

27732



National Library of Canada

Bibliothèque nationale du Canada

CANADIAN THESES ON MICROFICHE

THÈSES CANADIENNES SUR MICROFICHE

NAME OF AUTHOR/NOM DE L'AUTEUR Rita Schuller

TITLE OF THESIS/TITRE DE LA THÈSE Purification of Immunoglobulin heavy chain mRNAs and their use in hybridization studies

UNIVERSITY/UNIVERSITÉ University of Alberta, Edmonton, Alberta

DEGREE FOR WHICH THESIS WAS PRESENTED/GRADE POUR LEQUEL CETTE THÈSE FUT PRÉSENTÉE M.Sc.

YEAR THIS DEGREE CONFERRED/ANNÉE D'OBTENTION DE CE GRADE 1976

NAME OF SUPERVISOR/NOM DU DIRECTEUR DE THÈSE Dr. R.C. van Berstel

Permission is hereby granted to the NATIONAL LIBRARY OF CANADA to microfilm this thesis and to lend or sell copies of the film.

The author reserves other publication rights, and neither the thesis nor extensive extracts from it may be printed or otherwise reproduced without the author's written permission.

L'autorisation est, par la présente, accordée à la BIBLIOTHÈQUE NATIONALE DU CANADA de microfilmer cette thèse et de prêter ou de vendre des exemplaires du film.

L'auteur se réserve les autres droits de publication; ni la thèse ni de longs extraits de celle-ci ne doivent être imprimés ou autrement reproduits sans l'autorisation écrite de l'auteur.

DATED/DATE 23 December, 1975 SIGNED/SIGNÉ Rita Schuller

PERMANENT ADDRESS/RÉSIDENCE FIXÉ 8910 - 88 Avenue
Edmonton, Alberta

INFORMATION TO USERS

THIS DISSERTATION HAS BEEN
MICROFILMED EXACTLY AS RECEIVED

This copy was produced from a microfiche copy of the original document. The quality of the copy is heavily dependent upon the quality of the original thesis submitted for microfilming. Every effort has been made to ensure the highest quality of reproduction possible.

PLEASE NOTE: Some pages may have indistinct print. Filmed as received.

Canadian Theses Division
Cataloguing Branch
National Library of Canada
Ottawa, Canada K1A 0N4

AVIS AUX USAGERS

LA THESE A ETE MICROFILMEE
TELLE QUE NOUS L'AVONS RECUE

Cette copie a été faite à partir d'une microfiche du document original. La qualité de la copie dépend grandement de la qualité de la thèse soumise pour le microfilmage. Nous avons tout fait pour assurer une qualité supérieure de reproduction.

NOTA BENE: La qualité d'impression de certaines pages peut laisser à désirer. Microfilmée telle que nous l'avons reçue.

Division des thèses canadiennes
Direction du catalogage
Bibliothèque nationale du Canada
Ottawa, Canada K1A 0N4

THE UNIVERSITY OF ALBERTA

PURIFICATION OF IMMUNOGLOBULIN HEAVY CHAIN mRNA'S
AND THEIR USE IN HYBRIDIZATION STUDIES

by

RITA SCHULLER



A THESIS

SUBMITTED TO THE FACULTY OF GRADUATE STUDIES AND RESEARCH
IN PARTIAL FULFILMENT OF THE REQUIREMENTS FOR THE DEGREE
OF MASTER OF SCIENCE

DEPARTMENT OF GENETICS

EDMONTON, ALBERTA

SPRING, 1976

THE UNIVERSITY OF ALBERTA
FACULTY OF GRADUATE STUDIES AND RESEARCH

The undersigned certify that they have read, and recommend to the Faculty of Graduate Studies and Research, for acceptance, a thesis entitled "Purification of Immunoglobulin Heavy Chain mRNA's and Their Use in Hybridization Studies," submitted by Rita Schuller in partial fulfillment of the requirements for the degree of Master of Science.

E. M. Steinberg
.....
Co-supervisor

S. P. von Döbel
.....
Co-supervisor

M. R. ...
.....

P. J. ...
.....

Verner Paetkau
.....

Date *4 December 1975*
.....

for my mother

ABSTRACT

Techniques have been developed which allow the isolation of immunoglobulin heavy chain mRNA to a degree of purity suitable for detailed hybridization studies. These techniques involve the purification of nondegraded membrane-bound polysomes from mouse myelomas; successive oligo(dT)-cellulose chromatographies of the phenol-extracted RNA (each chromatography being preceded by a heat treatment which was found to be extremely critical in the removal of 18S rRNA); preparative sucrose density gradient centrifugations; and improved techniques of polyacrylamide gel electrophoresis in 99% formamide. The heavy chain mRNA's obtained in this way were characterized by the comparison of their cell-free translation products with the corresponding *in vivo* secreted heavy chains, using both SDS-polyacrylamide gel electrophoresis and two-dimensional high voltage electrophoresis of tryptic digests.

For α mRNA purified from H2020 myelomas and μ mRNA purified from MOPC 104E myelomas, hybridization studies with mouse liver DNA resulted in corrected gene reiteration frequencies of 3 and 4, respectively. On the basis of the monophasic natures of the C_0t curves obtained, there was no evidence whatsoever to prevent the assignment of these reiteration frequencies to both the variable and the constant regions of the α and μ mRNA's. Moreover, it seems that those rapidly-hybridizing sequences accounting for the biphasic kinetics reported in previous studies of hybridizations with immunoglobulin mRNA's, and for the tails on the C_0t curves in the present report, are due to repetitive portions of contaminating mRNA's and not of the immunoglobulin mRNA in question.

Hybridizations of the α mRNA to homologous and heterologous myeloma DNA's showed certain significant variations in the final levels and in the kinetics of hybridization: taking the hybridization with its homologous myeloma DNA as a standard, H2020 α RNA hybridized with S28 (γ_1), MPC11 (γ_{2b}) and Y5781 (μ) DNA's to an equal extent, with J558 (α) DNA to a greater extent, and with 104E (μ) DNA to a lesser extent. Hybridization studies with a 13S 3'-end containing fragment of H2020 α RNA indicated that these results are primarily attributable to differences in the α gene composition of the J558, H2020 and 104E DNA's. Consequently, these data suggest that the commitment of a particular lymphocyte to the production of a specific immunoglobulin class occurs concurrently with the loss of certain heavy chain constant region (C_H) genetic sequences. Considering the linkage relationship of C_H genes in the mouse, a mechanism of V_H - C_H gene integration based on excision and loss of interspersing DNA material seems to be implicated.

ACKNOWLEDGEMENTS

I wish to thank my co-supervisors, Dr. Charles Steinberg and Dr. R.C. von Borstel, for coordinating my research program between the University of Alberta and the Basel Institute for Immunology.

I am indebted to F. Hoffman-La Roche and Company, Basel, Switzerland, for supporting this research. In particular, I would like to express my deep appreciation to Dr. Susumu Tonegawa for the opportunity to work and learn in his laboratory, and for all his assistance and advice. Special thanks also go to Dr. Steinberg, for helpful discussion and encouragement during both the experimental work and the thesis preparation; Dr. T. Staehelin, for the translation of my mRNA preparations in his cell-free system; Ms. L. Forni, for carrying out the immunofluorescent studies; Ms. S. Witschi, for valuable assistance with the animal work; and the many other members of the Institute for Immunology who contributed either directly or indirectly to my research.

Finally, I am grateful to my family, for their constant understanding and support throughout my stay in Basel, and to Jürg Lenhard, without whom this research would never have been undertaken.

TABLE OF CONTENTS

| | Page |
|--|------|
| DEDICATION | iii |
| ABSTRACT | iv |
| ACKNOWLEDGEMENTS | vi |
| LIST OF TABLES | x |
| LIST OF FIGURES | xi |
| LIST OF PLATES | xiii |
| | |
| CHAPTER | |
| I. INTRODUCTION | 1 |
| Structure and Classification of Antibody Molecules | 2 |
| Problem of V and C Gene Integration | 4 |
| Basis of the "Two Gene — One Polypeptide" Concept | 4 |
| Structural Studies on Immunoglobulin mRNA | 5 |
| Proposed Mechanisms of Integration | 6 |
| Problem of the Origin of Antibody Diversity | 7 |
| Nature and Extent of Diversity | 7 |
| Numbers of V and C Genes per Linkage Group | 8 |
| Means of Distinguishing between the "Multiple Germ Line Gene" and the "Somatic Generation" Hypotheses. | 8 |
| Results of Hybridization Studies with Immunoglobulin mRNA's | 10 |
| Purpose of the Present Study | 12 |

| Chapter | | Page |
|---------|--|------|
| II. | MATERIALS AND METHODS | 14 |
| | Materials | 14 |
| | DE Medium | 14 |
| | DE-Methionine Medium | 15 |
| | Oligo(dT)-Cellulose | 16 |
| | RLS-100 | 17 |
| | Biological Material | 18 |
| | Methods | 18 |
| | Handling of Mouse Myeloma Lines | 18 |
| | DNA Preparation | 19 |
| | Preparation of <i>in vivo</i> Markers | 22 |
| | Isolation and Purification of Heavy Chain mRNA | 24 |
| | Characterization of Heavy Chain mRNA | 31 |
| | Preparation of ¹²⁵ I-labelled RNA | 33 |
| | DNA-RNA Hybridization | 35 |
| III. | RESULTS | 37 |
| | Immunofluorescence | 37 |
| | DNA Preparation | 37 |
| | Preparation of Radioactive <i>in vivo</i> Markers | 45 |
| | Preparation of Heavy Chain mRNA's | 48 |
| | Characterization of Heavy Chain mRNA's | 53 |
| | Further Purification of the Heavy Chain mRNA's | 67 |
| | Preparation of ¹²⁵ I-labelled RNA | 76 |
| | Preparation of a 3'-end Containing Fragment of H2020 α mRNA | 79 |

| Chapter | Page |
|--|------------------|
| III. (Cont'd) | |
| Hybridization Experiments | 82 |
| Hybridization Kinetics of H2020 α and 104E μ RNA Preparations with Mouse Liver DNA | 82 |
| Hybridization of H2020 α and 104E μ RNA's with DNA's from Various Heavy Chain- Producing Myelomas | 86 |
| Hybridization Studies with the H2020 α 3'-end Containing Fragment | 93 |
| Effect of the DNA Excess on the Final Hybridization Level | 95 |
| IV. DISCUSSION | 99 |
| Purification and Characterization of Heavy Chain mRNA's | 99 |
| Hybridization Kinetics of H2020 α and 104E μ RNA's with Mouse Liver DNA | 102 |
| Hybridization Studies with Myeloma DNA's | 104 |
| BIBLIOGRAPHY | 110 _o |

LIST OF TABLES

| Table | Description | Page |
|-------|---|------|
| 1. | Summary of existing reports on hybridization studies with immunoglobulin mRNA's | 11 |
| 2. | Immunofluorescent staining patterns of mouse myelomas | 38 |
| 3. | Summarized results of the preparation of DNA for use in hybridization experiments | 42 |
| 4. | Oligo(dT)-cellulose chromatography of membrane-bound polysomal (MBP) RNA | 51 |
| 5. | Incorporation of ^{35}S into acid-insoluble material, by a cell-free translation system supplemented with various RNA preparations | 56 |
| 6. | Percent hybrid formed by H2020 α and 104E μ RNA's with the DNA from various heavy chain-producing myelomas | 89 |
| 7. | Percent hybrid formed by H2020 α 'complete sequence' and 3'-end containing fragments with H2020, 104E, and J558 DNA's | 94 |
| 8. | Effect of the DNA excess on the final hybridization level | 98 |

LIST OF FIGURES

| Figure | Page |
|--|------|
| 1. Size determination of a sonicated RNA preparation by sucrose density gradient centrifugation in comparison with a ribosomal and transfer RNA standard | 17 |
| 2. Elution profile of sonicated 104E RNA from a SP-Sephadex C-50 column | 44 |
| 3. Sucrose density gradient centrifugation of the cell supernatant of [³⁵ S]methionine-labelled myeloma cells. | 46 |
| 4. Separation of heavy and light chains of reduced <i>in vivo</i> immunoglobulins by chromatography on G200 Sephadex. | 47 |
| 5. Sucrose density gradient centrifugation of membrane-bound polysome preparations | 49 |
| 6. Analytical sucrose density gradient centrifugation of oligo(dT)-cellulose fractions from H2020 membrane-bound polysomal RNA | 52 |
| 7. Preparative sucrose density gradient centrifugation of the TE-II fractions obtained by two successive oligo(dT) chromatographies, each preceded by heat treatment | 54 |
| 8. Preparative polyacrylamide gel electrophoresis in 99% formamide of the H2020 and 104E RNA preparations, in comparison with a ribosomal RNA standard | 75 |
| 9. Polyacrylamide gel electrophoresis in 99% formamide of eluted H2020 and 104E RNA, in comparison with a ribosomal RNA standard | 77 |
| 10. Sucrose density gradient centrifugation of iodinated RNA preparations | 78 |
| 11. Fractionation of a highly degraded ¹²⁵ I-labelled 104E RNA preparation by successive sucrose density gradient centrifugations | 80 |
| 12. Fractionation of 3'-end containing fragments and 'complete sequence' fragments of a ¹²⁵ I-labelled H2020 RNA preparation by successive sucrose density gradient centrifugations | 81 |

| Figure | Page |
|--|------|
| 13. Hybridization kinetics with mouse liver DNA (#1) | 83 |
| 14. Competition hybridization of 104E μ RNA (#1) with mouse liver DNA (#1) in the presence of 2 μ gm/ml unlabelled mouse 18S ribosomal RNA | 85 |
| 15. Homologous and heterologous hybridizations of H2020 α and 104E μ RNA's (#1) and DNA's (#1) | 88 |
| 16. Hybridization of H2020 α RNA (#2) with various myeloma DNA's | 91 |
| 17. Hybridization kinetics of H2020 α RNA (#2) with H2020 DNA (#2), 104E DNA (#2) and J558 DNA | 92 |
| 18. Hybridization kinetics of H2020 α RNA 'complete sequence' and 3'-end containing fragment with 104E DNA (#2) | 96 |
| 19. Simplistic model of V-C gene integration by excision of interspersing DNA sequences | 106 |

LIST OF PHOTOGRAPHIC PLATES

| Plate | Description | Page |
|-------|--|------|
| 1. | Intracellular immunofluorescent staining pattern of mouse myeloma lines. | 40 |
| 2. | Autoradiograph of SDS-polyacrylamide gel electrophoresis of the products synthesized in a cell-free translation system in response to the H2020 16S RNA preparation | 58 |
| 3. | Autoradiograph of SDS-polyacrylamide gel electrophoresis of the products synthesized in a cell-free translation system in response to various 104E RNA sucrose gradient fractions | 60 |
| 4. | Autoradiograph of the high voltage electrophoresis at pH6.5 of tryptic peptides from the cell-free products of 104E RNA fractions and from <i>in vivo</i> μ chain | 64 |
| 5. | Autoradiograph of the second-dimensional high voltage electrophoresis at pH3.5 of the 104E basic peptides obtained by the pH6.5 electrophoresis | 66 |
| 6. | Autoradiograph of the high voltage electrophoresis at pH6.5 of tryptic peptides from the cell-free products of H2020 16S RNA and rabbit globin mRNA and from <i>in vivo</i> α chain | 69 |
| 7. | Autoradiograph of the second-dimensional high voltage electrophoresis at pH3.5 of the H2020 acidic and basic peptides obtained by the pH6.5 electrophoresis | 71 |
| 8. | Analytical polyacrylamide gel electrophoresis in 99% formamide | 74 |

INTRODUCTION

Eukaryotic messenger RNA (mRNA) is of great potential usefulness for detailed studies on the organization and expression of genes in higher organisms. In this respect, the study of immunoglobulin mRNA is particularly important because of two unique features of the immune system:

1. The sequence of one immunoglobulin polypeptide chain appears to be controlled by two separate structural genes. Therefore, integration of genetic information must occur at some level.

2. A vast amount of diversity in terms of amino acid sequence exists among antibody molecules. The information required for this diversity must somehow be incorporated into the cellular genome. A lower limit of the extent of this diversity has been derived as follows (Fudenberg *et al.*, 1972): upon immunization with an antigen, the concentration of a specific antibody in an animal's serum may increase as much as 10^6 -fold, without a corresponding increase in total immunoglobulin production. If each antibody was originally present in equal concentration in the unimmunized animal, it can be deduced that antibodies of at least 10^6 different specificities exist.

The existing contributions, as well as the potential usefulness, of the study of purified immunoglobulin mRNA molecules towards the solving of these two fundamental immunological problems will be discussed in detail below. However, a critical evaluation of such studies is dependent, initially, on a thorough understanding of the basic structure of antibody molecules and of the precise relationship between specificity and amino acid sequence.

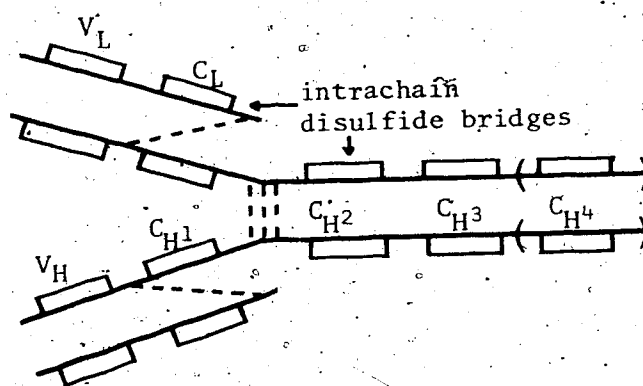
Structure and Classification of Antibody Molecules

The basic structure of a typical antibody molecule was elucidated by Porter and Edelman as early as 1960, and shown to consist of two heavy chains (450—700 amino acids each) and two light chains (approximately 200 amino acids each) joined by disulfide bridges. However, because antibodies from normal sera are very heterogeneous in antigenic characteristics and in amino acid sequence, more detailed structural studies were dependent on the recognition that the homogeneous myeloma and Bence-Jones proteins are related to normal immunoglobulins (Hiltschmann and Craig, 1965). These proteins, which usually show no antibody activity, are produced by the malignant proliferation of a single immunoglobulin-producing cell. Such malignancies were found to occur naturally in both the man and the mouse, and have since been induced in the mouse by intraperitoneal injection of mineral oil. The homogeneity of these proteins provides a unique opportunity to study individual molecules apparently selected at random from the immunoglobulin pool. By peptide mapping and later by amino acid sequencing of these homogeneous proteins, it was recognized that each immunoglobulin chain has a unique sequence consisting of approximately 100 amino acid residues, at its amino terminal end. Because this sequence is different for each chain, it is therefore referred to as the variable region. In contrast, the remainder of each chain consists of a constant region that can be used to define particular classes and subclasses of immunoglobulins. More than 99% of the total human and mouse immunoglobulins have been identified as belonging to one of three classes (IgG, IgA, or IgM) which are defined by the presence of specific heavy chains (γ , α , or μ , respectively). Two light chain types, κ and λ , have also been defined, and each may combine with any one of the heavy chains to produce the final

immunoglobulin molecule. (Within one molecule, the two light and two heavy chains are each of the same class.)

Furthermore, in humans, four subclasses of γ chains have been identified which differ in biological properties but which have a sequence homology of about 90%; although only limited sequence data are available, there is serological evidence for two subclasses each of α and μ , as well. In contrast, subtypes of light chains appear to be extremely rare. Only in human λ chains have subtypes been found; these differ in the constant region by a single amino acid substitution. Little homology exists between any variable and any constant region; however homology units, consisting of approximately 100–110 amino acid residues, are definitely evident in the constant regions of each class of immunoglobulin, and these units correspond to the loops formed by intrachain disulfide bridges.

In summary, then, the basic structural unit of an immunoglobulin molecule can be depicted as follows (adapted from Fudenberg *et al.*, 1972):



In this diagram, V denotes the variable region; C, the constant region; L, the light chain; and H, the heavy chain. The interchain disulfide

bridges are shown as dotted lines because their exact number and position vary between classes and species. C_L and C_{H1-4} represent homology units. The IgM molecule contains one extra homology unit in the heavy chain (C_{H4}) as compared with the IgG or IgA molecule.

Problem of V and C Gene Integration

Basis of the "Two Gene - One Polypeptide" Concept

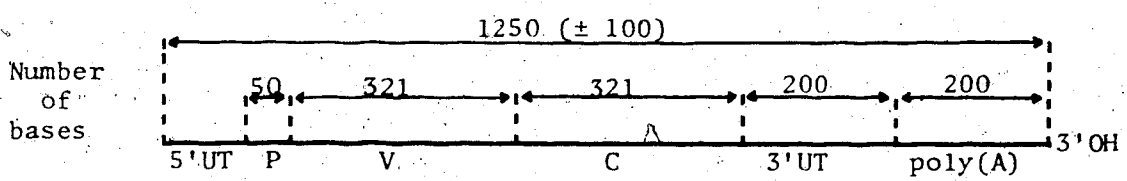
A consideration of the peptide maps and/or amino acid sequences of a large number of myeloma proteins, combined with classical genetic studies, suggests that the variable region is coded for by any one of more than a thousand genes, while the constant region is the product of a single gene. This observation was incorporated by Dreyer and Bennett (1965) into the hypothesis that two genes are involved in the synthesis of each immunoglobulin chain, one controlling the constant portion of the chain and the other, the variable portion. The former is specific for each type of light or heavy chain, and has been designated as the C gene; the latter is different from one chain to another and can be any one of a gene cluster designated as V genes.

Probably the most convincing piece of experimental evidence in support of this hypothesis comes from the work of Wang *et al.* (1970) on a rare human serum with monoclonal IgG and IgM proteins. From amino acid sequencing, it was determined that the heavy chains of these proteins, while differing by their possession of γ or μ constant regions, were identical in the amino acid sequence of their variable regions. Since it is highly improbable that two genes could maintain one-quarter of their corresponding polypeptide chains identical to each other throughout the evolution of the immune system, the best interpretation

of these data is that the constant and variable regions of each chain are under separate genetic control, and that the κ and μ C genes of this serum share the same V gene.

Structural Studies on Immunoglobulin mRNA

The hypothesis of "two genes - one polypeptide" necessitates the existence of some mechanism by which the information encoded by the V and the C genes is joined to produce the final polypeptide. Theoretically, such joining may occur at one of three levels: DNA, mRNA, or protein. However, recent studies on the nucleotide sequence of immunoglobulin mRNA's isolated from mouse myelomas have provided conclusive evidence that both variable and constant region amino acid sequences are represented in the same mRNA molecule. In particular, the structure of the κ light chain mRNA from the MOPC21 mouse myeloma was determined by Milstein *et al.* (1975) to be the following:



In this diagram, V represents the variable region sequence; C, the constant region sequence; P, the precursor sequence (i.e. those nucleotides corresponding to an amino acid sequence at the N-terminal end of the κ light chain which is apparent in *in vitro* translates but not in *in vivo* secreted κ chains); and UT, the untranslated sequences (i.e. those nucleotide sequences which do not correspond to any amino acid sequences in either *in vitro* or *in vivo* κ chains).

Proposed Mechanisms of Integration

Since the mRNA's used for sequence studies were invariably isolated from the microsomal cell fraction, the possibility is not eliminated that joining of V and C region information occurs at some stage between transcription of the mRNA and attachment by ribosomes. It appears, however, that only constant and variable regions coded by the same chromosome can be associated in a single immunoglobulin polypeptide chain, the evidence for this being the predominantly 'cis' combination of allelic markers in rabbits heterozygous at both C_H and V_H region loci (Tosi *et al.*, 1970). Hence, it seems more likely that a DNA level of association is involved.

Considering, then, that association of V and C region information does occur at the genetic intrachromosomal level, several mechanisms of gene integration have been proposed. The translocation mechanism, brought forth by Dreyer and Bennett (1965) and later expanded by Gally and Edelman (1970), suggests that V genes tandemly arranged on a chromosome can form an 'episome-like' structure by an intrachromosomal recombinational event, diffuse a short distance to a nearby C gene in the same chromosome, and be inserted adjacent to the C gene by a specific integration enzyme. Implicit in this mechanism is the concept that joining of particular V and C genes would simultaneously commit the cell to the production of that immunoglobulin polypeptide. Alternatively, the branched network model of DNA was used by Smithies (1968) to devise a mechanism in which V genes are all arranged parallel to one another and are simultaneously adjacent to a parallel stack of C genes. Protein switches between the two stacks would direct the path of RNA polymerase

and thereby specify which of the many possible V-C combinations were to be expressed. At present, no direct experimental evidence exists in support of either of these proposed mechanisms.

Problem of the Origin of Antibody Diversity

Nature and Extent of Diversity

The phenotypic basis of antibody specificity, and consequently diversity, has been clearly elucidated: antibodies of different specificity, as well as different antibodies directed against the same antigen, have different amino acid sequences. As indicated above, the variability is concentrated in the amino terminal 110-120 residues of the light or heavy chains, particularly in three regions of higher-than-usual variability within these residues (Wu and Kabat, 1970). By affinity labelling studies, these regions have been shown to comprise the antibody combining site (Singer and Doolittle, 1966).

Furthermore, studies of the amino acid sequences of large numbers of myeloma variable regions have shown that each region can be unambiguously classified as belonging to κ , λ or heavy chains (Edelman and Gall, 1966). That is, there appears to exist among immunoglobulin structural genes three linkage groups: a group of V genes associated only with the κ chain C gene(s), a group of V genes associated only with the λ chain C gene(s), and a group of V genes associated with any one of the heavy chain C genes. V regions from each group can be further classified into subgroups by the degree of amino acid sequence homology, using the following criteria: all V regions of the same subgroup show at least 80% identity in sequence, while V regions of different subgroups are less than 60% identical.

Numbers of V and C Genes per Linkage Group

Genetic studies have provided convincing evidence that only one C gene exists per linkage group for each immunoglobulin class or subclass (Lieberman and Potter, 1966; Herzenberg *et al.*, 1968). However, a great deal of controversy still remains as to the number of V genes in each linkage group. In general, two opposing views exist. The "multiple germ line gene" hypothesis predicts that all antibody sequences are encoded by genes directly transmittable from parent to offspring; that is, by germ line genes (Dreyer and Bennett, 1965; Hood and Talmage, 1970). Using the previously estimated value of 10^6 different antibody sequences, a minimum of 10^3 V genes per linkage group are required by this hypothesis, assuming nonpreferential recombination of heavy and light chain types. The "somatic generation" hypothesis, on the other hand, predicts that the diversity in the variable region arises by somatic events, presumably recombination (Gally and Edelman, 1970) and/or mutation (Burnet, 1969; Jerne, 1970). Therefore, only a few master copies of the variable region genetic sequences are required in the germ line. Generally, this hypothesis recognizes that each V region subgroup is likely coded for by a different germ line gene, since it is very difficult to imagine somatic mechanisms which could produce, from one gene, two sequences which differ by more than 40% of their amino acid residues. Consequently, the minimum number of V genes predicted by the "somatic generation" hypothesis is generally considered to be equal to the number of subgroups of V_K , V_λ , and V_H regions.

Means of Distinguishing between the "Multiple Germ Line Gene"

and the "Somatic Generation" Hypotheses

It is possible to present arguments both for and against each of

these hypotheses. For example, the Mendelian inheritance of genetic markers associated with the sequences of variable regions, and the great selection pressure required to produce and maintain in the germ line the immense variety of different V sequences, seem to argue against the "multiple germ line gene" hypothesis. On the other hand, the "somatic generation" hypothesis requires an especially high rate of somatic recombination and/or mutation acting preferentially on V genes, or else a very strong selection to preserve or proliferate any cells in which such somatic events have occurred (Fudenberg *et al.*, 1972).

In general, all attempts to distinguish between the two hypotheses on the basis of classical genetical methods combined with sequence studies on immunoglobulin polypeptides have produced ambiguous or inconclusive results. However, there exists on the molecular genetic level, a direct approach to determining the actual origin of antibody diversity; that is, to count the numbers of polynucleotide sequences in the genome which correspond to variable regions. Such an approach would take the following experimental form: isolation, in a pure form, of the mRNA coding for a specific immunoglobulin class; demonstration of the identity and purity of this mRNA; radioactive labelling of the mRNA or its complementary DNA to a high specific activity; determination of the characteristics of hybridization of this radioactive probe with the corresponding DNA. From the hybridization data, it should then be possible to determine, according to the principles elucidated by Bishop *et al.* (1972), the reiteration frequencies of those DNA sequences responsible for the production of the particular mRNA.

In performing such hybridization studies, it must be recognized that complete mRNA molecules consist of both V and C region sequences,

as discussed above; consequently, each sequence must be separately identified as contributing to a particular portion of the hybridization kinetics. Also, in this way the hybridization studies can be used to confirm the genetical evidence for unique C genes.

Results of Hybridization Studies with Immunoglobulin mRNA's

To date, mouse myelomas, either as *in vivo* tumor lines or as cell culture lines, have provided the most useful source of immunoglobulin mRNA. Reports of the preparation of mRNA fractions which have demonstrable activity in the *in vitro* synthesis of myeloma proteins, and the subsequent iodination and hybridization of these mRNA's with mouse DNA, are summarized in Table 1. In most of these reports, similar results were obtained with undifferentiated DNA (liver, spleen, embryo) as with myeloma DNA, indicating that specific amplification of immunoglobulin genes does not occur during lymphocyte differentiation. The major points evident from this summary are:

a. The majority of each mRNA preparation contains sequences which hybridize with unique (or nearly unique) genes.

b. In each mRNA preparation, there exist some sequences which hybridize more rapidly than the majority of the sequences. The exact proportion of these rapidly-hybridizing sequences, as well as their corresponding gene frequencies, varies greatly between reports. It remains to be determined if these variations are significant or if they merely represent differences in the purity of the mRNA probe or in the method of hybridization.

In regard to the problem of assigning V and C sequences to a particular portion of the hybridization kinetics, Storb (1974) and Premkumar

TABLE 1. Summary of Existing Reports on Hybridization Studies with Immunoglobulin mRNA's

| Class and source of mRNA | Estimated purity of mRNA | Maximum hybridization achieved | Rapidly-hybridizing portion of hybridized sequences | Corresponding gene frequency | Gene frequency of slowly-hybridizing portion | Reference |
|--------------------------|--------------------------|--------------------------------|---|------------------------------|--|--------------------------------|
| λ -mRNA Y5380 | not stated | 50% | 50% | 245 | 5 | Delovitch and Baglioni (1973) |
| δ -mRNA MPC 11 | not stated | 50% | 50% | 245 | 5 | Delovitch and Baglioni (1973) |
| MOPC 41 | not stated | 25% | not stated | 2500-5000 | not stated | Storb (1974) |
| MOPC 70E | 70-80% | 50% | 16% | 230 | 1-2 | Tonegawa et al. (1974) |
| MOPC 41 | not stated | 70% | 25% | 30-50 | 1-2 | Leder et al. (1974) |
| MOPC 21 | 50% | 50% | not stated | 250 | 1-2 | Milstein et al. (1975) |
| α -mRNA 315 | not stated | 70% | 20% | 5300 | 4 | Prenkumar et al. (1974) |
| γ -mRNA MPC 11 | 50% | 55% | 13% | 290 | 1-2 | Bernardini and Tonegawa (1974) |

et al. (1974) assume, on the basis of purely *ad hoc* arguments, that the first transition (i.e. that representing rapidly hybridizing sequences) corresponds to V sequences, and the second transition corresponds to a unique C sequence. They therefore interpret their data as a confirmation of the "multiple germ line gene" hypothesis for the origin of antibody diversity.

However, more judicious analyses have been carried out by Tonegawa *et al.* (1974) using competition hybridization experiments involving κ chain mRNA's isolated from both the same and different subgroups, and by Milstein *et al.* (1975) using either 3'-end fragments of the mRNA or complementary DNA transcripts containing varying proportions of C and V sequences. These experiments have confirmed that the unique (slowly-hybridizing) portion does correspond to the C region sequences. Furthermore, they provided no evidence whatsoever that excludes the assignment of the V region sequences as well to this slowly-hybridizing portion. Therefore, it seems entirely possible that only one or a few V region germ line genes exist per subgroup, and that antibody diversity is generated by somatic events. The origin of the rapidly-hybridizing portion could be either repetitive untranslated sequences at the 5'-end of the immunoglobulin mRNA, or repetitive sequences at the 5'-ends of contaminating RNA species. The existing data do not distinguish between these two possibilities.

Purpose of the Present Study

It was desired, primarily, to extend the hybridization studies of the type described above to include additional heavy chain mRNA species, and thereby to provide a broader basis of evidence for distinguishing

between the "multiple germ line gene" and the "somatic generation" hypotheses of the origin of antibody diversity. However, since the value of any hybridization study is dependent on the purity of the mRNA probe, and since heavy chain mRNA's appear to be intrinsically more difficult to purify than light chain mRNA's, the initial step was an attempt to improve existing methods for the purification of immunoglobulin mRNA's.

Furthermore, the fact that all heavy chain constant region genes belong to one linkage group, suggests that such highly purified heavy chain mRNA's might also be valuable for investigating the integration of V and C region information at the genetic level.

MATERIALS AND METHODS

Materials

In all procedures to be described, Merck analytical grade chemicals were used unless otherwise designated; glassware was autoclaved; and solutions were prepared with tridistilled water and autoclaved when possible. During critical steps in the isolation of mRNA (for example, oligo(dT)-cellulose chromatography and sucrose density gradient centrifugation), glassware was treated with Baycovin (Diethylpyrocarbonate; Bayer) by soaking in a 1% solution overnight followed by autoclaving, and solutions were treated by stirring with 0.1% Baycovin overnight followed by air evacuation.

Reagents or materials requiring special preparation were as follows:

DE medium

Dulbecco's modified Eagle medium, obtained in powder form from GIBCO Co., was dissolved in glass-distilled water and supplemented with 10 ml per liter of each of the following solutions: 200 mM L-Glutamine, 100X Non Essential Amino Acids, and an antibiotic mixture consisting of 15,000 units Penicillin plus 15,000 mcg Streptomycin per ml (each of these solutions being obtained from GIBCO). The medium was then filter sterilized and stored frozen at -20°C . Immediately prior to use, 0.05% NaHCO_3 and 10mM HEPES (N-2-Hydroxyethylpiperazine-N-2'-Ethanesulfonic Acid, Calbiochem A grade) were added to adjust the pH. This final solution is hereafter referred to as DE medium.

DE - Methionine medium

Since the commercially available powder form of Dulbecco's modified Eagle medium contains the essential amino acids, this methionine-free medium had to be made completely from starting materials. The following solutions, in the quantities given, were mixed and made up to 1 liter with glass-distilled water:

| | |
|--|--------|
| 10X Salt Mix ¹ | 100 ml |
| 50X Essential Amino Acid Solution - Methionine ² | 40 ml |
| 100X Non Essential Amino Acid Solution ³ | 20 ml |
| 100X Sodium Pyruvate Solution ³ | 10 ml |
| 100X Vitamin Solution ³ | 40 ml |
| 0.5% Phenol Red Solution ³ | 3 ml |
| 7.4% NaHCO ₃ | 50 ml |
| 0.12% NaH ₂ PO ₄ ·H ₂ O | 100 ml |
| <hr/> | |
| 200mM L-Glutamine ³ | 10 ml |
| Antibiotic mixture ³ (10,000 units/ml Penicillin 10,000 mcg/ml Streptomycin) | 10 ml |

¹10X Salt Mix: 2.6 gm/l CaCl₂·2H₂O, 4.0 gm/l KCl, 2 gm/l MgSO₄·7H₂O, 64 gm/l NaCl, 1.0 mgm/l Fe(NO₃)₃·9H₂O, 11 gm/l Glucose·H₂O

²50X Essential Amino Acid Solution - Methionine: 4mM each L-Tryptophan, L-Threonine; 10mM each L-Cystine, L-Histidine; 20mM each, L-Arginine·HCl, Glycine, L-Serine, L-Tyrosine, L-Phenylalanine; 40mM each L-Valine, L-Isoleucine, L-Lysine·HCl (all amino acids being obtained from Sigma).

³These solutions were obtained from GIBCO Co.

The resulting solution was sterilized by filtration and stored frozen at -20°C . Immediately prior to use, the pH was adjusted by blowing through gaseous CO_2 until the solution was an orange-red color.

Oligo(dT)-Cellulose

The preparation method according to Gilham (1964) involved three steps:

1. *Preparation of the pyridinium salt of TMP (thymidine monophosphate):* TMP-Na_2 (Miles or Sigma) dissolved in water was loaded on a column of Dowex 50 H^+ ion exchange resin (5gm TMP-Na_2 being used per 350ml wet volume Dowex). The column was washed with water and eluted fractions were monitored for optical density at 267nm (maximum absorption of TMP). The OD-containing fractions were pooled and concentrated in a flash evaporator to approximately 20ml per 10^5 OD_{267} units of recovered TMP-H_2 . (All the following quantities are based on this amount of TMP-H_2 .)

2. *Polymerization of TMP-H_2 :* Polymerization occurs only under completely anhydrous conditions. Therefore, all glassware and compounds used in the following procedure were first carefully dried. For the TMP-H_2 solution, this drying was accomplished by the repeated addition and evaporation of 15 ml of dry pyridine (anhydrously redistilled and stored over KOH pellets). Polymerization was then carried out by the addition of 4.5gm dry DCC (N,N'-dicyclohexylcarbodiimide, Fluka) to the TMP-H_2 in 18ml dry pyridine, followed by vigorous shaking at room temperature for 5 days.

3. *Binding of oligo(dT) to cellulose:* Following the further addition of 300ml of dry pyridine and 12gm of DCC, 30gm of Whatman CC31

cellulose (prewashed with alcohol and HCl and prebaked) were added to the solution of polymerized TMP-H₂. Shaking was continued for five to six days.

At the end of the procedure, the oligo(dT)-cellulose was collected by filtration on a sintered glass funnel and washed extensively with absolute ethanol at 37°C, followed with distilled H₂O, until the optical density at 267nm was negligible. It was then dried in a vacuum oven at 37°C and stored at -20°C.

RLS-100

A high-speed supernatant of rat livers, which has been reported by Blobel and Potter (1966) to contain an effective inhibitor of RNase activity, was prepared as follows: male albino rats of the Wistar strain (300—350 grams in weight) were asphyxiated by CO₂ vapor and bled by slitting the throats. Livers were removed immediately upon death of the animal, and each liver was put into 25ml of ice-cold Buffer B (0.3M sucrose, 50mM KCl, 10mM Tris-HCl pH7.5, 5mM MgCl₂, 1mM dithiothreitol), chopped with scissors, and homogenized 14 strokes in a motor-driven Teflon-glass tissue grinder (1200rpm, 0.3mm clearance). The microsomal fraction was removed by centrifuging in the Sorvall RC 2-B for 20 minutes at 15,000rpm, and the post-microsomal supernatant was recentrifuged at 40,000rpm for 4 hours in the International Preparative Ultracentrifuge B-60 (rotor A170). After removal of the overlying fat layer, the supernatant obtained in this step was collected and frozen at -70°C. Immediately prior to use, it was carefully thawed at 37°C and spun once more in the Sorvall at 5000rpm for 20—30 minutes to remove any cloudiness.

Biological Material

Mouse myeloma lines were obtained from the Salk Institute Cell Distribution Center and from Dr. M. Potter, with the following designations concerning the class of immunoglobulin produced by each: MOPC 104E and Y5781 (IgM), S28 (IgG₁), MPC11 (IgG_{2b}), H2020 and J558 (IgA). They were received as solid tumors growing subcutaneously in female Balb/C mice. The mice used for the further passage of these lines were obtained from the Institut für biologische-medizinische Forschung, Füllinsdorf, Switzerland. The MOPC 104E (hereafter referred to more simply as 104E) and the H2020 myeloma lines were used as sources of μ and α heavy chain mRNA, respectively, and all six lines, as well as livers from uninjected mice, were used as sources of DNA.

Methods

Handling of Mouse Myeloma Lines

The myeloma lines were maintained as solid tumors in 8 to 20 week old female Balb/C mice by the serial subcutaneous injection of $1-2 \times 10^7$ cells at intervals of 10-14 days. For this purpose, cell suspensions from dissected tumors were made in DE medium containing 1% fetal calf serum (FCS). A reserve stock of each myeloma was also maintained by freezing small aliquots of cell suspensions at -70°C in DE medium containing 20% FCS and 10% dimethylsulfoxide.

At the completion of the experimental work described in this report, each myeloma line was checked by immunofluorescence to ensure that the production of immunoglobulin had been maintained as designated. This was done by intracellularly staining an acetic acid-fixed cell suspension of each myeloma with the fluorescently-labelled antiserum specific for

its immunoglobulin class, as well as with an unrelated antiserum (Holborow and Johnson, 1967).

DNA Preparation

Methods described by Bishop (1972) were essentially followed throughout.

1. *Purification of Nuclei*: Livers from Balb/C mice were taken into Buffer C (0.3M sucrose, 50mM KCl, 10mM Tris-HCl pH7.5, 5mM MgCl₂, 4mM CaCl₂) at a ratio of approximately 1gm liver per 2ml buffer, and homogenized 12 strokes at 1200rpm in the glass-Teflon homogenizer described previously. The homogenate was filtered through 4 layers of cheesecloth and spun 2500rpm for 10 minutes in the I.E.C. PR-6. The upper phase was aspirated and the remaining sediment was resuspended in an additional 1/2 volume of Buffer C. This suspension was then diluted to 0.22M sucrose by the slow addition of water, layered over an equal volume of 0.34M sucrose containing 0.01M Tris-HCl pH7.5 and 4mM CaCl₂, and centrifuged 2500rpm for 15 minutes in the I.E.C. PR-6. The resulting pellet was suspended in 9 volumes of 2.2M sucrose containing Tris and CaCl₂ as above. The nuclei were sedimented by centrifugation at 26,000rpm for one hour in the Spinco SW27 rotor, and stored frozen at -70°C.

With the myeloma tumors, it was found that a simpler purification procedure resulted in equally satisfactory preparations of nuclei. Briefly, 10-14 day old tumors were dissected and homogenized as described for the livers. However, when this homogenate was centrifuged at low speed, a distinct pellet was obtained, in contrast to the liver homogenate. This pellet was suspended in Buffer C (10ml per gram) and

NP-40 was added to 0.5%. After stirring for 10 minutes in ice, the mixture was centrifuged at 2000rpm for 10 minutes in the Sorvall. The resulting pellet was then suspended in sucrose and the nuclei sedimented as described for the liver nuclei preparation.

2. *Extraction of DNA:* The purified tumor or liver nuclei were suspended in TE-I buffer (0.05M Tris-HCl pH8.5, 0.05M Na₂EDTA) at a ratio of 1ml nuclei per 10ml buffer. SDS and pronase were added to 0.2% and 500 µgm/ml, respectively, and the suspension was incubated at 37°C for 5 hours, then shaken gently at room temperature overnight. When all the DNA was dissolved, NaCl was added to 0.5M, followed by 1/2 volume of water-saturated phenol. After shaking at room temperature for 60 minutes, 1/2 the starting volume was added of a chloroform: isoamyl-alcohol solution (25:1). Shaking was continued for 10 minutes, then the mixture was spun 2000rpm for 10 minutes in the I.E.C. PR-6. The aqueous phase was collected and reextracted 2 more times, as above. Two volumes

of ethanol were added to the final aqueous phase. The precipitated DNA was spooled on glass pipettes and redissolved in TE-I buffer by shaking overnight (the volume being the same as that originally used to suspend the nuclei). 5 units T₁RNase and 50 µgm RNaseA (both heat-treated at 80°C for 10 minutes) were added per ml of dissolved DNA. After incubation at 37°C for 5 hours, SDS and pronase were added to 0.2% and 200 µgm/ml, respectively. Incubation at 37°C was continued for at least 30 minutes when NaCl was added to 0.25M and the phenol-chloroform extraction was carried out three more times. DNA was collected from

the precipitate of the final aqueous phase by spooling or by low speed centrifugation, dried under vacuum and dissolved in a minimal volume of SP50 buffer (0.3M NaCl, 0.01M NaAcetate, pH5.5). If the DNA

appeared cloudy at this stage (due to aggregated glycogen which is also water soluble), it was cleared by centrifuging 40,000rpm for 20 minutes in the I.E.C. A170 rotor. The clear supernatant was then measured for optical density at 260 and 280 nm.

3. *Sonication and Size Determination:* After dilution to 50 OD₂₆₀ units per ml in SP50 buffer, the DNA was sonicated in ice at an amplitude of 7 μ . for 6 times 30 seconds with 30 second intervals (sonicator from M.S.E. Co.). The size of the resulting DNA fragments was determined by subjecting an aliquot to sucrose gradient centrifugation in comparison with a RNA standard. Linear 5—20% sucrose gradients (4ml each) were made in DAMON/IEC polyallomer tubes (#2841) using stock solutions of 5% and 20% sucrose in TSE (10mM Tris-HCl pH7.5, 100mM NaCl, 2mM Na₂EDTA). 0.25 to 0.5 OD₂₆₀ units of sonicated DNA, as well as 20D₂₆₀ units of a mouse ribosomal and transfer RNA preparation, were made up to 0.1ml in TSE and layered on the gradients. Centrifugation was at 55,000rpm for 180 minutes in the Spinco SW56 rotor at 18°C. Gradients were collected from the bottom of the tube with the optical density at 260nm being monitored continuously by a Gilford 2400 spectrophotometer fitted with an I.R.C. 4mm flowthrough cell. By comparison with the peaks of known S values formed by the RNA; the peak position of the sonicated DNA was assigned an S value.

4. *Gel Filtration:* In order to remove heavy metals, as well as remaining partially digested RNA, the sonicated DNA preparation was passed through a SP-Sephadex C-50 column (5 x 45cm) equilibrated in SP50 buffer. 2000 OD₂₆₀ units of a DNA preparation were loaded per column, and 15 minute fractions of approximately 10ml were collected by washing with the SP50 buffer. Fractions were measured for OD₂₆₀ and pooled

accordingly. Between each run, the column was washed with a high salt buffer (1M NaCl, 0.01M NaAc, 0.02% NaN₃). The pooled DNA was ethanol-precipitated by the addition of 1/10 volume of 3M NaAcetate and two volumes of absolute ethanol. After leaving this solution overnight at -20°C, the precipitate was collected in siliconized glass tubes by centrifugation, dried, and dissolved in 0.1xSSC (15mM sodium chloride - 1.5mM sodium citrate; that is, 1/10 concentration of a standard saline-citrate solution) at concentrations appropriate for hybridization experiments.

Preparation of in vivo Markers

1. *Isolation of ³⁵S-labelled Immunoglobulins:* Cell suspensions of 104E and H2020 tumors were made at a concentration of 2 x 10⁶ live cells per ml in DE - Methionine medium containing 1% dialyzed FCS. One ml of each suspension was plated and incubated 30 minutes at 37°C.

Approximately 400 µCi of [³⁵S]-methionine (obtained from the Radiochemical Center, Amersham, with a specific activity of 338 Ci/mmol) were added. After incubation at 37°C for 4 hours, the cells were spun down and the supernatant was collected. Incorporation of the [³⁵S]-methionine into acid-insoluble material of the cell supernatant was measured by TCA-precipitation: a 20 µl aliquot of each supernatant was taken into 1 ml H₂O and 0.5 mgm of bovine serum albumin was added as a carrier. Trichloroacetic acid was added to 5% and the solution was heated at 80°C for 20 minutes. After quick-cooling in ice, it was filtered through Whatman GF/A paper (2.4cm circles). The filter paper was washed three times with cold 50% TCA, dried at 100°C, and counted in Toluene/Triton x 100/PPO/POPOP Scintillation fluid in a Packard Liquid Scintillation Spectrometer (Model 3375).

³⁵S-labelled immunoglobulins were isolated from the total proteins secreted into the medium by sucrose gradient centrifugation of the cell supernatant. Exponential 10–28% sucrose gradients (12 ml each) were prepared in DAMON/IEC polyallomer tubes (#2841) which had been cut to fit the Spinco SW41 rotor. Stock solutions consisted of 10% and 40% sucrose in 10X PBS (phosphate-buffered saline, GIBCO). One ml of cell supernatant was layered on each gradient and centrifugation was carried out at 41,000 rpm for 20 hours in the Beckman Spinco 12 65B at 4°C. Gradients were collected (0.4 ml per fraction) and OD₂₆₀ scanned continuously, as described above. The radioactivity of each fraction was measured by TCA-precipitation. The peak fractions were pooled and dialyzed against 0.2M Tris-HCl pH8.2.

2. *Separation of Light and Heavy Chains*: Procedures used were modifications of those previously described (Eisen *et al.*, 1968). Immunoglobulin preparations were reduced by the addition of 100 µg/ml dithiothreitol per ml in the presence of 5.5M Guanidine-HCl (Schwarz-Mann, ultrapure), followed by incubation at 37°C for 90 minutes. Alkylation was carried out by the addition to 0.02M of iodoacetic acid (Fluka, recrystallised twice from chloroform). After incubation for one hour at room temperature, the solution was passed through a G-200 Sephadex column equilibrated with 5M Guanidine-HCl in 0.1M Acetic acid. Fractions of 1.8 to 2 ml were collected and the radioactivity of each was measured directly by counting an aliquot in Toluene/PPO/POPOP scintillation fluid. Appropriate fractions were pooled, dialyzed extensively against 1% NH₄HCO₃, concentrated by lyophilization, and kept at -70°C.

Isolation and Purification of Heavy Chain mRNA.

1. *Preparation of Membrane-Bound Polysomes (MBP)*: Tumor-bearing mice (usually 70 to 80 at a time) were sacrificed when the size of the tumor reached approximately 1cm in diameter. This usually required 12 to 14 days after injection for both 104E and H2020. The whole tumors were taken immediately into ice-cold DE medium containing 100 µgm/ml cycloheximide (Calbiochem B grade). All operations hereafter were carried out below 4°C. In this medium, the tumors were dissected into several pieces each, with fatty material, connective tissues, and necrosis being carefully cut away. The 'clean' pieces of tumor were then transferred to a mixture consisting of one part RLS-100 and one part Buffer B, plus 100 µgm/ml cycloheximide (approximately 8 grams of tumor material per 35ml mixture), and homogenized 12 strokes in the Teflon-glass tissue grinder. Unbroken cells, nuclei, and large membrane fragments were removed by centrifuging the homogenate at 6000rpm for 10 minutes in the Sorvall RC 2-B. The supernatant was then subjected to higher centrifugation (20,000rpm, 10 minutes, Sorvall) to sediment the remaining membrane fragments which contain the bound polysomes. The pellet obtained in this step was gently resuspended in a mixture composed of one part RLS-100, one part TKM buffer (20mM Tris-HCl pH7.5, 100mM KCl, 5mM MgCl₂) plus 100 µgm/ml cycloheximide (10ml of this mixture being used per 8 grams of starting tumor material). Nonidet P-40 (Bender and Hobein Co.) was added to this suspension to a final concentration of 1.2% (v/v), in order to release the MBP into the solution. After clearing by low speed centrifugation, the MBP solution was layered on a cushion of 1.8M sucrose in TKM (approximately 33ml of

MBP per 7ml cushion in Damon/IEC polyallomer tubes #2847), and centrifuged at 26,000rpm for 20—24 hours at 4°C in a Spinco SW27 rotor. Under these conditions, the released MBP sedimented through the sucrose and formed a translucent pellet, which was then gently dissolved in ice-cold water (5—7ml per pellet) and cleared by centrifuging 10,000rpm for 10 minutes in the Sorvall. OD₂₆₀ was measured and the preparation was stored at -70°C until further use.

2. *Analysis of MBP*: Prior to use, an aliquot of each preparation was subjected to sucrose gradient centrifugation, in order to check the quality of the MBP. Exponential sucrose gradients (5 ml each) were prepared in Beckman cellulose nitrate tubes (#305050), using TKM buffer and 1.5M sucrose in TKM as stock solutions. Three OD₂₆₀ units of each MBP preparation, diluted to 0.2ml with TKM, were loaded per gradient, and centrifugation was carried out at 50,000rpm in the SW 50.1 rotor of a Beckman Spinco 12-65B for 20 minutes at 4°C with no brake. Gradients were collected from the bottom of the tubes and OD₂₆₀ was monitored continuously, as previously described.

3. *Extraction of RNA from MBP*: Frozen MBP, at a concentration of 30—50 OD₂₆₀ units/ml, were thawed carefully at 4°C. Lithium dodecyl sulphate (LDS) was added to 0.2% and proteinase K (chromatographically pure) to 200 µg/ml. After incubation at 0°C for 10 minutes, the LDS concentration was raised to 1.0%, and the resulting solution was made 100mM in Tris-HCL pH9.0 and 2mM in Na₂EDTA. An equal volume of a phenol:cresol:water mixture (100:14:40) was added, and the resulting mixture was shaken at 4°C for 30 minutes. The phases were separated by centrifuging at 10,000rpm for 10 minutes in the Sorvall. The upper

aqueous phase was removed and kept at 4°C, while the cloudy-white inter-phase was collected, suspended in 20ml of a buffer consisting of 100mM Tris HCl pH9.0 and 2mM Na₂EDTA, and reextracted by shaking for 15 minutes at 4°C with 20ml of a chloroform:isoamylalcohol mixture (25:1). Again the phases were separated by centrifugation. The aqueous phase so obtained was combined with the first, and the phenol:cresol:water extraction was repeated 2 times more. The final aqueous phase was made up to 0.5M in sodium acetate pH5, 2 volumes of absolute ethanol were added, and this solution was kept at -20°C overnight. The resulting RNA precipitate was collected by centrifugation (30 minutes at 1200rpm in the IEC PR6 centrifuge), dried under vacuum, and dissolved in a minimal volume of TE-II buffer (10mM Tris-HCl pH7.5, 0.2mM Na₂EDTA). Optical densities at 260 and 280nm were determined with a Beckman DB GT spectrophotometer.

4. *Oligo(dT)-Cellulose Chromatography*: Oligo(dT)-cellulose, at a ratio of 1 gm per 1000 OD₂₆₀ units of membrane-bound polysomal RNA, was packed in a glass jacketed column (diameter 2cm) with water circulating at 25°C, and equilibrated in TEK(0.5) buffer (TE-II plus 0.5M KCl). The extracted RNA was diluted to 100 OD₂₆₀ units per ml in TE-II buffer, heated in an Erlenmeyer flask having a large surface area:volume ratio at 70°C for 5 minutes, and quick-cooled in ice water. KCl was then added to 0.5M, and the resulting solution was warmed to 25°C and loaded on the oligo(dT)-cellulose column with a flow rate of not more than 10ml per hour. After the RNA solution had completely entered the cellulose, the column was sequentially washed with TEK(0.5) buffer, TEK(0.1) buffer (which is TE-II plus 0.1M KCl), and TE-II buffer. The column outflow

was continuously monitored for UV-transmittable material by a LKB UV Absorbtiometer and Recorder and the buffers were changed each time when the percent transmission returned to the base line. During the first 2 washes, 30 minute fractions of 5-10ml per fraction were collected, and during the final TE-II elution, 15 minute fractions of not more than 2ml per fraction were collected. Fractions eluted at each step were pooled, and the OD₂₆₀ and the volume were measured accurately. The TE-II pool was subjected to a second oligo(dT)-cellulose chromatography by repeating exactly the above procedure including the heat treatment. Appropriate fractions were again pooled and the RNA was ethanol-precipitated.

5. *Sucrose Density Gradient Centrifugation:* Exponential 10-28% sucrose gradients (13ml each) were made in Damon/IEC polyallomer tubes (#2841), using stock solutions of 10% and 37.5% sucrose in TLE buffer (5mM Tris-HCl pH7.5, 0.1% LDS, 0.2mM Na₂EDTA). The ethanol precipitates of the oligo(dT)-cellulose columns were collected by centrifugation (20,000rpm for 30 minutes in Spinco SW27 or SW41 rotors), dried, and dissolved in TLE buffer at a maximum concentration of 40 OD₂₆₀ units/ml. This dissolved RNA was then heated at 70°C for 3 minutes, quick-cooled in ice water, and layered on the sucrose gradients (0.5ml/gradient). Centrifugation was at 40,000rpm for 24 hours in an I.E.C. SB283 rotor at 6°C. Fractions of 0.4ml each were collected from the bottom of the tubes with the OD₂₆₀ being monitored continuously. Those fractions which were thought to contain heavy chain mRNA were made up to 0.5ml with the 37.5% sucrose in TLE, measured more accurately for OD₂₆₀ in the Beckman DB GT Spectrophotometer, and ethanol precipitated. The

precipitates were collected by centrifugation, dried, and dissolved in 0.01M Tris-HCl pH7.5 at a concentration of 2500D₂₆₀ units/ml (equivalent to 1 µgm RNA/ml).

6. *Polyacrylamide Gel Electrophoresis*: RNA samples in 0.01M Tris or in water were subjected to polyacrylamide gel electrophoresis in the presence of formamide, according to the following procedure (which contains only minor modifications of the one described by Berns *et al.*, 1974). Merck analytical grade formamide was deionized by stirring overnight with 10% Biorad mixed bed ion exchange resin. After removal of the resin by filtration, Na₂HPO₄ and NaH₂PO₄ were added to 0.01M each, and the pH was adjusted to 6.5 with 100% acetic acid. 3.5% polyacrylamide gels (0.6 x 8 cm) were polymerized in plexiglass tubes, using a solution of 3.5% acrylamide, 0.175% bis-acrylamide, 0.2% (v/v) TEMED, (N,N,N',N'-Tetramethylethylene diamine, Fluka) and 0.1% ammonium persulphate prepared in water. (Acrylamide and bis-acrylamide, obtained from Fluka, were recrystallized before use.) After polymerization was complete, the gels were blown out from the tubes into phosphate-buffered formamide solution (approximately 200ml per 10 gels) in a shallow glass container; and shaken gently at room temperature for 5-7 days with the formamide solution being changed every 24 hours during this time. By the end of this equilibration in formamide, the gels had elongated considerably. They were then cut back to the original length of 8cm, sucked back into the plexiglass tubes, and pre-electrophoresed at 15 volts per cm for 1/2 hour.

A maximum of 10 µgm of RNA was first made up to 10 µl in Tris or H₂O and then adjusted to 80% in formamide by adding 4 volumes of sample

buffer (phosphate-buffered formamide containing 15% sucrose and 0.01% Bromophenol Blue). The final volume of 50 μ l was applied per gel. Electrophoresis was carried out at 5 volts/cm until the samples had completely entered the gels (approximately 30 minutes) followed by 15 volts/cm for 20 hours. Buffer was circulated from the bottom to the top chambers during the electrophoresis, and the bottom chamber was cooled with tap water (approximately 16°C). After the electrophoresis, the gels were scanned at 260nm in a Gilford 2500 Spectrophotometer adapted with a 2410-S linear transport device. When the electrophoresis was performed for analytical purposes, the gels were then stained overnight with a 0.005% solution of "Stain-All" (Eastman Kodak Co.) in 50% formamide. Destaining was by tap water, out of direct light. Alternatively, when the electrophoresis was performed as a preparative step in the purification procedure, a 1-2mm slice was cut out of the heavy chain mRNA-containing band immediately after scanning. The band position could be located very precisely in the following way. First, its approximate position in the gel was estimated from the peak on the optical density scan. A small amount of 1% Bromophenol blue solution was then injected transversely into the gel at either side of the estimated band center, not more than 5mm apart, using a fine gauge syringe needle. When the gel was rescanned at 260nm, the injected BPB produced two sharp absorption lines. The relation of these lines to the center of the peak on the recording paper was used to locate precisely the center of the band between the two thin blue lines formed by the BPB in the gel. The appropriate gel slice was then cut out accordingly.

7. *Elution of RNA from Gels*: The gel slices obtained in the above steps were homogenized in a buffer consisting of 2ml of 0.5M NaAcetate pH6.0, 1 drop of 2M Tris-HCl pH9.0, and a few drops of phenol, using a loose-fitting glass tissue grinder. All the glassware used throughout the elution procedure was well siliconized. The crushed gel was incubated at 37°C for 20 minutes, vortexed 10 seconds, frozen quickly in a dry ice-methanol bath, and thawed quickly at 37°C. After this incubating-vortexing-freezing-thawing procedure was repeated 2 more times, the suspension of crushed gel was centrifuged 3000rpm for 5 minutes in the I.E.C. PR-6, and the supernatant was saved. The gel was then subjected to three more rounds of extraction, using one ml of buffer mix. The resulting supernatant was combined with the first and, after the addition of 2 volumes of ethanol, was kept at -20°C for at least 24 hours.

8. *Hydroxyapatite-Chromatography of the Gel Eluant*: In the above procedure, linear polyacrylate also elutes from the gel and coprecipitates with the RNA at the addition of ethanol. It was removed as follows by taking advantage of the fact that RNA binds nonspecifically to hydroxyapatite under low salt conditions. A small hydroxyapatite column (approximately 1.5 x 0.5 cm) was prepared using Hypatite C from Clarkson Chemical Co., and was washed with NP(0.05) (0.025M Na₂HPO₄, 0.025M NaH₂PO₄). The precipitate of the formamide gel eluant was collected by centrifugation, dried, dissolved in 0.5ml of NP(0.05), and loaded on the column at a flow rate of not more than one ml per 10 minutes. The column was washed extensively with NP(0.05) to remove all unbound material, with the outflow being monitored for optical density at 207nm

(the maximum absorption of acrylamide). When OD could no longer be detected, the RNA was eluted with NP(0.4) (0.2M Na₂HPO₄, 0.2M NaH₂PO₄) in as small a volume as possible, monitoring the OD at 260nm. The eluted RNA was then dialyzed against H₂O, concentrated by lyophilization, ethanol-precipitated, and redissolved in 20 µl of water.

Characterization of Heavy Chain mRNA

1. *In vitro Translation*: Translation of the heavy chain mRNA preparations was carried out in the mammalian cell-free system of Schreier and Stachlin (1973) with separated initiation factors being substituted for the partially purified preparation originally described. Purified globin mRNA was translated in parallel with the 104E and H2020 samples to be tested. Labelling of the translation products was by [³⁵S]-Methionine.

At the completion of translation, incorporation of ³⁵S into the TCA-precipitable material was determined for a 5 µl aliquot of the reaction mixture. The remainder of the cell-free products were precipitated with 1ml of 10% TCA and left overnight at 4°C. The precipitates were collected by centrifugation and washed one time with cold 5% TCA and three times with cold acetone (by vortexing and centrifuging). The final precipitate was dried and dissolved in a minimal volume of 1% NH₄HCO₃.

2. *SDS - Polyacrylamide Gel Electrophoresis*: The procedure was based on that of Laemmli (1970). Stock solutions were prepared as follows: Solution A, 30 gm acrylamide plus 0.8 gm bis-acrylamide made up to 100 ml with water, filtered through 50 Whatmann, and stored cold and dark; Solution B, 18.15 gm Tris (Trizma base, Sigma) plus 50 ml

water, pH adjusted to 8.8 with 1M HCl, volume adjusted to 100 ml with water; Solution C, 10% sodium dodecyl sulphate (SDS) in water; Solution D, 6 gm Tris plus 40 ml water, pH adjusted to 6.8 with 1M HCl, volume adjusted to 100 ml with water. A 13%-acrylamide solution (containing 0.35% bis-acrylamide, 2.25% Tris, and 0.1% SDS) was then prepared using appropriate volumes of Solutions A, B and C. After the addition of 0.025% (v/v) Temed, and 0.30% APS (ammonium persulphate, Fluka), this solution was polymerized in a glass form to give a slab gel approximately 14 cm long and 2 mm thick. This was overlaid with a 4%-acrylamide spacer gel, having a lower pH and containing 0.11% bis-acrylamide, 1.5% Tris and 0.1% SDS from the appropriate additions of Solutions A, D, and C, plus 0.05% (v/v) Temed and 0.1% APS. Slits for the application of samples were made by inserting a plexiglass form before polymerization of the spacer gel was complete in such a way that the samples would migrate through approximately 2cm of spacer gel before entering the 13% gel.

A portion of each washed cell-free product containing the desired number of cpm's, as well as portions of the *in vivo* markers (see above for preparation), were lyophilized to dryness and redissolved in 50 μ l of sample buffer (0.6% Tris-HCl, pH 6.8, 1.0% SDS, 1.0% [v/v] β -Mercaptoethanol, 10% [v/v] Glycerol, and 0.005% Bromophenol Blue). The samples were then heated at 100°C for 3 minutes to prevent aggregation, and applied to the gel. Electrophoresis was carried out in a Tris:glycine:SDS buffer (0.6%:2.88%:0.1%) at 120 volts for 12 to 14 hours. The gel was then removed from the form, dried under vacuum with the help of an infrared lamp, and autoradiographed using Kodak X-ray film.

3. *Two-Dimensional High Voltage Electrophoresis*: Tryptic digests of cell-free products and *in vivo* markers were prepared and analyzed by high voltage electrophoresis, according to the following procedure. Since immunoglobulin chains are resistant to tryptic digestion unless their intrachain disulphide bridges are broken, the cell-free products were first reduced and alkylated by the procedure described previously for the *in vivo* immunoglobulin preparations, and dialyzed against 1% NH_4HCO_3 . A portion containing the desired number of cpm's from each reduced cell-free product and heavy chain *in vivo* preparation was then made up to 2mgm in protein by adding bovine serum albumin. Tryptic digestion was carried out by adding 20 μgm of trypsin per 2mgm of total protein and incubating 4 hours at 37°C. After lyophilization, the resulting tryptic digests were dissolved in 75 μl of pH6.5 buffer (10% pyridine, 0.4% acetic acid), and applied in 2cm lines to the center of Whatmann 3MM paper. Electrophoresis was carried out in the same buffer at 300 volts for 47 or 60 minutes, in the Gilson Model DW high voltage electrophoreter. Autoradiography was performed to locate the positions of the peptides on the paper. The peptides were then cut apart as desired, sewed on to a new paper, and run in the perpendicular direction in pH3.5 buffer (1% pyridine, 10% acetic acid), again at 3000 volts for 47 or 60 minutes.

Preparation of ^{125}I -labelled RNA

Iodination was carried out according to Commerford (1971). I^{125} was obtained from the Eidg. Institut für Reaktorforschung (Würlingen, Switzerland) in portions of 5mCi in 10 μl . The pH was adjusted to 5.0

by adding 10^{-2} mmoles of NH_4 Acetate pH5.0 and 10^{-7} mmoles of HCl; then the volume was made up to 50 μl with H_2O . A 100 μl reaction mixture, containing the RNA sample to be iodinated, plus the desired number of mCi of ^{125}I from the above solution, plus ammonium acetate pH5.0, potassium iodide, and thallium chloride in final concentrations of 100mM, 1×10^{-2} mM and 1mM respectively, was assembled in ice, with the thallium chloride being added last. This reaction mixture was incubated at 60°C for 40 minutes, during which time binding of the iodine to the RNA occurs in conjunction with the reduction of Tl^{+3} . The reaction mixture was then chilled in ice, and excess Tl^{+3} was reduced by adding 10^{-2} mmoles Tris-HCl pH9.0, 10^{-3} mmoles Na_2SO_3 and 10^{-4} mmoles Na_2EDTA and reincubating at 60°C for 18 minutes.

Immediately following this incubation, unbound iodine was removed by passing the reaction mixture through a small HAP column, according to the method already described, with the NP(0.05) wash and the NP(0.4) eluant being monitored for radioactivity rather than for optical density. This was done by counting a 5 μl aliquot of each collected fraction directly in a Nuclear-Chicago Autogamma Scintillation Spectrometer (efficiency of ^{125}I = 80%). NP(0.4) fractions were pooled according to the counts, dialyzed extensively against H_2O after the addition of 50 $\mu\text{g}/\text{ml}$ carrier RNA (purified yeast tRNA or *E. coli* rRNA), and ethanol precipitated. The precipitates were collected and run on 10--28% sucrose gradients in TLE, according to the method described above. Gradient fractions of approximately 0.4ml each were collected manually from the bottom of the tubes, and ^{125}I activity was measured in the Nuclear Chicago. Appropriate fractions were ethanol precipitated, again

after the addition of 50 $\mu\text{g}/\text{ml}$ carrier. The precipitated material was collected, counted, and dissolved in 0.1xSSC at the concentration desired for use in hybridization experiments.

DNA-RNA Hybridization

Experiments were performed in order to determine the final level and/or the kinetics of hybridization between various combinations of DNA's and RNA's. In general, the procedure described by Tonegawa *et al.* (1974) was followed:

Hybridization was carried out at 70° in 2xSSC at a final concentration of 0.22, 2.2, or 22 mg of DNA per ml. DNA in 0.1xSSC was denatured by heating at 100° for 5 min. in siliconized conical tubes under mineral oil. [¹²⁵I]RNA in 0.1xSSC was added and the heating was continued for another 2 min. An aliquot was withdrawn for determination of the "intrinsic RNase-resistant fraction." The tube was then transferred to a 70° water bath. After 30 sec, one-ninth volume of preheated 20xSSC was added and quickly mixed; this was taken as time 0. At intervals, 50- to 200- μl samples were withdrawn and quickly mixed with 10-20 ml of precooled 2xSSC. The diluted hybridization mixture was divided into four equal parts. In two parts, the nucleic acid was directly precipitated with one-fifth volume of 50% trichloroacetic acid. When the DNA concentration for annealing was 0.22 or 2.2 mg/ml, 500 μg of yeast RNA (Worthington) was added as precipitation carrier. The other two parts were treated with 20 $\mu\text{g}/\text{ml}$ of bovine pancreatic RNase and 2 units/ml of T-1 RNase at 37° for 20 min. (Both nucleases had been preheated at 80° for 10 min in 2xSSC at pH 5.0 in order to inactivate contaminating DNase.) The RNase-treated samples were chilled in ice (carrier added if necessary), and precipitated with one-fifth volume of 50% trichloroacetic acid.

Minor modifications of this procedure in the work to be described were as follows: DNA concentrations sometimes varied by 1-10% from those given above; in some experiments which studied only the final level, and not the kinetics, of hybridization, the intrinsic RNase-resistant fraction was not determined; some hybridizations were carried out with 6xSSC at 75°C as well as with 2xSSC at 70°C.

The precipitated nucleic acid from each sample was collected by filtration on Whatman GFA paper (2.4cm circles) and washed 3 times with cold 5% TCA and once with 98% ethanol. The filter papers were then dried at 100°C and counted for ^{125}I activity in the Nuclear-Chicago. The fraction hybridized at each time point was determined by the ratio of the radioactivity in the RNase-treated samples to the radioactivity in the untreated samples. For the C_{ot} curves, the values so obtained were corrected by subtraction of the intrinsic RNase-resistant fraction.

RESULTS

Immunofluorescence

For the myeloma lines H2020, J558, 104E, Y5781, and S28, no discrepancies were found between the designated immunoglobulin class and the immunofluorescent staining pattern. Data concerning the proportions of cells stained by each fluorescently-labelled antiserum, as well as an estimate of the intensity of staining, are given in Table 2. Photographs of each cell suspension, stained with the antiserum specific for its heavy chain class, are shown in Plate 1.

The IgG_{2b}-producing myeloma, MPC11, showed an unexpected staining pattern with anti- γ_{2b} : only one positive cell was found out of more than 1000 cells scored. This likely represents the arisal in our myeloma line of variant cells which are incapable of producing γ heavy chains; such instances have been reported previously for other MPC11 cell lines (Scharff *et al.*, 1975). The failure of an attempt to isolate γ mRNA from our cell line (my own unpublished results) indicates that, in this case at least, the presence of such variant cells is the result of events at the transcriptional or the gene level, rather than at the translational level.

In all cases, a control staining made with an unrelated antiserum (anti- γ_1 in the case of the IgM myelomas and anti- μ in all other cases) was found to be completely negative.

DNA Preparation

It was found that a convenient amount of starting material for the preparation of DNA was approximately 200 tumors or 300 livers, from which 10-20ml of purified nuclei were usually obtained, yielding a

TABLE 2. Immunofluorescent Staining Patterns of Mouse Myelomas

| Myeloma | Specific anti-serum | Proportion of stained cells | Intensity of staining |
|---------|---------------------|-----------------------------|--|
| 104E | anti- μ | 75% | ranged from bright to faint |
| Y5781 | anti- μ | 15—20% 75—80% | bright ranged from faint to almost negligible |
| S28 | anti- γ_1 | 50% | moderately bright |
| J558 | anti- α | 90% | bright |
| H2020 | anti- α | 90% | moderately bright |

Plate 1. Intracellular immunofluorescent staining pattern of mouse myeloma lines.

Antisera used: H2020 and J558, anti- α ; S28, anti- γ_1 ; 104E and Y5781, anti- μ .



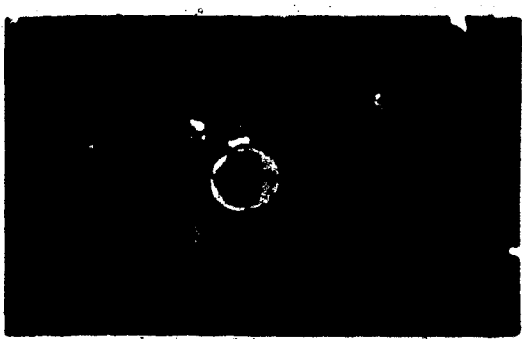
H2020



J558



S28



104E



Y5781

final amount of 75—150mgm DNA. Therefore, those types of DNA required in large quantities were prepared on separate occasions. Since the results obtained at each step of the procedure were entirely comparable on each occasion and for each DNA type, the final results only are summarized in Table 3. Detailed results of the size determination and the SP50 column fractionation are given below for one preparation as an example.

The OD₂₆₀ scan of the sucrose density gradient centrifugation of a 104E sonicated DNA preparation is shown in Figure 1, in comparison with that of ribosomal and transfer RNA. The distances of migration of the two RNA components of known S values (distance A for the 4S tRNA and distance B for the 18S rRNA) were correlated to the average distance of migration of the DNA in the parallel gradient, as shown in Figure 1. In this way, the S value of the DNA peak was determined to be 8.5. According to the formula of Studier (1965), $S = 0.0882 M^{0.36}$, the average single-stranded molecular weight of the sonicated DNA was therefore calculated to be 1.6×10^5 (equivalent to 500 nucleotides per strand, assuming an average molecular weight per nucleotide of 320). The elution profile from an SP-50 column of this same 104E preparation is shown in Figure 2. More than 90% of the OD₂₆₀-absorbing material was eluted in one peak, representing the sonicated DNA. The tail of this peak probably contains DNA fragments which are considerably smaller than the average size. By pooling fractions as indicated, such DNA fragments, plus the small amount of OD-absorbing material eluted after extensive washing of the column (probably digested RNA fragments), were excluded from the DNA used for hybridization experiments. Furthermore,

TABLE 3. Summarized Results of the Preparation of DNA for Use in Hybridization Experiments

| DNA # | Isolation of Nuclei and Extraction of DNA | | | Sonication and Size Determination | | Final amount of purified DNA obtained after gel filtration (mgm) |
|----------|---|--|--------------------------------------|-----------------------------------|---|--|
| | Amount of nuclei (ml) | Total OD ₂₆₀ units after extraction | OD ₂₆₀ /OD ₂₈₀ | S value of extracted DNA | Corresponding single-stranded molecular weight ($\times 10^{-5}$) | |
| Liver #1 | 20 | 3540 | 1.86 | 7.5 | 1.15 | 153 |
| Liver #2 | 20 | 3850 | 1.88 | 7.5 | 1.15 | 169 |
| 104E #1 | 10 | 1780 | 1.82 ₀ | 8.5 | 1.60 | 67 |
| 104E #2 | 20 | 4590 | 1.89 | 8.7 | 1.70 | 183 |
| H2020 #1 | 10 | 1840 | 1.73 | 8.9 | 1.85 | 63 |
| H2020 #2 | 15 | 3990 | 1.84 | 8.5 | 1.60 | 162 |
| J558 | 15 | 2360 | 1.89 | 7.8 | 1.25 | 102 |
| Y5781 | 15 | 2880 | 1.84 | 8.3 | 1.50 | 138 |
| MPC 11 | 15 | 3760 | 1.87 | 8.4 | 1.55 | 146 |
| S28 | 15 | 3680 | 1.88 | 8.3 | 1.50 | 132 |

#1 and #2 refer to preparations of the same type of DNA made on different occasions.

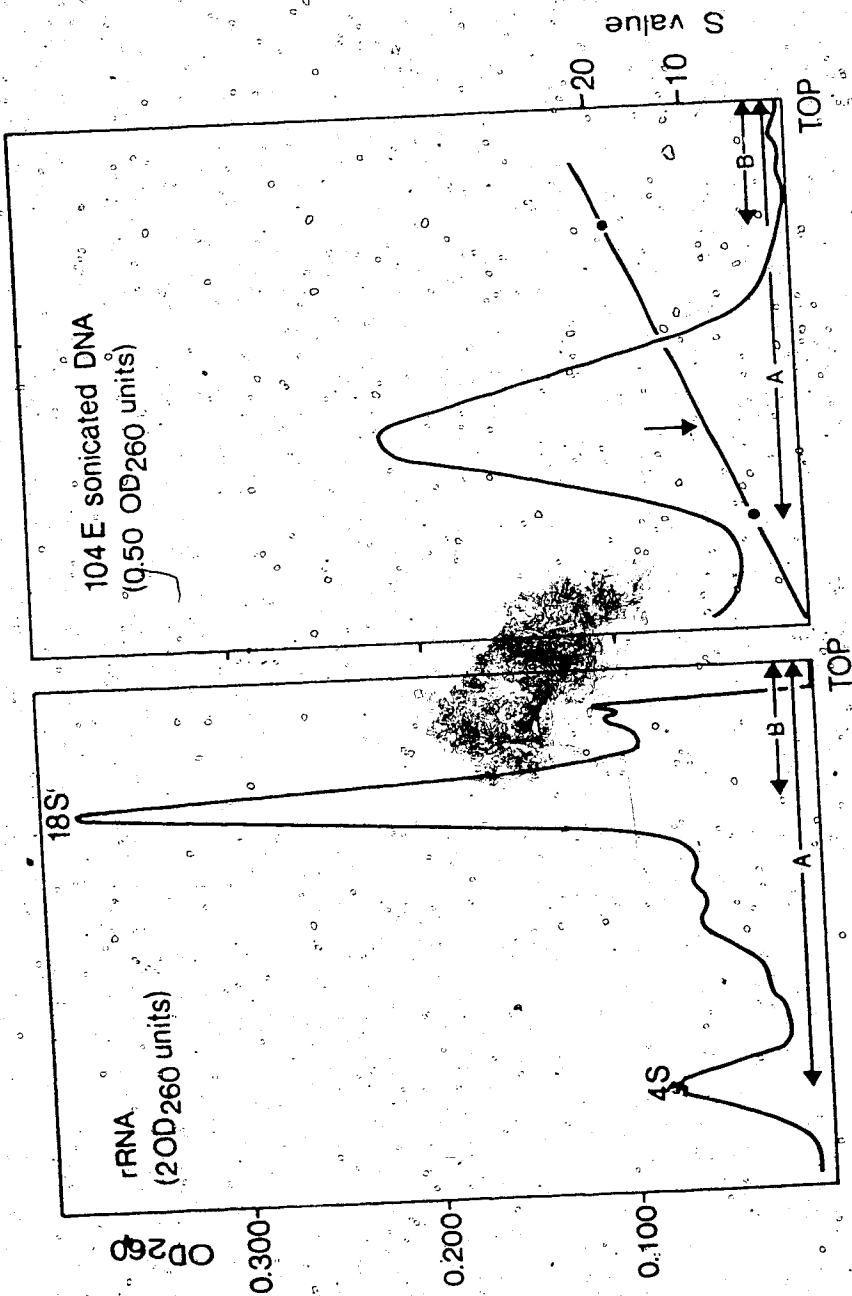


Figure 1. Size determination of a sonicated DNA preparation by sucrose density gradient centrifugation in comparison with a ribosomal and transfer RNA standard.

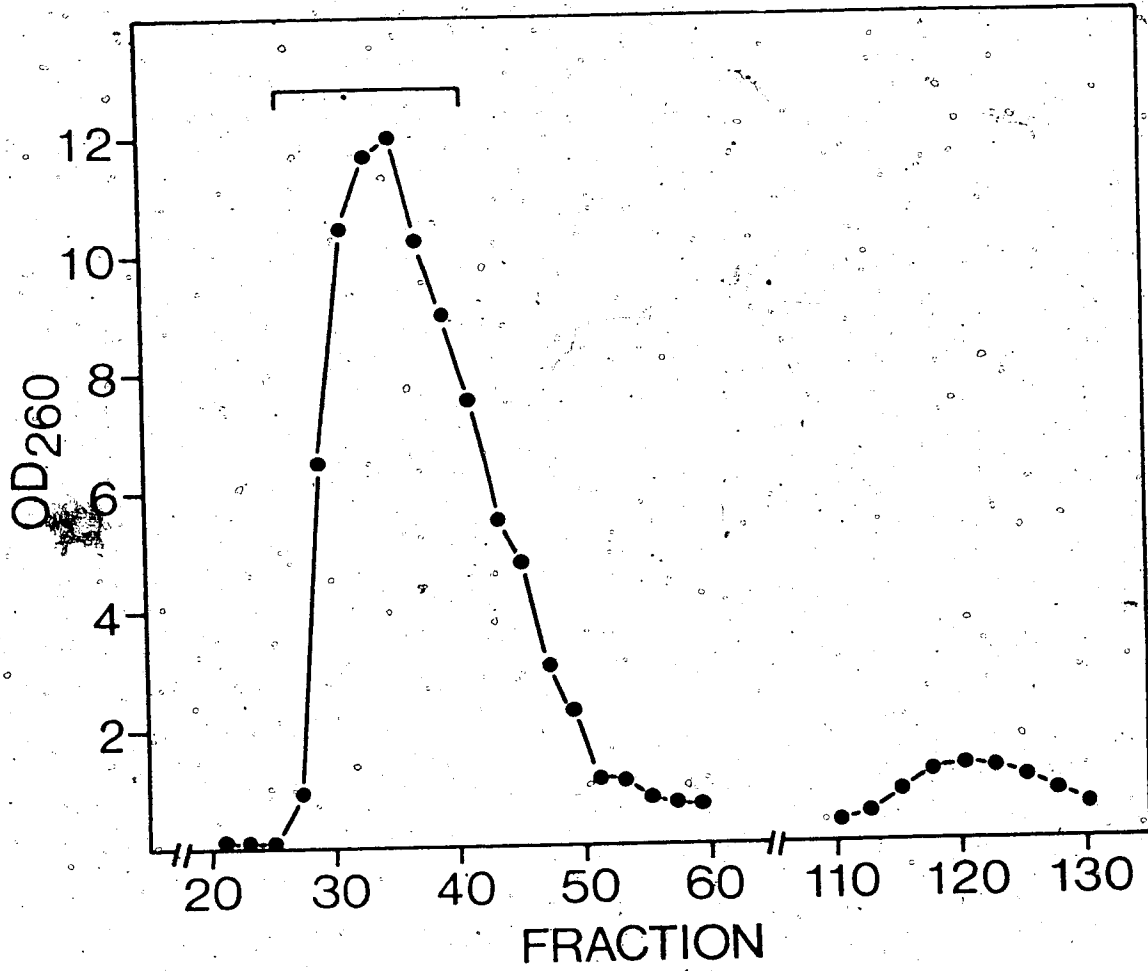


Figure 2. Elution profile of sonicated 104E DNA from an SP-Sephadex C-50 column.

since SP50 is a cation exchanger, the DNA pooled from this column should be free of all heavy metals which might influence the hybridization reaction.

Preparation of Radioactive *in vivo* Markers

104E and H2020 myeloma cells were labelled with [^{35}S]-methionine as described in Materials and Methods. Incorporation of ^{35}S into the acid-insoluble material of the cell supernatant was 6.25×10^7 cpm per ml for H2020 and 2.05×10^7 cpm per ml for 104E. In each cell suspension, approximately 80% live cells were present at the start of the labelling time and 60% at the end. This indicates that the acid-insoluble radioactivity has actually been secreted into the medium, and not merely released by the lysis of dead cells.

The labelled immunoglobulins were then isolated from the total secreted proteins by fractionation of the cell supernatants on sucrose gradients. The OD_{260} scans and the TCA-precipitable counts of the peak fractions are given in Figure 3. Fractions 5-7 were pooled from the 104E gradient as [^{35}S]-IgM (1.8×10^6 cpm) and fractions 17 and 18 from the H2020 gradient as [^{35}S]-IgA (2.3×10^7 cpm).

From each of these pools, approximately 10% was saved as complete *in vivo* IgM or IgA for future use. Pure heavy chain markers were prepared from the remaining 90% by reduction and alkylation of the disulphide bridges, followed by G200 Sephadex column chromatography under acidic conditions. Clean separation of the heavy and light chains was achieved in each case, as shown by the elution profiles in Figure 4. Fractions were pooled as indicated, yielding *in vivo* [^{35}S] μ chain (1.0×10^6 cpm) and *in vivo* [^{35}S] α chain (1.4×10^7 cpm).

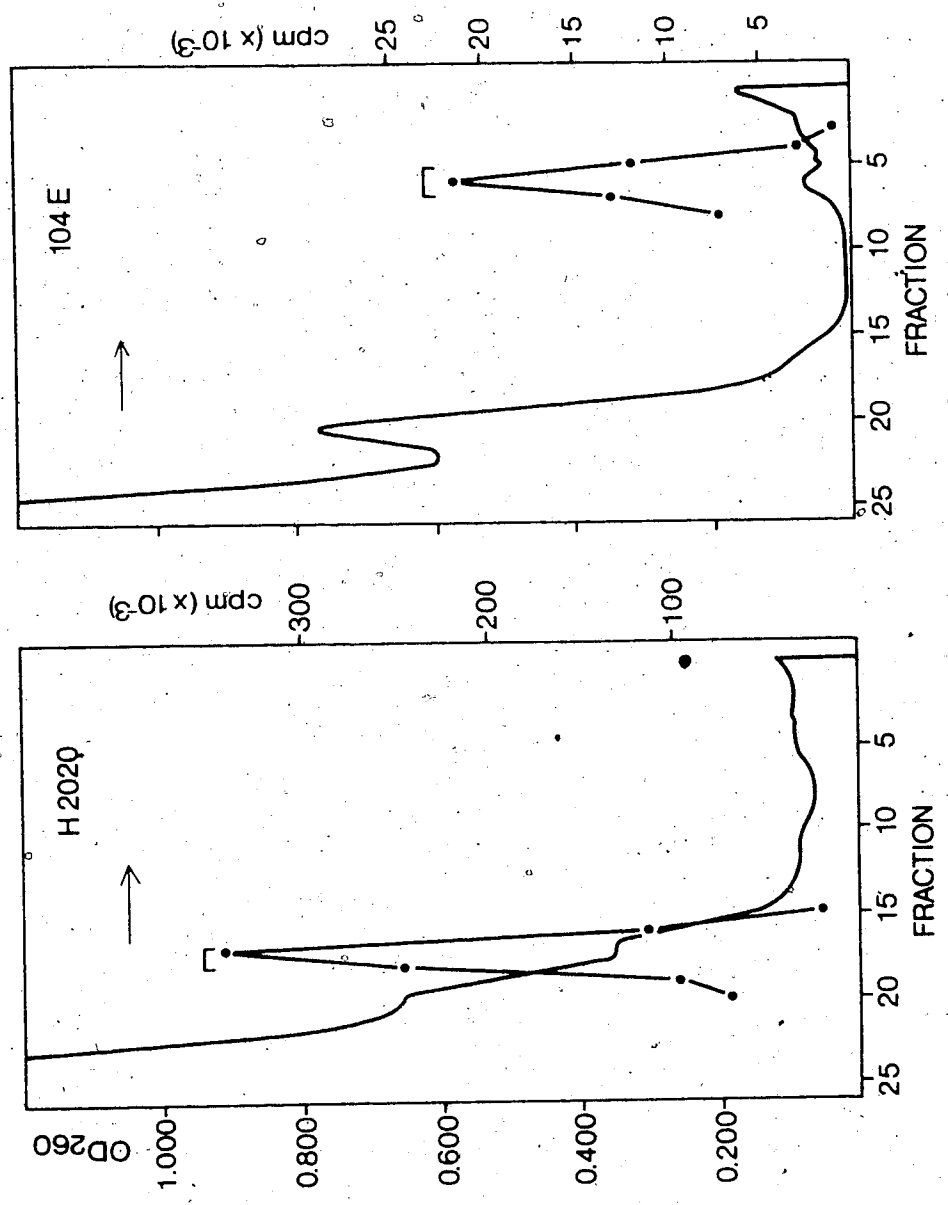


Figure 3. Sucrose density gradient centrifugation of the cell supernatant of [³⁵S]-methionine-labelled myeloma cells. Optical density at 260nm represented by continuous scan, incorporation of ³⁵S into TCA-precipitable material by points.

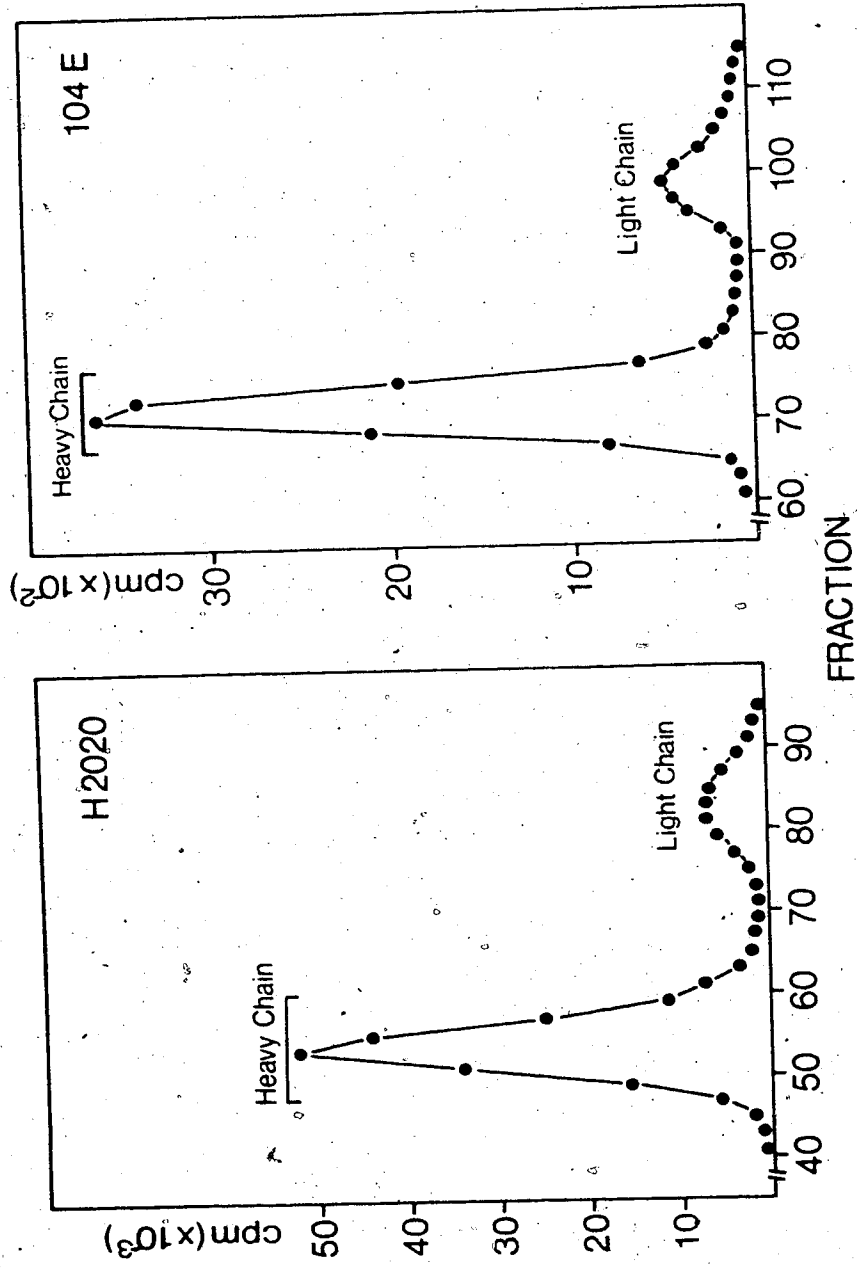


Figure 4. Separation of heavy and light chains of reduced *in vivo* immunoglobulins by chromatography on 6200 Sephadex.

Preparation of Heavy Chain mRNA's

Since it has been shown that the majority of immunoglobulin synthesis occurs on polysomes bound to the endoplasmic reticulum (Sherr and Uhr, 1970; Tonegawa and Baldi, 1973), the first step in the preparation procedure was the isolation of nondegraded membrane-bound polysomes (MBP). Sucrose density gradient centrifugation profiles of such preparations derived from H2020 and 104E myeloma tumors and considered usable for the isolation of mRNA are shown in Figures 5A and 5B, respectively. In comparison is the profile from a preparation considered too degraded for use (Figure 5C). The major factor considered in estimating the quality of the preparation was the relative proportions of material at the light and the heavy ends of the gradient. That is, a gradual decrease in peak heights towards the smaller polysomes, as in Figures 5A and 5B, indicates that degradation is minimal; on the other hand, a relative lack of material at the heavy end of the gradient plus increasing peak heights towards the monosomes, as in Figure 5C, indicates that the majority of polysomes have been degraded. Approximately 200 tumor-bearing mice of each of 104E and H2020 yielded about 3000 OD₂₆₀ units of MBP from which the heavy chain mRNA was isolated in each case.

The phenol extraction of these MBP preparations resulted in 53mgm of H2020 RNA and 80mgm of 104E RNA, assuming that 1 OD₂₆₀ unit is equivalent to 25mgm of RNA, with OD₂₆₀/OD₂₈₀ ratios of 1.81 and 1.85, respectively. These membrane-bound polysomal RNA's were each subjected to two successive chromatographies on oligo(dT)-cellulose. The quantities of RNA obtained by each wash, as well as the recovery and retention values

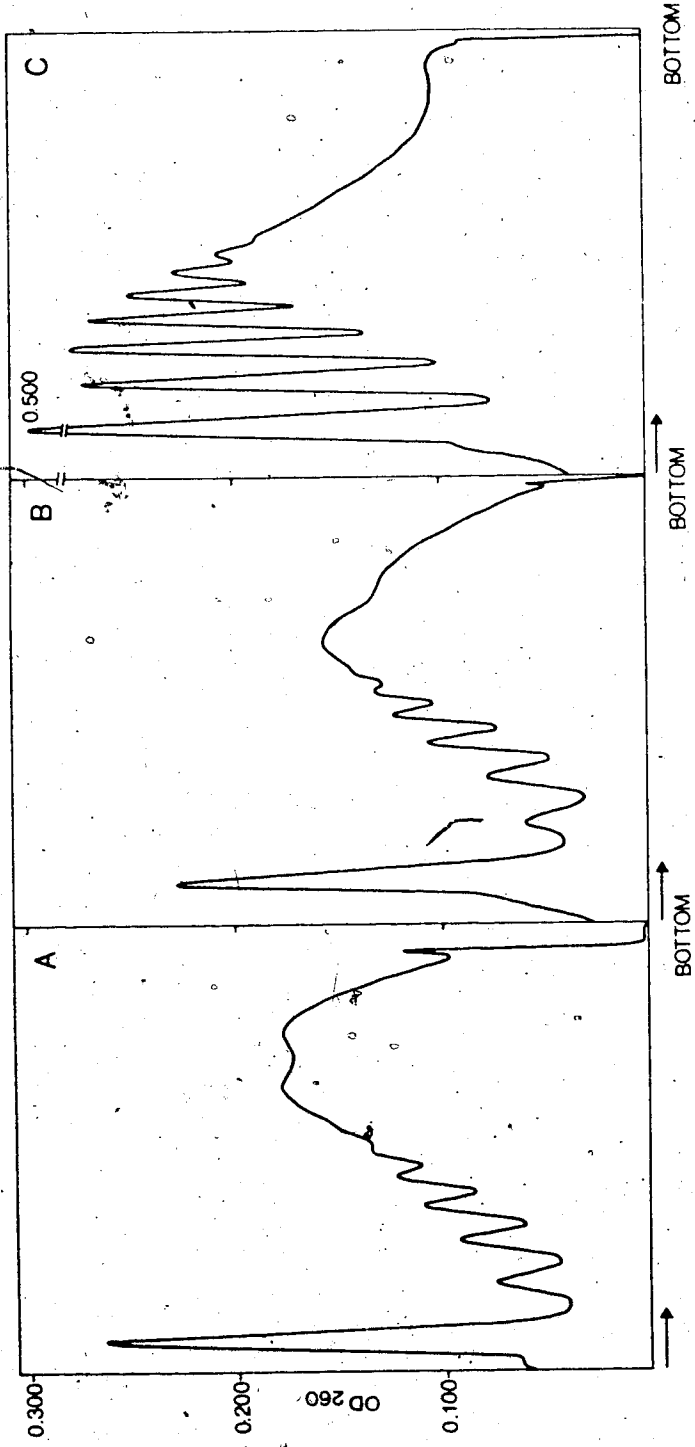


Figure 5. Sucrose density gradient centrifugation of membrane-bound polysome preparations. A, H2020; B, 104E; C, a preparation considered too degraded for use.

of each column, are given in Table 4. The rationale for this step is that most eukaryotic mRNA's contain a sequence of poly(A) at their 3'-end (Lee *et al.*, 1971). This sequence binds to oligo(dT) under high salt conditions and is released in the absence of salt. It has further been shown (Aviv and Leder, 1972) that the large portion of the MBP RNA which does not bind at the high salt concentration (TEK[0.5] buffer) consists mainly of tRNA and the 5S, 18S and 28S rRNA's. The relatively smaller amount of loosely bound material that is eluted with the intermediate salt concentration (TEK[0.1] buffer) consists primarily of 18S and 28S rRNA's. In the present work, the poly(A)-containing fraction that eluted with the TE-II buffer of the first oligo(dT)-cellulose column comprised 2.5% and 2.9% of the input MBP RNA, for H2020 and 104E respectively. However, when these TE-II fractions were subjected to a second oligo(dT) chromatography, they were found to still contain significant amounts of material which did not bind in TEK(0.5) buffer. In fact, although essentially all the input RNA was recovered from each of these second columns, only 41% (H2020) and 31% (104E) were recovered in the TE-II eluant, resulting in a final retention value of approximately 1% in each case. By analysis in sucrose gradients, the major component of this second TEK(0.5) wash was found to be 18S rRNA, as shown by the third OD₂₆₀ scan in Figure 6. In addition, the heat treatment before each chromatography was found to be very critical, as is evident by a comparison of the first two OD₂₆₀ scans in Figure 6: in a trial preparation of H2020 RNA, chromatographed without heat treatment, a significant amount of 18S material was still present in the poly(A)-containing fraction even after the second oligo(dT)-cellulose column. In contrast,

TABLE 4. Oligo(dT)-Cellulose Chromatography of
Membrane Bound Polysomal (MBP) RNA

| H2020 Input | 1st Column 1320 OD ₂₆₀ units of H2020 MBP RNA | | | 2nd Column 33 OD ₂₆₀ units of 1st Column TE-II wash | | |
|--------------------------------------|--|----------|-------|--|----------|-------|
| | TEK(0.5) | TEK(0.1) | TE-II | TEK(0.5) | TEK(0.1) | TE-II |
| Wash buffer | | | | | | |
| Volume of wash (ml) | 45 | 45 | 11.5 | 17 | 10 | 13.3 |
| Total OD ₂₆₀ units eluted | 1170 | 9 | 33 | 17 | 0.5 | 13.6 |
| Column Recovery | | 92% | | | 94% | |
| Column Retention* | | 2.5% | | | 41% | |
| Overall Retention | | | | | | 1.03% |

| 104E Input | 1st Column 2000 OD ₂₆₀ units of 104E MBP RNA | | | 2nd Column 58 OD ₂₆₀ units of 1st Column TE-II eluant | | |
|--------------------------------------|---|----------|-------|--|----------|-------|
| | TEK(0.5) | TEK(0.1) | TE-II | TEK(0.5) | TEK(0.1) | TE-II |
| Wash buffer | | | | | | |
| Volume of wash (ml) | 55 | 30 | 16 | 23.5 | 13 | 21.5 |
| Total OD ₂₆₀ units eluted | 1925 | 12 | 58 | 35.6 | 4 | 18 |
| Column Recovery | | 99.8% | | | 99% | |
| Column Retention | | 2.9% | | | 31% | |
| Overall Retention | | | | | | 0.91% |

*Retention refers to proportion bound at 0.5 and 0.1M salt.

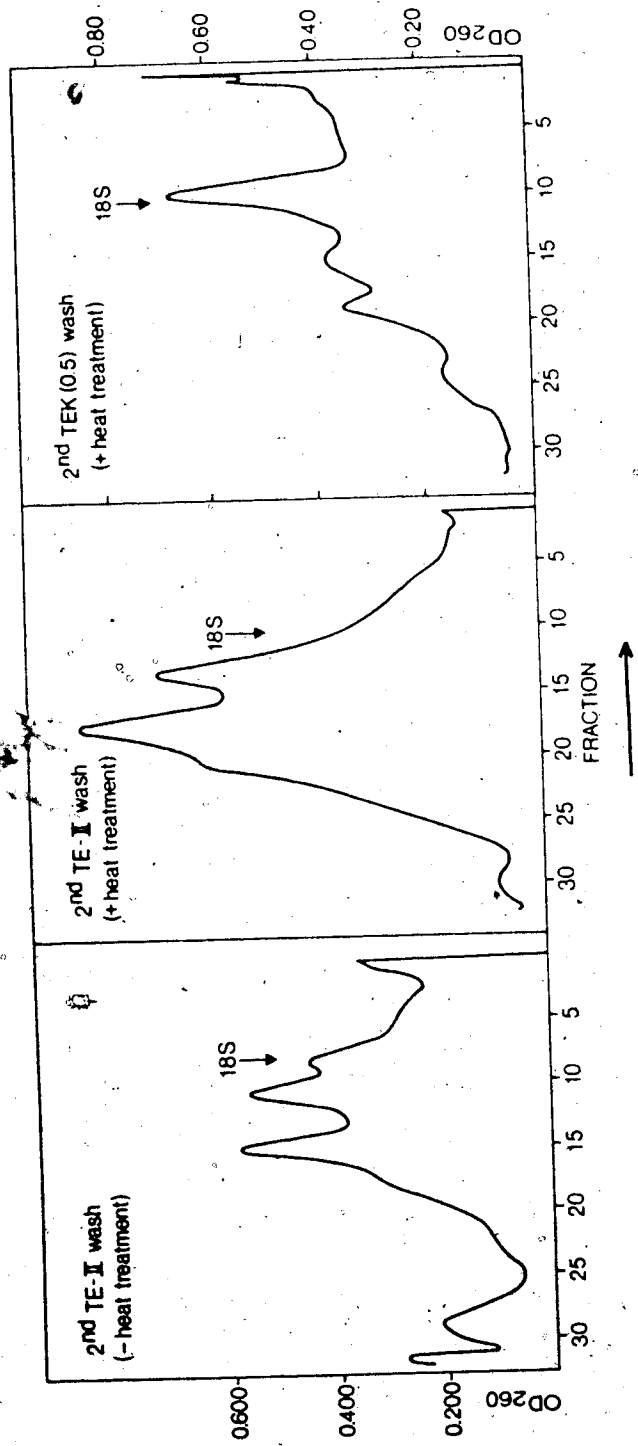


Figure 6. Analytical sucrose density gradient centrifugation of oligo(dT)-cellulose fractions from H2020 membrane-bound polysomal RNA. The 18S position was determined by centrifugation of a ribosomal RNA standard in a parallel gradient.

with heat treatment virtually no 18S material could be detected in the second TE-II eluant.

The poly(A)-containing mRNA's from the second TE-II wash were then fractionated by preparative sucrose density gradient centrifugation. Figure 7 gives the OD₂₆₀ scans of each gradient, as well as manual OD measurements of selected fractions. With both H2020 and 104E, the majority of the RNA sedimented in two clearly distinguishable portions of the gradient. In each case, one major peak was observed at approximately the 13S position, which corresponds to the sedimentation value of light chain mRNA. In the case of H2020, most of the remaining RNA sedimented as a clearly distinguishable, relatively homogeneous peak at approximately 16S. With 104E, the majority of the remaining RNA sedimented rather diffusely in the 17-18S region. The ratio of the amount of material in the heavier portion to the amount in the 13S peak was significantly greater for H2020 than for 104E. The fractions in the 16S region of the H2020 gradient and in the 17-18S region of the 104E gradient which were thought to contain the heavy chain mRNA (indicated by the small arrows in Figure 7) were used for further analysis and purification.

Characterization of Heavy Chain mRNA's

The presumptive heavy chain mRNA fractions, obtained from oligo(dT)-cellulose chromatography and sucrose gradient fractionation, were tested for their ability to stimulate the synthesis of polypeptides *in vitro*. On the basis of the relative sharpness of the sucrose gradient peak, the two H2020 16S RNA fractions were pooled prior to translation. However, since the 17-18S 104E peak was rather indistinct, fractions 9 to 13 were

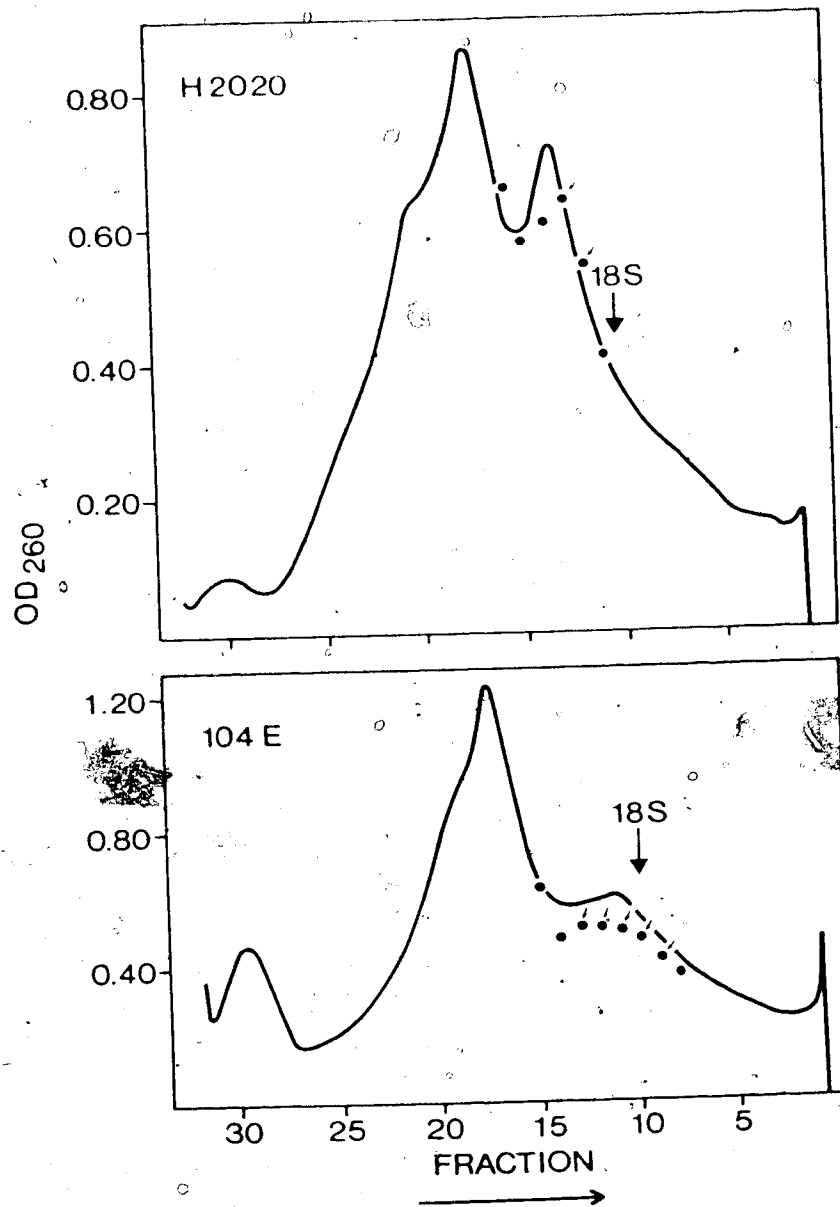


Figure 7. Preparative sucrose density gradient centrifugation of the TE-II fractions obtained by two successive oligo(dT) chromatographies, each preceded by heat treatment. Solid curves represent continuous OD₂₆₀ scans, points represent manual OD₂₆₀ measurements. Arrows indicate those fractions taken for further purification and/or translation. The 18S position was determined by centrifugation of a ribosomal RNA standard in a parallel gradient.

translated separately to determine if any differences could be detected in their cell-free products. Five μgm of the H2020 pool and 3 μgm of each 104E fraction were translated in the cell-free system described in Materials and Methods, along with 1 μgm of globin mRNA as a control. Incorporation of ^{35}S into the TCA-precipitable material in each case is given in Table 5. These figures show that the addition of each RNA fraction to the cell-free system resulted in a significant stimulation of incorporation over that obtained endogenously. No significant differences were evident in the activities of the various 104E fractions. However, each showed approximately 25% less stimulation than the H2020 pool, which in turn gave about 50% of the stimulation obtained with the globin mRNA.

Preliminary analysis of the products synthesized in response to the H2020 16S pool and the 104E 17-18S fractions was performed by electrophoresis in SDS-polyacrylamide slab gels. Autoradiographs of each gel are shown in Plates 2 and 3. From Plate 2, it is evident that the majority of the H2020 cell-free products migrate as a single band, with a mobility very slightly greater than the *in vivo* IgA heavy chain; that is, the majority of the components translated from the H2020 16S sucrose gradient pool are very closely related to authentic α chains. In fact, precise coelectrophoresis was not expected, since the *in vivo* secreted forms of immunoglobulin heavy chains are known to have attached carbohydrate moieties which slow their electrophoretic mobilities in SDS-acrylamide gels; these moieties would not be added in a cell-free translation system (Schubert, 1970). The H2020 cell-free products also formed a number of minor bands, each with a mobility greater than that

TABLE 5. Incorporation of ^{35}S into Acid Insoluble Material, by a Cell-Free Translation System Supplemented with Various RNA Preparations

| Added RNA | Total TCA-precipitable counts per minute | |
|----------------------|--|---------------------------------|
| | per reaction mixture | per μgm of added RNA |
| | ($\times 10^{-6}$) | ($\times 10^{-6}$) |
| — | 0.52 | — |
| Purified globin mRNA | 3.83 | 3.83 |
| H2020 16S RNA | 9.61 | 1.91 |
| 104E RNA fractions | | |
| 9 | 4.2 | 1.40 |
| 10 | 4.0 | 1.33 |
| 11 | 4.2 | 1.40 |
| 12 | 3.7 | 1.23 |
| 13 | 4.0 | 1.33 |

Plate 2. Autoradiograph of SDS-polyacrylamide gel electrophoresis of the products synthesized in a cell-free translation system in response to the H2020 16S RNA preparation.

1.5×10^6 cpm of these cell-free products were co-electrophoresed with *in vivo* IgA isolated from H2020 cells (1×10^6 cpm) and with the cell-free products of purified rabbit globin mRNA (5×10^5 cpm). Electrophoresis carried out at 120 volts for 14 hours. Exposure time for the autoradiograph, 3 days.

heavy chain →

light chain →



'in vivo' IgA

H2O2O 16S RNA
cell-free products

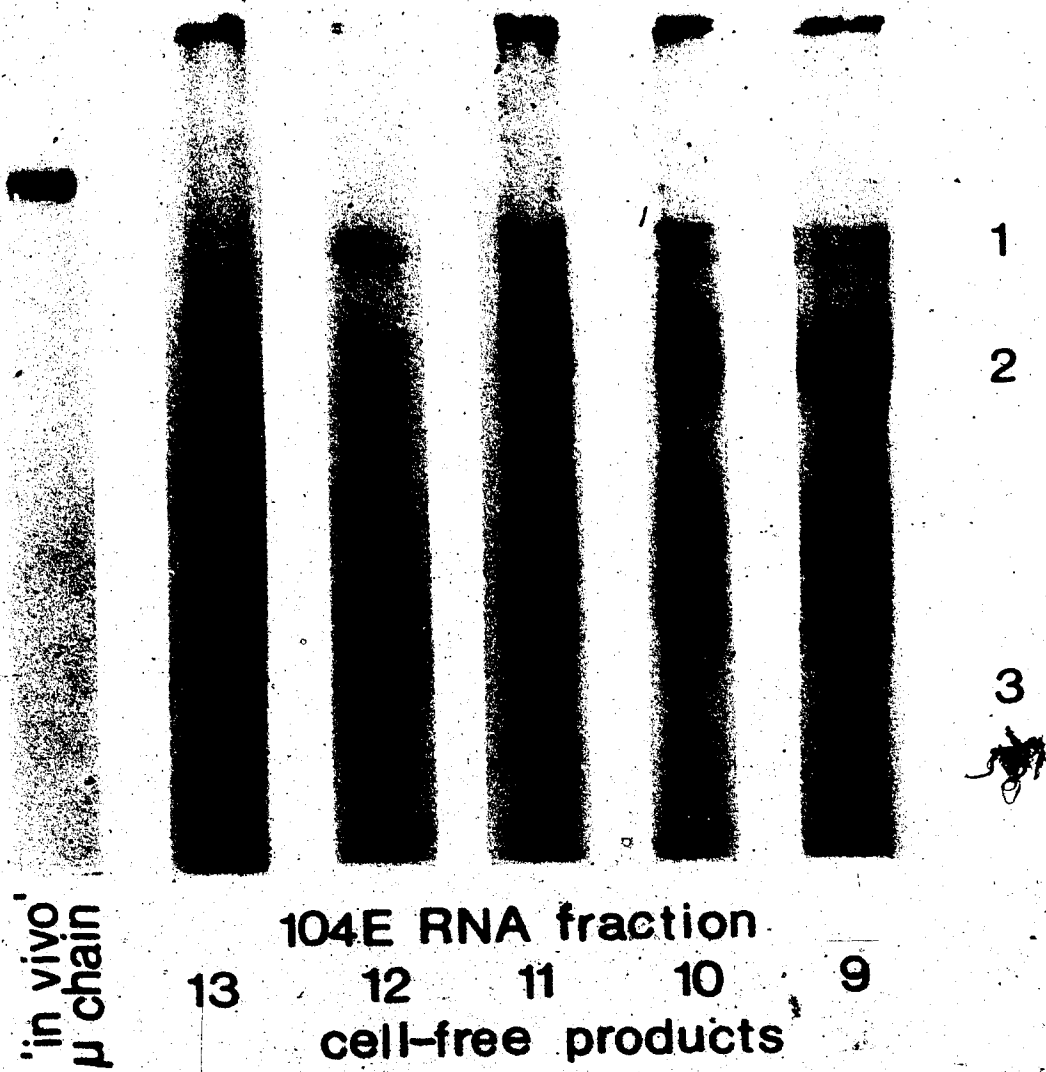


Globin mRNA
cell-free products



Plate 3. Autoradiograph of SDS-polyacrylamide gel electrophoresis of the products synthesized in a cell-free translation system in response to various 104E RNA sucrose gradient fractions.

5×10^4 cpm from each fraction were coelectrophoresed with *in vivo* μ chain isolated from 104E cells. Electrophoresis carried out at 120 volts for 14 hours. Exposure time for the autoradiograph, 10 days.



of the major band. These minor bands cannot be attributed to contaminating mRNA's in the cell-free system, as the globin control is completely free of corresponding bands. The possibility cannot be excluded that they represent the cell-free products of mRNA's other than that coding for the α chain. However, it is equally possible that at least some of them represent peptide fragments of the α chain itself. Such fragments could arise by false initiation or premature termination of translation, or by post-translational cleavages. In fact, it is thought that immunoglobulin chains synthesized *in vitro* lack proper disulphide bridges, and are therefore more susceptible to such cleavages (Swan *et al.*, 1972).

In the second gel (Plate 3), the cell-free products of the 104E sucrose gradient fractions 9-13 were electrophoresed in parallel with the *in vivo* IgM heavy chain. As in the case of the H2020 electrophoresis, it was not expected to find a band in the cell-free products corresponding directly to that of the *in vivo* μ chain. However, in actuality, a large number of bands of relatively equal intensities were found, all with mobilities greater than that of the *in vivo* μ chain. The possibility that some of these bands represent peptide fragments of the slowest migrating band (as discussed for H2020) is supported by the correlations between the intensities of certain bands. For example, in Plate 3 the intensities of the bands in region 1 of fraction 13 are relatively less than in fractions 10 and 11, and so is the intensity of band 2. However, for band 3, the intensity is greater in fraction 13 than in fractions 10 and 11. Therefore, band 2 probably represents a fragment of the bands in region 1, whereas band 3 is likely

caused by the cell-free product of a different mRNA. By such criteria, the RNA from fractions 10-12 of the 104E sucrose gradient can be said to be relatively similar in respect to the cell-free products produced. However, by the SDS-polyacrylamide gel electrophoresis alone, it is not possible to determine if all or any of these cell-free products correspond to authentic μ chains.

Further analysis of the cell-free products was therefore performed by tryptic digestion followed by two-dimensional high voltage electrophoresis. Plate 4 shows the autoradiograph of the electrophoresis in pH6.5 buffer of the tryptic peptides formed by the 104E sucrose gradient fractions 10-12 and by the *in vivo* μ chain. In each case, the majority of the radioactivity was found in one spot slightly on the basic side of the origin (position 1 in Plate 4), indicating either that the trypsin digestion was not effective or else that most of the peptides formed were neutral in the pH6.5 buffer. The *in vivo* μ chain showed at least one major peptide not found in the cell-free products (position 2). However, similarities do exist between the patterns formed by the *in vitro* and the *in vivo* preparations. Furthermore, when the basic peptides were cut out as indicated and reelectrophoresed in the perpendicular direction in pH3.5 buffer, the patterns formed by the *in vitro* and *in vivo* preparations definitely did correspond. (See Plate 5. Positions marked 1 and 2 are equivalent to those in Plate 4.) In particular, the extra peptide evident in the *in vivo* μ chain at position 2 in the pH6.5 buffer seemed to migrate to a distance equivalent to one of the peptides from position 1 of the 104E cell-free products. (These 'equivalent' peptides are indicated by a number 3 in Plate 5.)

Plate 4. Autoradiograph of the high voltage electrophoresis at pH6.5 of tryptic peptides from the cell-free products of 104E RNA fractions and from *in vivo* μ chain.

3.5×10^5 cpm of each sample applied. Electrophoresis carried out at 3000 volts for 60 minutes. Exposure time for the autoradiograph, 7 days.

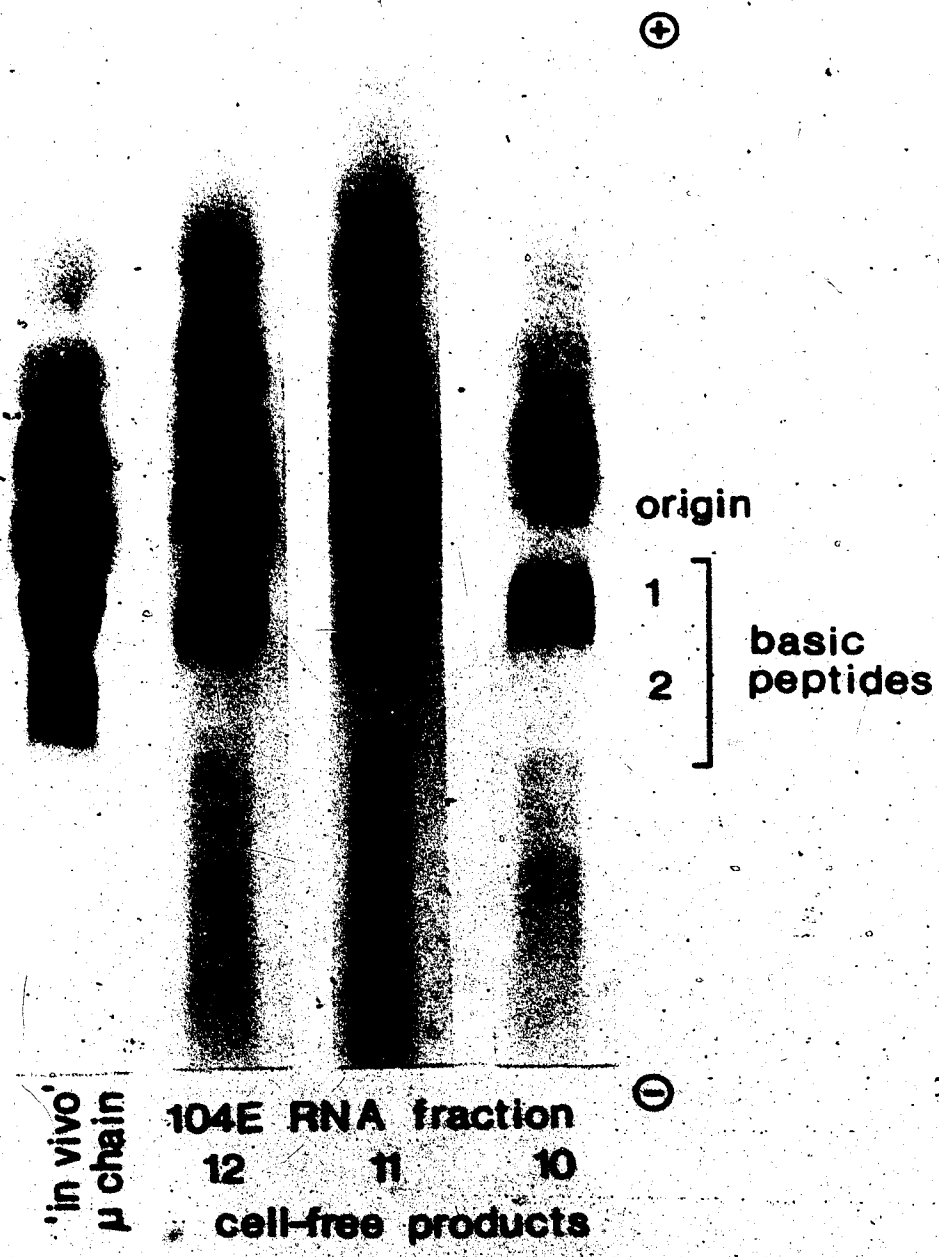
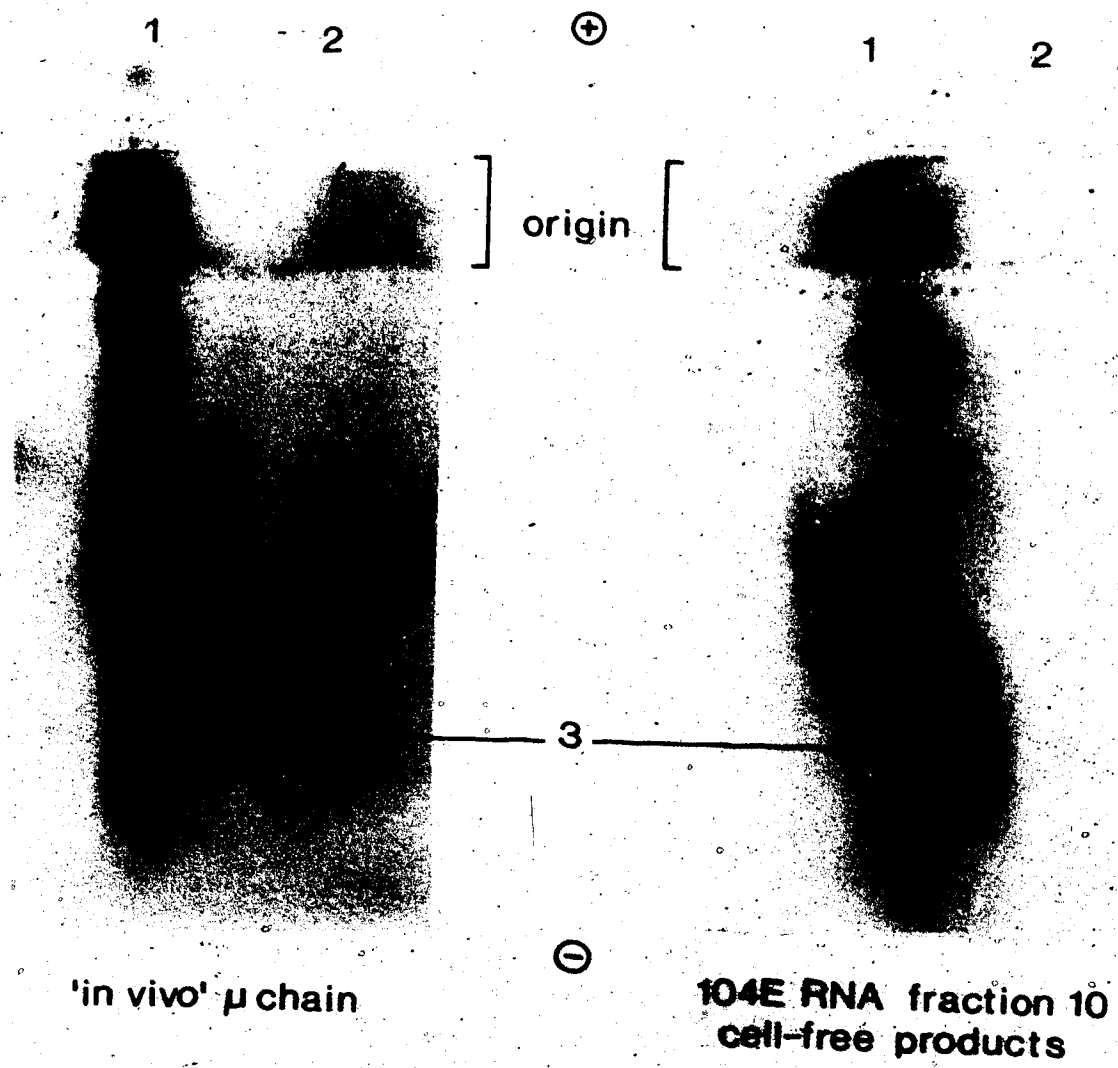


Plate 5. Autoradiograph of the second-dimensional high voltage electrophoresis at pH3.5 of the 104E basic peptides obtained by the pH6.5 electrophoresis.

Positions 1 and 2 are equivalent to those in Plate 4. Electrophoresis carried out at 3000 volts for 47 minutes. Exposure time for autoradiograph, 28 days.



A similar analysis was carried out for the cell-free products of the H2020 16S sucrose gradient pool, in comparison with the *in vivo* α chain. Plates 6 and 7 show the autoradiographs of the pH6.5 and pH3.5 electrophoresis, respectively. (Acidic and basic peptides were cut apart as indicated in Plate 6. Positions 1, 2, 3 and 4 are equivalent in both plates.) From this two-dimensional electrophoresis, it is evident that all the tryptic peptides of the *in vivo* α chain are also present in the *in vitro* preparation. This is very convincing evidence that authentic α chains were actually produced by the translation of the RNA from the H2020 16S sucrose gradient pool. Extra *in vitro* peptides, which do not correspond to any of the *in vivo* peptides, comprise only a very minor portion of the total preparation. Their possible origins have already been outlined in the preceding discussion on SDS-polyacrylamide gel electrophoresis.

Further Purification of the Heavy Chain mRNA's

Using as a guide the results obtained by the analysis of the cell-free products, the RNA from fractions 10-12 of the 104E sucrose gradient was taken as the source for the further purification of μ mRNA. Similarly, H2020 α mRNA was further purified from the 16S RNA sucrose gradient pool.

Each of these preparations was first examined by analytical formamide gel electrophoresis to obtain some idea of their purity independent of that obtained from the analysis of their translation products. Samples and gels were prepared and electrophoresed as described in Materials and Methods, using 5 μ gm of the H2020 preparation and 10 μ gm

8

Plate 6. Autoradiograph of the high voltage electrophoresis at pH6.5 of tryptic peptides from the cell-free products of H2020 16S RNA and rabbit globin mRNA and from *in vivo* α chain.

1×10^6 cpm of each sample applied. Electrophoresis carried out at 3000 volts for 47 minutes. Exposure time for the autoradiograph, 4 days.

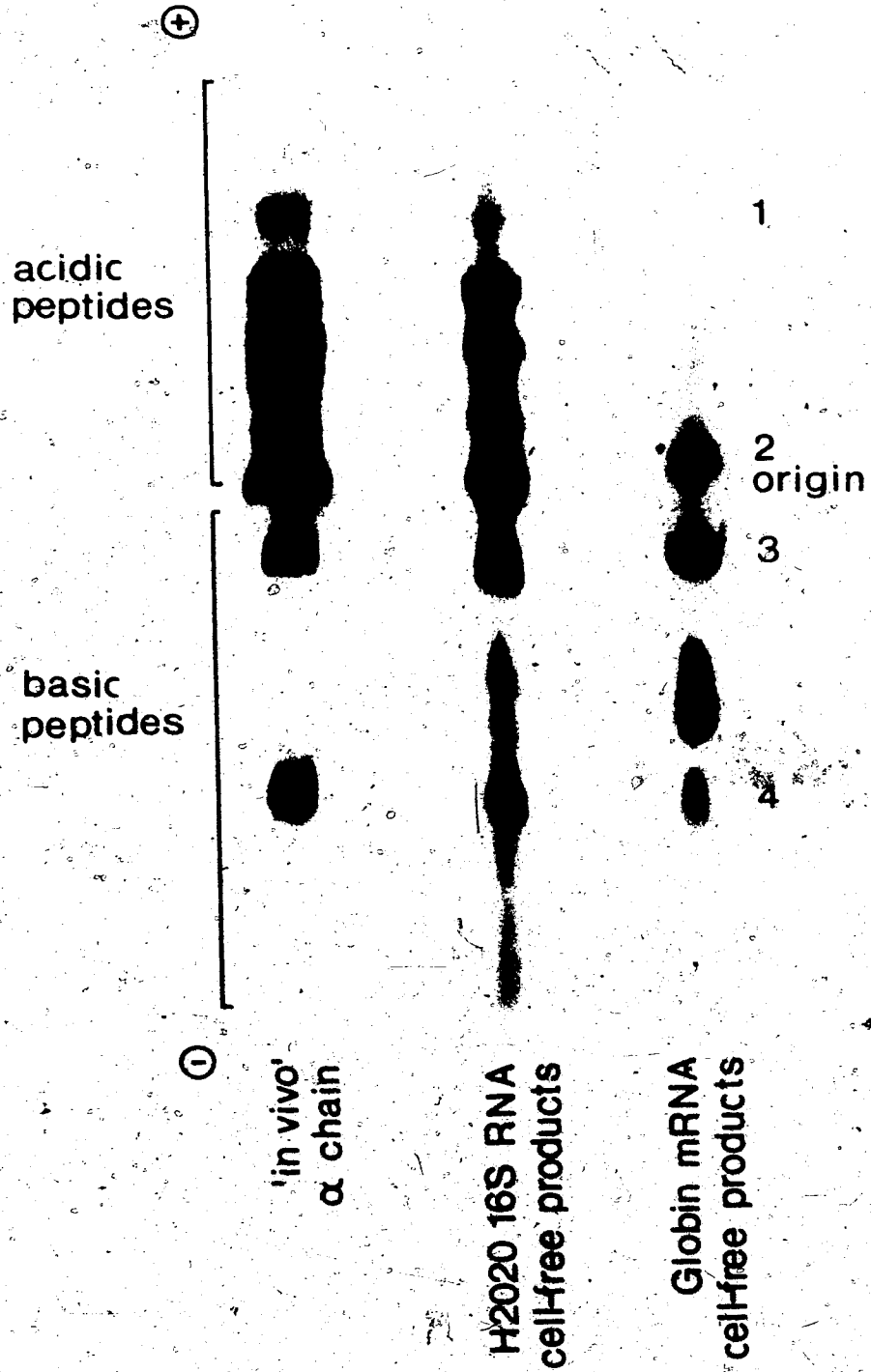


Plate 7. Autoradiograph of the second-dimensional high voltage electrophoresis at pH3.5 of the H2O2O acidic and basic peptides obtained by the pH6.5 electrophoresis.

Positions 1, 2, 3 and 4 are equivalent to those in Plate 6. Electrophoresis carried out at 3000 volts for 60 minutes in the case of the acidic peptides; at 3000 volts for 47 minutes in the case of the basic peptides. Exposure time for the autoradiographs, 14 days.

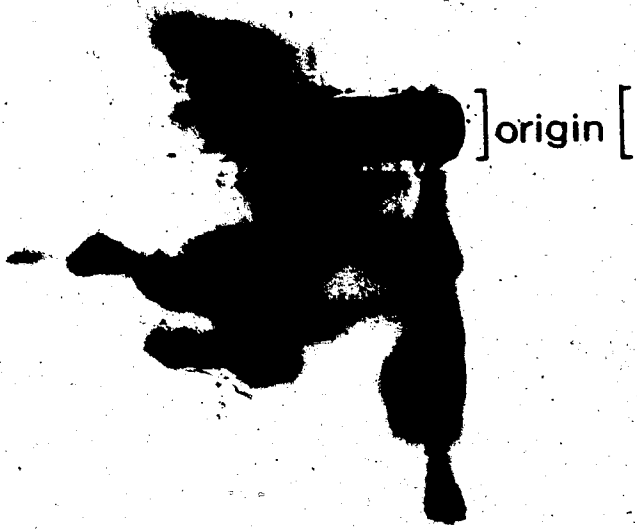
1

2

⊕

1

2



'in vivo'
α chain

H2020 16S RNA
cell-free products

4

3

⊕

4

3

]origin [



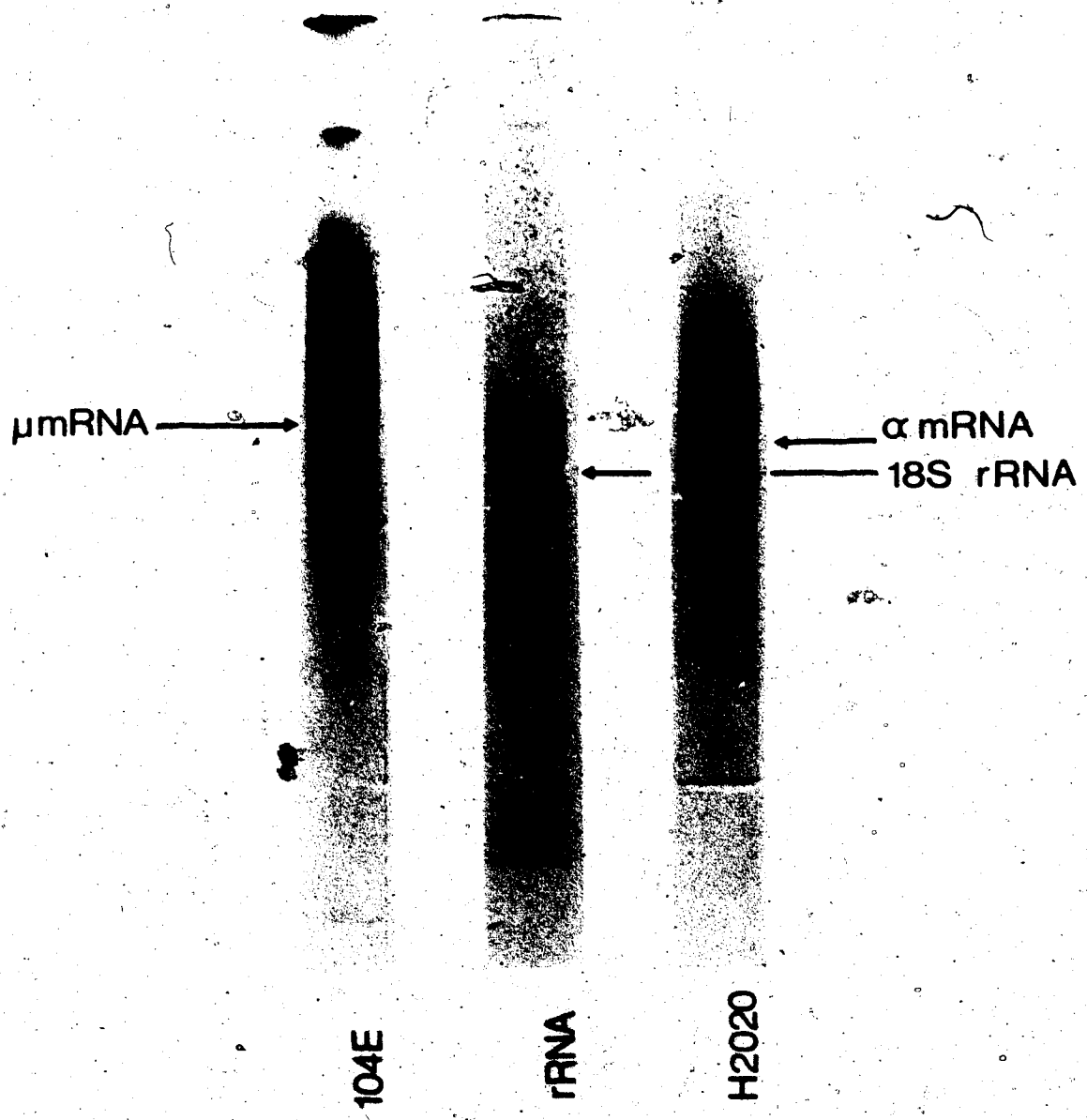
⊖

of the 104E preparation per gel. Two μgm of mouse 18S rRNA were run on a parallel gel. Stained gels are shown in Plate 8. In the H2020 gel, the majority of the RNA migrated as one band with a mobility very slightly less than 18S rRNA. Only a small amount of lightly stained material is noticeable on either side of this major band. In the 104E gel, the μ mRNA migrated significantly slower than 18S rRNA, and the proportion of diffuse material surrounding this band was much greater than in the case of H2020. In addition, a second band is evident at exactly the 18S position. However, the distance between these two bands is great enough that a significant increase in the purity of the μ mRNA should be attainable by cutting out the corresponding gel slice. Also by such a procedure it should be possible to eliminate large proportions of the diffuse material around each major band. With this purpose, therefore, the remaining portions of the 104E and the H2020 sucrose gradient preparations (45 μgm and 20 μgm , respectively) were subjected to preparative formamide gel electrophoresis. Representative gel scans of each are shown in Figure 8, and the portion cut out from each gel is indicated. The elution of RNA from these gel slices and the removal of coeluted polyacrylate was carried out as described in Materials and Methods. The final yield in the NP(0.4) fractions, in the case of both H2020 and 104E, was measured at 0.1 OD_{260} units (equivalent to 4 μgm of RNA). After dialysis of the NP(0.4) fractions against water and concentration by lyophilization, the eluted material was ethanol-precipitated and dissolved in 20 μl H_2O . At this point, therefore, the RNA concentration could be estimated as 0.2 $\mu\text{gm}/\mu\text{l}$ for both H2020 and 104E.

To ensure that the eluted material still had the characteristics of

Plate 8. Analytical polyacrylamide gel electrophoresis in 99% formamide.

H2020 and 104E RNA preparations were electrophoresed in parallel with a ribosomal RNA standard. Staining by a 0.005% solution of Stains-All in 50% formamide; destaining by tap water. Direction of electrophoresis was from top to bottom.



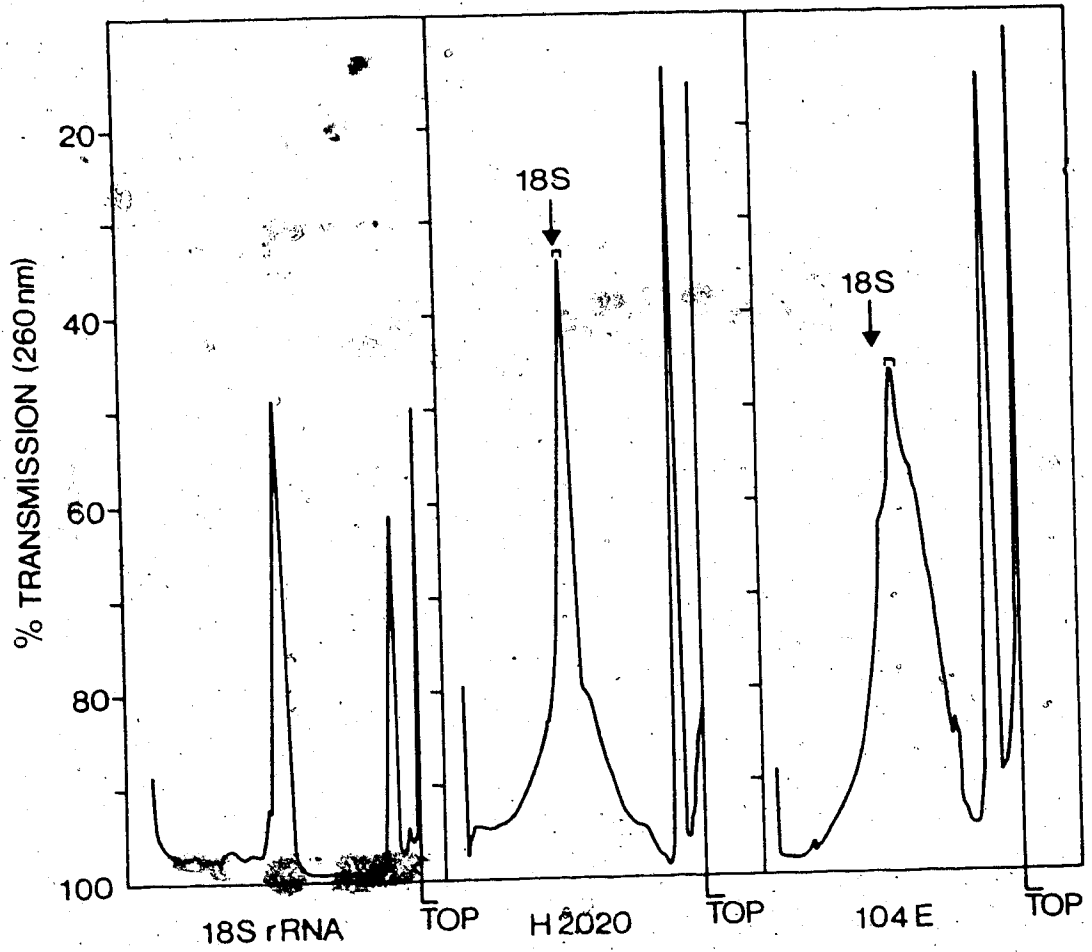


Figure 8. Preparative polyacrylamide gel electrophoresis in 99% formamide of the H2020 and 104E RNA preparations, in comparison with a ribosomal RNA standard.

the corresponding heavy chain mRNA, and to obtain some estimate of the increase in purity, 5 μ l of each preparation was then rerun on formamide gels, in parallel with 2 μ gm of 18S rRNA. Gel scans are shown in Figure 9. In both cases, a definite peak was evident at the expected position and the eluted material migrated as a significantly narrower band than in the original gels. However, when the relative heights of the H2020, 104E, and rRNA peaks are compared, it seems as though 0.2 μ gm/ μ l was an overestimation of the concentration of the μ and α mRNA's. That is, either the OD measurements of the NP(0.4) fractions were in error, or significant amounts of RNA were lost during the lyophilization and precipitation steps. In particular, the concentration of H2020 α mRNA appears to be about one half that of the 104E μ mRNA.

Preparation of ^{125}I -labelled RNA

The H2020 and 104E heavy chain mRNA preparations obtained by elution from formamide gels were radioactively labelled with ^{125}I . Because this isotope has a relatively short half life, the RNA preparations had to be iodinated on two separate occasions in order to carry out all the hybridization experiments described below. Since the specific activity of the resulting ^{125}I -labelled RNA is likely to be different on each occasion, the first iodination is indicated in all future work by a #1, and the second by a #2.

On both occasions, 5 μ l of each preparation were iodinated using 2mCi of ^{125}I , in parallel with 1 μ gm of 18S rRNA as a control. Figure 10 shows the 10-28% sucrose gradient profiles of the first iodinated preparations. Degradation of the RNA during iodination appears to be more extensive with the 104E and H2020 mRNA preparations than with the

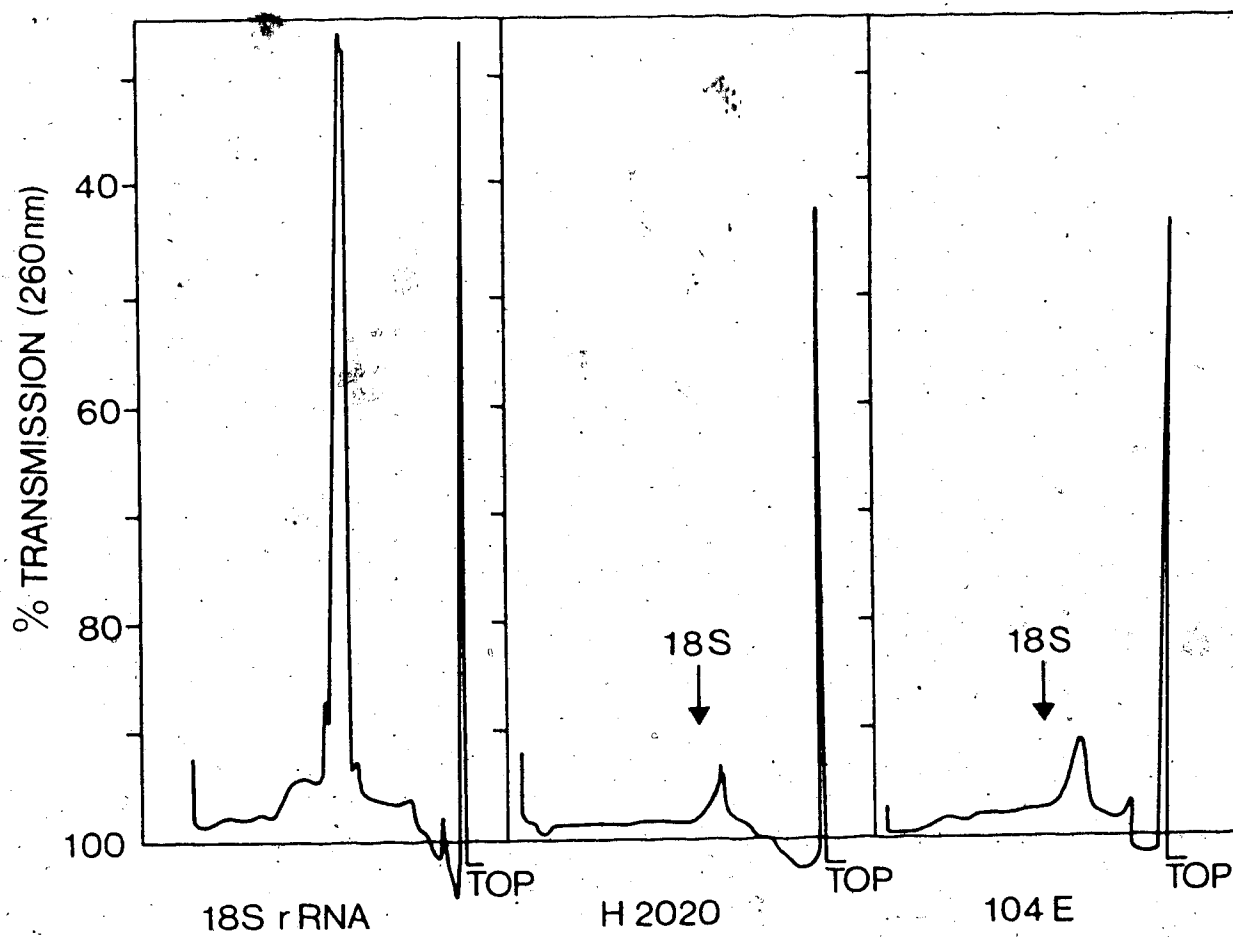


Figure 9. Polyacrylamide gel electrophoresis in 99% formamide of eluted H2020 and 104E RNA, in comparison with a ribosomal RNA standard.

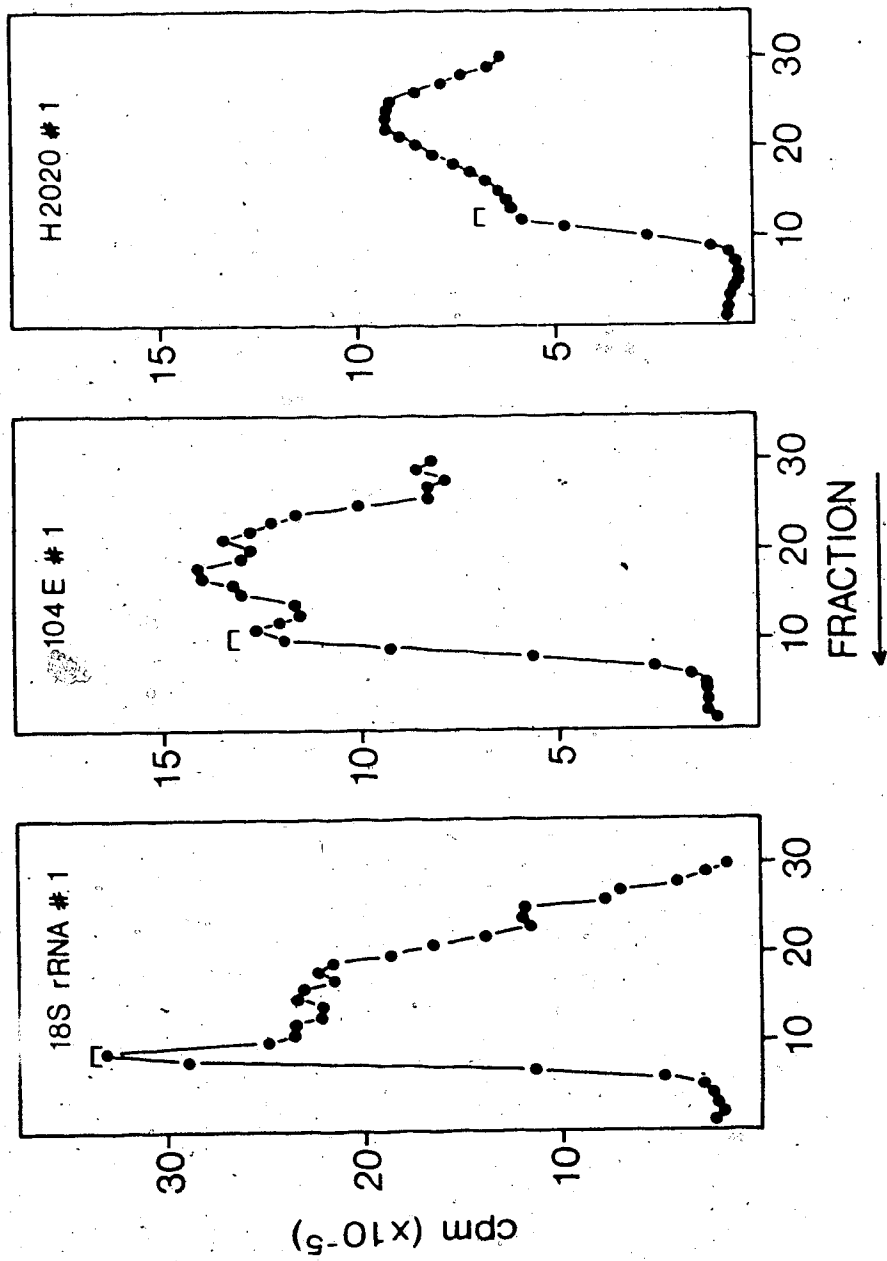


Figure 10. Sucrose density gradient centrifugation of iodinated RNA preparations.

18S rRNA. Since the number of cpm's of ^{125}I -labelled RNA obtained vastly exceeds the required amount for hybridization experiments, only the heaviest peak fractions were pooled and ethanol-precipitated as indicated in Figure 10. Because the 104E #2 preparation appeared excessively degraded in the first gradient, the heaviest fractions were rerun on a second gradient before pooling for use in hybridization experiments (see Figure 11).

Preparation of a 13S 3'-end Containing Fragment of H2020 α mRNA

Approximately 90% of the second H2020 iodinated preparation was subjected to two successive steps of chromatography on oligo(dT)-cellulose in order to separate intact molecules and those fragments containing the poly(A) 3'-terminal sequence from those fragments containing only internal and 5'-terminal sequences. Of the input radioactivity, 11% was bound to the first column and 90% to the second column under high salt conditions, indicating that the second TE-II wash consisted almost entirely of poly(A)-containing material. This material was then fractionated according to size by two successive steps of 10—28% sucrose density gradient centrifugation (Figure 12). Parallel gradients were run with that portion of H2020 RNA from the second iodination which had not been subjected to oligo(dT)-cellulose chromatography (that is, which contains all the sequences of the complete RNA molecule). The fragments sedimenting at approximately 13S were collected as indicated from each gradient. In all experiments to be described involving this 13S 3'-end containing fragment, the 'complete sequence' RNA used as a comparison was that derived from these equivalent 13S fractions of the oligo(dT)-unfractionated H2020 #2 preparation. This eliminates completely any

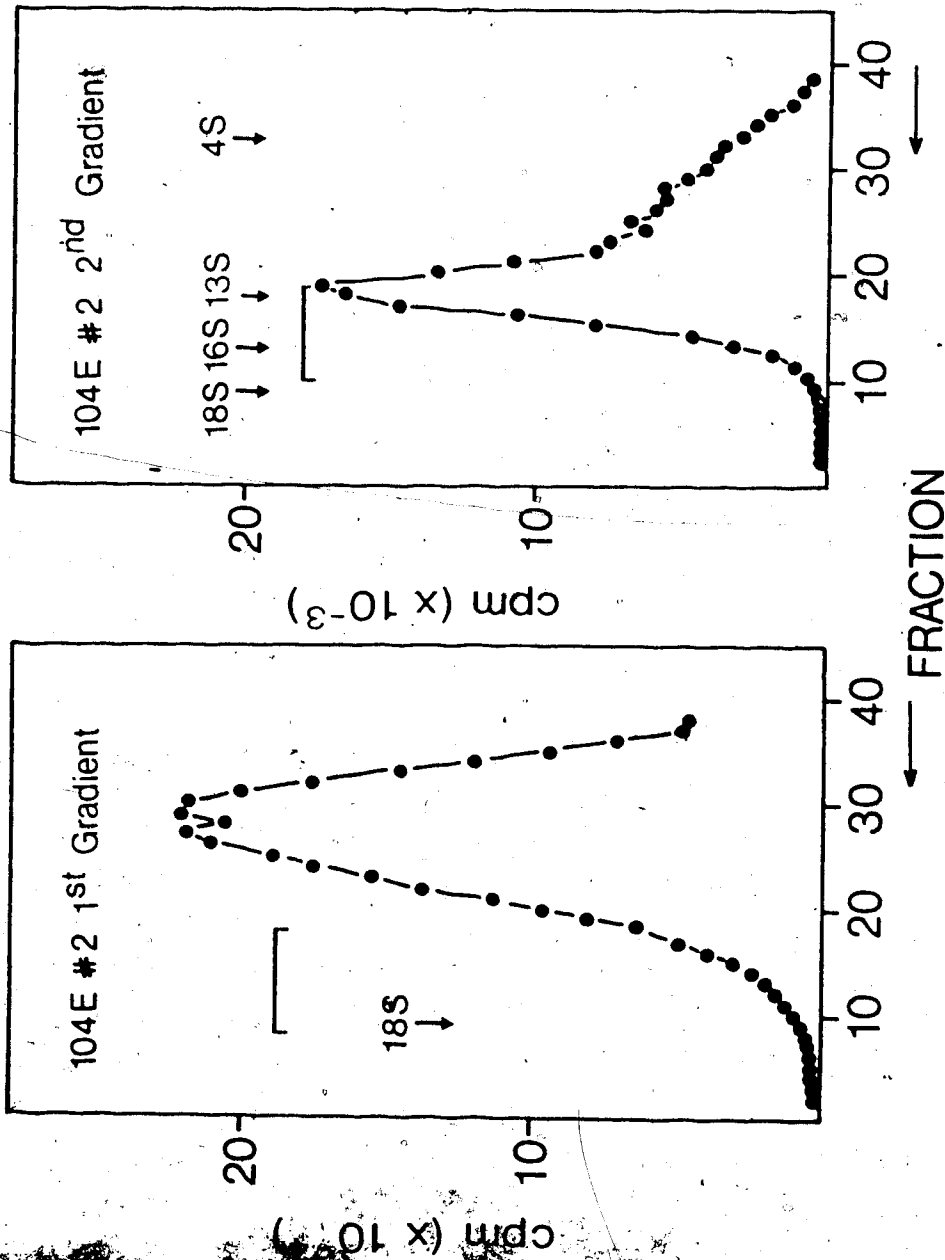


Figure 11. Fractionation of a highly degraded ^{125}I -labelled 104E RNA preparation by successive sucrose density gradient centrifugations. Reference positions were determined by the parallel centrifugation of the following markers: mouse ribosomal and transfer RNA (18S and 4S), *E. coli* ribosomal RNA (16S), MOPC 321 light chain mRNA (13S). Fractions pooled from the first gradient (indicated by the bracket) were resedimented in the second gradient.

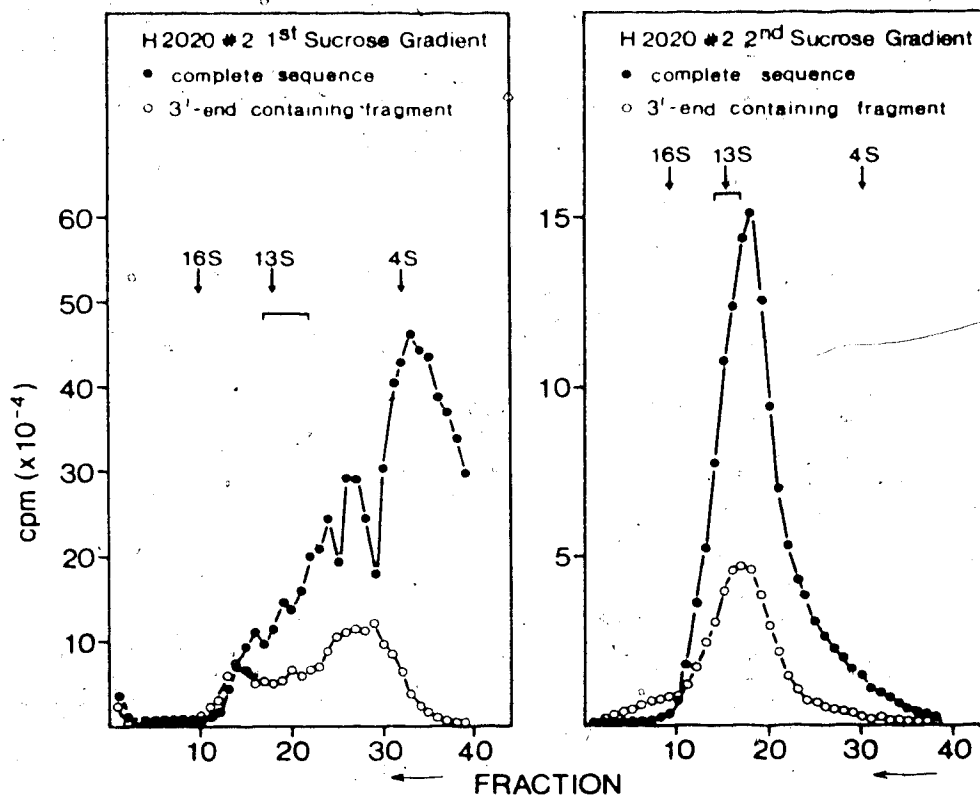


Figure 12. Fractionation of 3'-end containing fragments and 'complete sequence' fragments of a ^{125}I -labelled H2020 α RNA preparation by successive sucrose density gradient centrifugations. Reference positions determined as per Figure 11. Fractions pooled from the first gradient (indicated by the bracket) were resedimented in the second gradient.

possible variations due to a size difference between the 3'-end containing fragment and the complete-sequence containing fragment.

Remaining fractions from the first and second gradients of the 'complete sequence' RNA which had sedimentation values greater than 10S were also pooled, and used as an additional source of ^{125}I -labelled H2020 mRNA (that is, H2020 #2) for experiments which did not involve the 3'-end containing fragment.

Hybridization Experiments

In all results presented below, the preparations of DNA and iodinated RNA used were equivalent within, but not necessarily between, series of experiments. Because of the uncertainty discussed above in the actual concentrations of the final RNA preparations, it was initially assumed that each iodinated RNA had a specific activity of 2×10^7 cpm/ μg . This figure is based on experience with the iodination of immunoglobulin light chain mRNA (Tonegawa *et al.*, 1974).

Hybridization Kinetics of H2020 α and 104E μ RNA Preparations with Mouse Liver DNA

In order to scan as large a range of C_{ot} values as possible, hybridization was performed at a low DNA concentration (0.20 mgm/ml) as well as at a high DNA concentration (20 mgm/ml). In each case, 4×10^4 cpm's of RNA were added per ml of the final hybridization mixture, resulting in approximate DNA/RNA ratios of 1×10^5 and 1×10^7 , respectively. As a comparison, the hybridization kinetics of mouse 18S rRNA were also studied, at an intermediate concentration of 2.0 mgm/ml (DNA/RNA ratio = 1×10^6). As evident in Figure 13, the majority of the RNA sequences present in the H2020 α and the 104E μ RNA preparations hybridized with

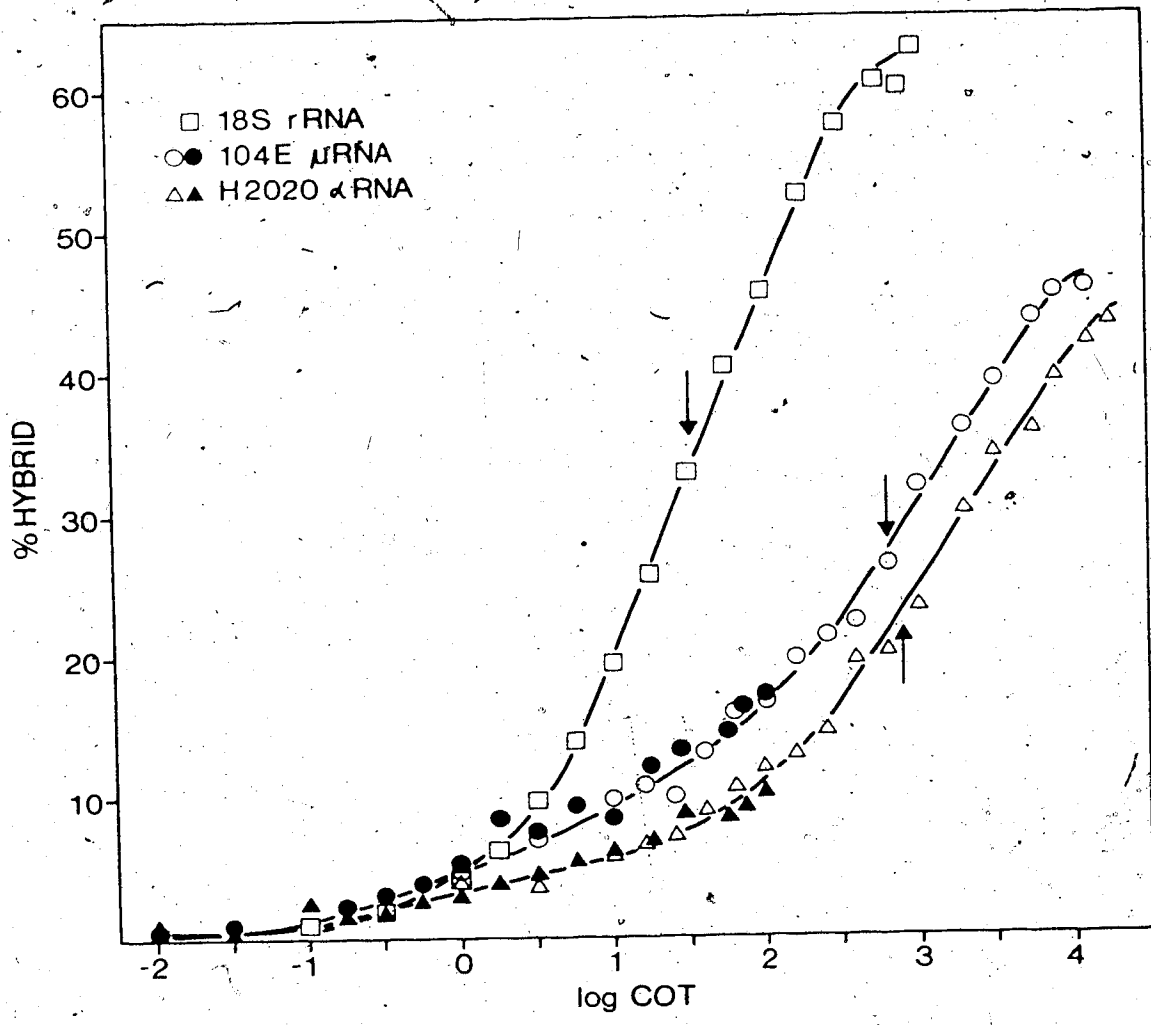


Figure 13. Hybridization kinetics with mouse liver DNA (#1). RNA from the first iodinated preparation was used in each case. Arrows indicate apparent $\log C_{0t}^{1/2}$'s.

- ▲ : DNA concentration, 0.20 mgm/ml
ratio of DNA to RNA, 1×10^5
- △ : DNA concentration, 20.0 mgm/ml
ratio of DNA to RNA, 1×10^7
- : DNA concentration, 2.0 mgm/ml
ratio of DNA to RNA, 1×10^6

Intrinsic RNase resistant factors: ●, 0.80%; ○, 2.73%;
▲, 0.16%; △, 0.92%; □, 0.58%.

mouse liver DNA at C_{0t} values greater than 10^2 (C_{0t} values being the product of the DNA concentration and the annealing times, expressed as mol.-sec./l.). The kinetics of hybridization were not distinctly biphasic in either case; however, the proportion of RNA sequences hybridizing at C_{0t} values lower than 10^2 was definitely greater for the μ RNA than for the α RNA. The possibility that this was due to some residual rRNA still present in the 104E preparation was investigated by a competition hybridization experiment, using an excess of cold 18S rRNA. This experiment was carried out at the low DNA concentration only. The kinetics of hybridization under these conditions are shown in Figure 14, where it is evident that, by the addition of excess 18S rRNA, the proportion of hybrid formed by the 104E preparation at low C_{0t} values was reduced by at least 5%. This reduction resulted in levels of hybridization at the low C_{0t} values not significantly different from those obtained with the H2020 α RNA. Therefore, of the 45% of the 104E preparation which hybridized at the maximum C_{0t} values, a minimum of 5% consisted of rRNA sequences.

At the highest C_{0t} value achieved, the portion of RNA hybridized had not yet reached a definite maximum value in either case. However, in order to obtain some estimate of the gene frequencies corresponding to these RNA sequences, the maximum percentage hybridization was approximated as 45% for the H2020 RNA and 50% for the 104E RNA. From this, apparent $C_{0t_{1/2}}$ values (that is, the C_{0t} values at 1/2 the maximum hybridization) of 790 and 630, respectively, were obtained, with the 5% correction value for rRNA being applied in the case of 104E. (The values of the apparent $\log C_{0t_{1/2}}$'s are indicated by the arrows in

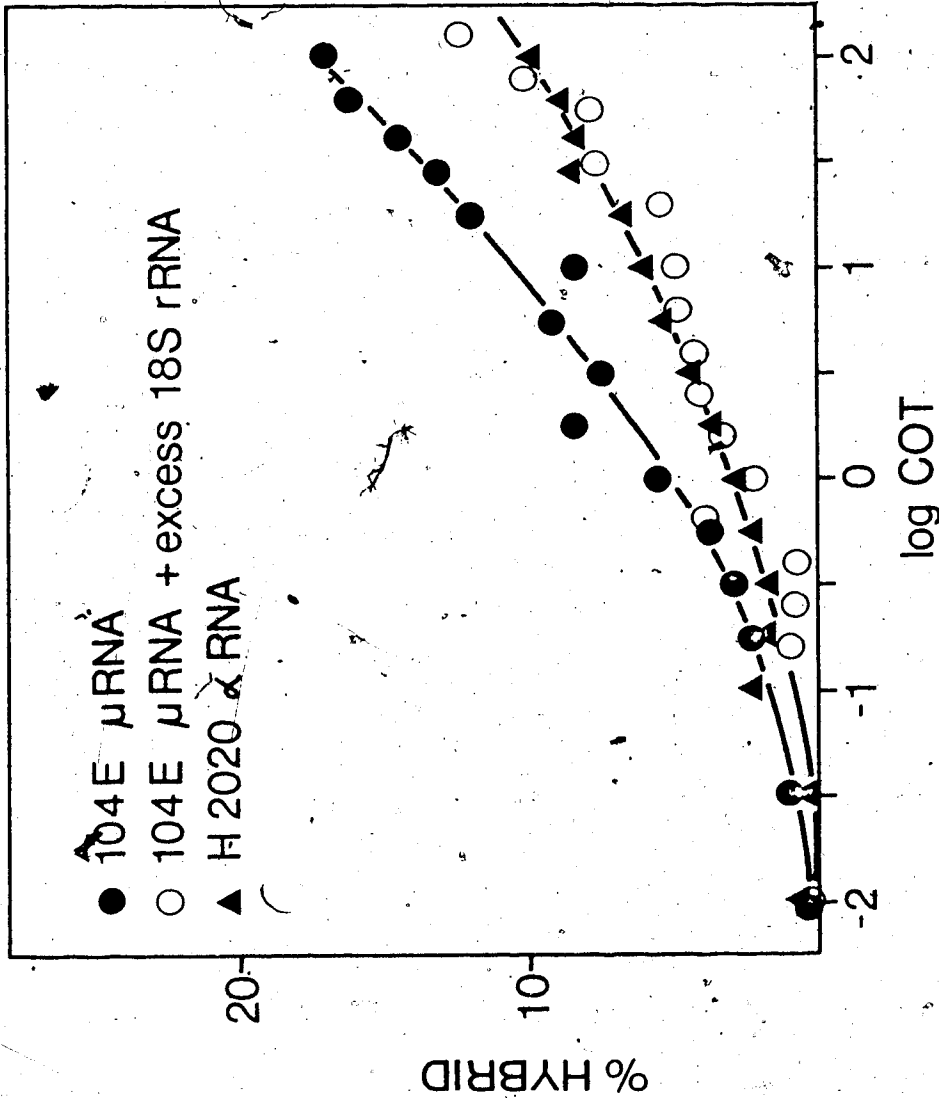


Figure 14. Competition hybridization of 104E μ RNA (#1) with mouse liver DNA (#1) in the presence of 2 μ g/ml unlabelled mouse 18S ribosomal RNA. DNA concentration, 0.20 mg/ml; ratio of DNA to RNA, 1×10^5 ; intrinsic RNase resistant factor, 1.59%. The hybridization kinetics of 104E μ RNA without competitor, and of H2020 α RNA, are reproduced from Figure 13.

Figure 13.) The following formula derived by Bishop *et al.* (1972) can be used to convert a $C_{ot}^{1/2}$ value to a reiteration frequency:

$$F = \frac{C_1}{C_2} \times \frac{G_2}{G_1}$$

where C_1 = $C_{ot}^{1/2}$ of *E. coli* crRNA in 2xSSC at 70°C (= 8.1)*,
 G_1 = Genome size of *E. coli* DNA (= 2.7×10^9 daltons)*,
 G_2 = Genome size of mouse liver DNA (= 1.8×10^{12} daltons)*,
 C_2 = $C_{ot}^{1/2}$ of the mouse RNA sequence in question,
 and F = reiteration frequency of the corresponding sequence
 in mouse liver DNA.

In this way, a nominal reiteration frequency of approximately 7 was obtained for the H2020 α gene, and approximately 8 for the 104E μ gene. In comparison, the reiteration frequency of the mouse 18S rRNA gene was determined to be 175, from an apparent $C_{ot}^{1/2}$ of 32. This is in good agreement with published results (Melli *et al.*, 1971; Tonegawa *et al.*, 1974).

Hybridization of H2020 α and 104E μ RNA's with DNA's from Various Heavy Chain-producing Myelomas

The question was asked: Do mRNA's containing one particular heavy chain sequence hybridize to the same extent with heterologous heavy chain myeloma DNA's as with their homologous myeloma DNA?

The first series of experiments performed to investigate this question involved the hybridization in all possible combinations of the H2020 and 104E RNA's and DNA's. In these initial experiments, the final level of hybridization was of major interest; consequently, only one

*Values taken from Melli *et al.* (1971).

sample was taken from the hybridization mixture at a low C_{ot} value. In order to obtain as high C_{ot} values as possible without excessively long incubation times, hybridizations were carried out in 6xSSC buffer at 75°C as well as in 2xSSC at 70°C. The C_{ot} value obtained at 6xSSC was then converted to the equivalent C_{ot} value which would have been obtained at 2xSSC by multiplication with a constant equal to 2.5, according to Britten *et al.* (1974). The final DNA concentration was 20 mgm/ml in each case; 2×10^4 cpm's of RNA were added per ml of final hybridization mixture in order to obtain as high a DNA/RNA ratio as possible (i.e. 2×10^7). The results are presented graphically in Figure 15. With the H2020 α RNA, the final level of hybridization obtained with the heterologous (104E) DNA was significantly lower than that obtained with the homologous (H2020) DNA. In contrast, the 104E μ RNA showed no significant differences between its homologous and heterologous hybridizations.

In the next series of experiments, this investigation of the final levels of heterologous hybridizations was repeated using different preparations of 104E and H2020 RNA's and DNA's, and was also expanded to include the following myeloma DNA's: Y5781 (IgM), MPC11 (IgG_{2b}), S28 (IgG₁) and J558 (IgA). Hybridizations were performed in 2xSSC only, and no samples were taken at low C_{ot} values. The final DNA concentration was 22.5 mgm/ml in each case, and RNA was added to give a DNA/RNA ratio of 2×10^7 . The homologous hybridizations of 104E μ RNA with 104E DNA, and H2020 α RNA with H2020 DNA, were included as controls. Results are presented in Table 6. With the 104E μ RNA, no differences could be detected in the final level of hybridization with any of the six DNA preparations. The results of the H2020 α RNA hybridizations are more

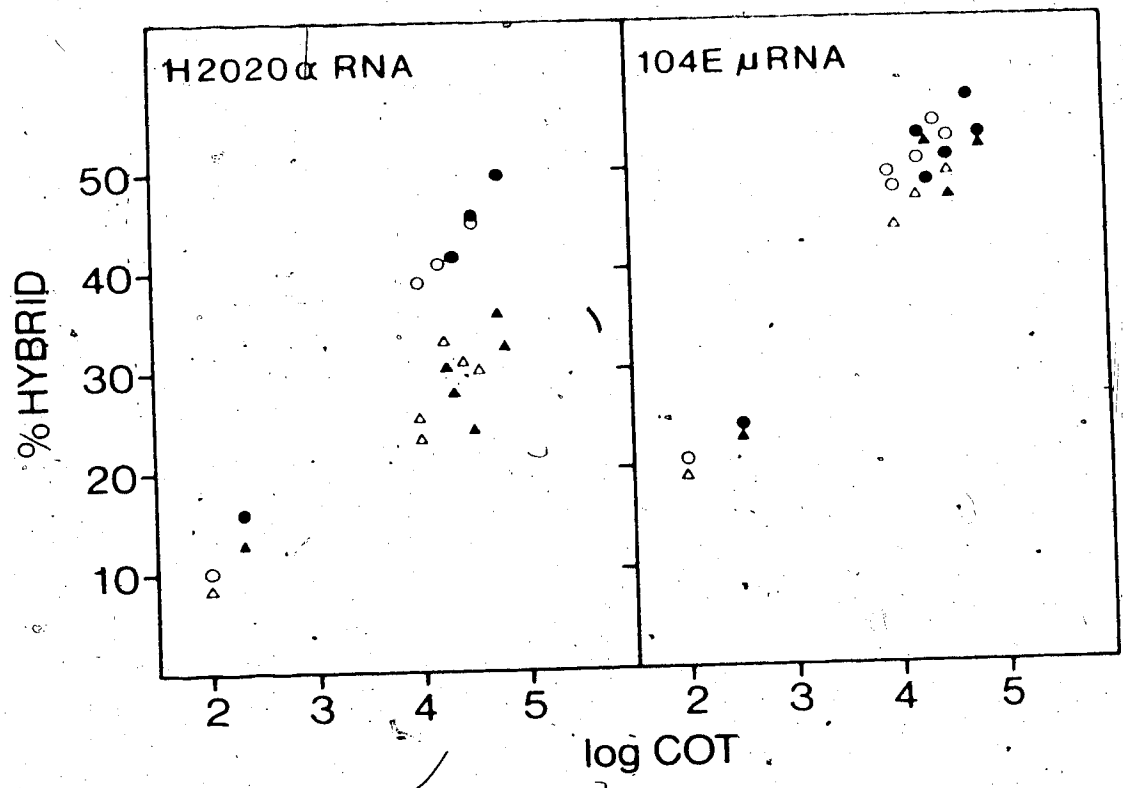


Figure 15. Homologous and heterologous hybridizations of H2020 α and 104E μ RNA's (#1) and DNA's (#1). Circles represent H2020 DNA and triangles, 104E DNA. Open figures represent hybridizations in 2xSSC at 70°C and closed figures, hybridizations in 6xSSC at 75°C. DNA concentrations, 20 mgm/ml. Ratio of DNA to RNA, 2x10⁷.

TABLE 6. Percent Hybrid Formed by H2020 α and 104E μ RNA's with the DNA from Various Heavy Chain Producing Myelomas

| RNA | DNA | Log C_0t | | | | | |
|----------|----------|------------|---------------|-------|-----|-------|------|
| | | 2 | 4 | 4.25 | 4.3 | 4.4 | 4.5 |
| H2020 #2 | Y5781 | 10.8 | 32.1 31.7 | 34.1 | | 35.8 | 35.0 |
| | MPC 11 | 14.3 | 31.3 34.8 | 38.6 | | 40.8 | 38.6 |
| | S28 | 10.2 | 32.8 31.5 | 35.0 | | 35.3 | 35.7 |
| | J558 | 15.3 | 44.8 45.5 | 47.8 | | 48.7 | 48.8 |
| | H2020 #2 | | 36.0 37.0 | 37.5 | | 39.2 | 38.5 |
| | 104E #2 | | 21.25 25.3 | 26.25 | | 27.25 | 26.2 |
| 104E #2 | Y5781 | 14.0 | 36.3 37.5 | 40.2 | | 39.6 | 40.4 |
| | MPC 11 | 17.0 | 35.3 36.8 | 41.0 | | 39.2 | 36.6 |
| | S28 | 16.1 | 34.9 34.2 | 37.1 | | 38.8 | 41.6 |
| | J558 | 16.0 | 33.5 32.8 | 36.8 | | 37.8 | 37.0 |
| | H2020 #2 | | 34.9 | | | 39.2 | |
| | 104E #2 | | 36.7 | | | 37.0 | |

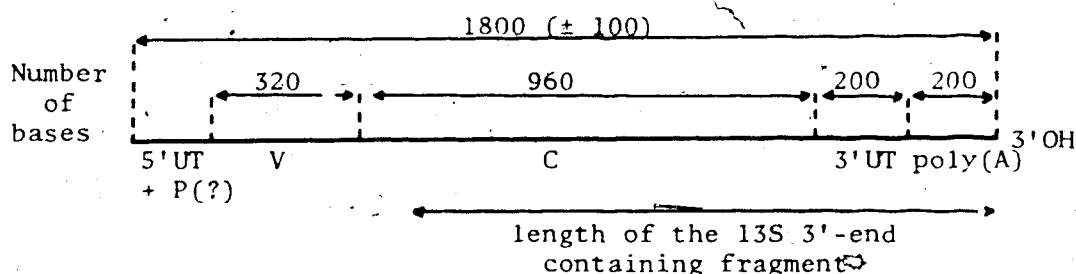
DNA concentration = 22.5 mg/ml; ratio of DNA to RNA = 2×10^7 .
Each row represents the results of a separate hybridization mixture.

clearly seen by the graphical presentation in Figure 16. The lower level of hybridization obtained with the 104E DNA is once again evident. S28, MPC11 and Y5781 DNA's all resulted in essentially equivalent levels of hybridization as H2020 DNA. The hybridization with J558 DNA produced a final level greater than that produced homologously.

Those combinations which showed significant differences in their final levels of hybridization were then studied more extensively by determining the kinetics of their hybridizations. C_0t curves are presented in Figure 17 (DNA concentration = 22.5 mgm/ml; DNA/RNA ratio = 2×10^7). In the hybridization of the H2020 α RNA with the J558 DNA, the slope of the C_0t curve was essentially the same as with the H2020 DNA, even though the final level was higher. In contrast, in the hybridization with 104E DNA, both the slope of the C_0t curve and the final level of hybridization were lower than with the H2020 DNA.

Hybridization Studies with the H2020 α 3'-end Containing Fragment

By analogy with the illustration of a κ mRNA molecule (see Introduction), the structure of the α mRNA can be depicted as follows:



The κ mRNA is known to be approximately 1250 bases in length (Tonegawa *et al.*, 1974; Milstein *et al.*, 1975), and it shows a sedimentation velocity of 13S in sucrose density gradients. Therefore, the radioactive-

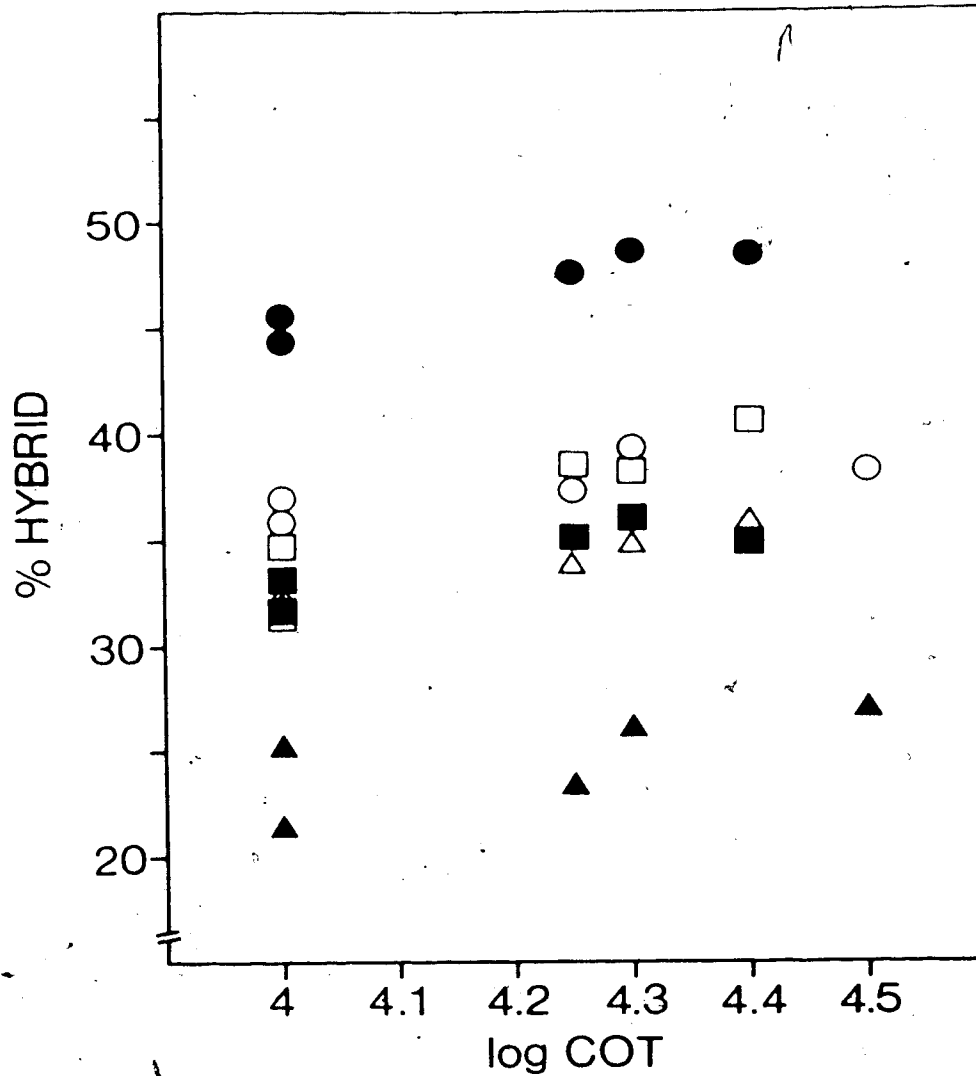


Figure 16. Hybridization of H2020 α RNA (#2) with various myeloma DNA's.
 ▲, 104E DNA (#2); ■, S28 DNA; ●, J558 DNA;
 △, Y5781 DNA; □, MPC11 DNA; ○, H2020 DNA (#2).
 DNA concentration, 22.5 mgm/ml; DNA to RNA ratio, 2×10^7 .

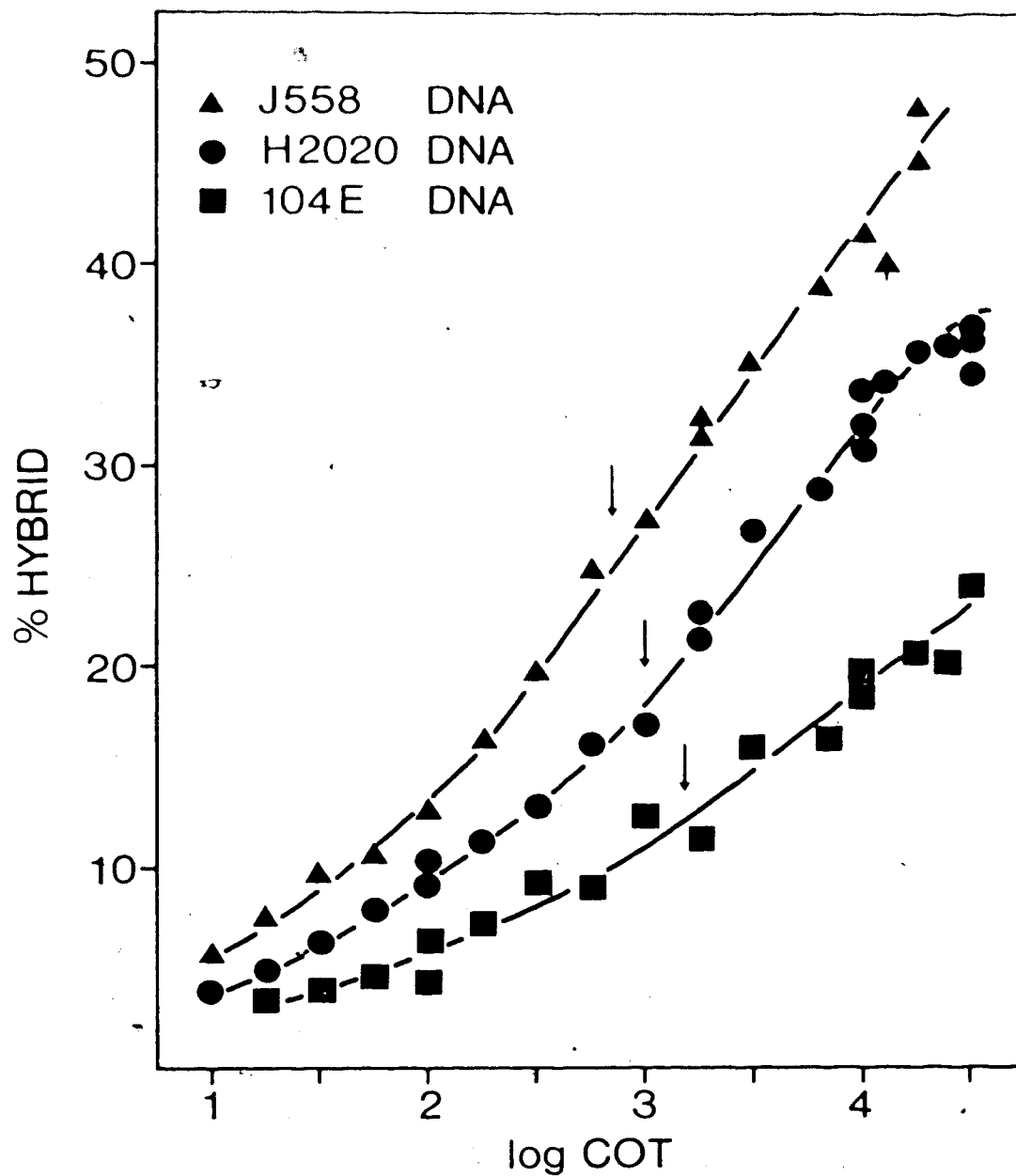


Figure 17. Hybridization kinetics of H2020 α RNA (#2) with H2020 DNA (#2), 104E DNA (#2) and J558 DNA. DNA concentration, 22.5 mgm/ml. Ratio of DNA to RNA, 1×10^7 . Intrinsic RNase resistant factor: \blacktriangle , 1.35%; \bullet , 1.68%; \blacksquare , 2.75%. Arrows indicate apparent $\log C_{0t_{1/2}}$'s.

labelled sequences of the 13S 3' end containing fragment which was prepared from the α mRNA should correspond exclusively to C region and 3' untranslated sequences. (According to Commerford [1971], the poly(A) tract is not labelled by ^{32}P .)

The first series of experiments involving this RNA fragment investigated the final level of its hybridization with H2020, 104E, and J558 DNA's (that is, the homologous DNA plus those heterologous DNA's which had shown variant hybridization levels with the H2020 α RNA containing all the sequences of the complete molecule). With each DNA, the 'complete sequence' RNA, prepared under equivalent conditions as the 3'-end containing fragment, was also hybridized as a control. The equivalent lengths of these two RNA sequences were considered (that is, the number of nucleotides corresponding to 16S and to 13S), and the DNA/RNA ratios were adjusted as follows in order to obtain as similar as possible DNA excesses: With the H2020 'complete sequence' α RNA, the sequence ratio of DNA to RNA is equal to 3×10^6 (taking the length of this 16S RNA as 1800 nucleotides, the average molecular weight per nucleotide as 320, and the molecular weight of the mouse genome as 1.8×10^{12} daltons). With the 3'-end containing fragment, the sequence ratio is 5×10^6 (taking the length of this 13S RNA as 1200 nucleotides). Therefore, in order to achieve an arbitrary DNA excess of 3 in each case, the experimental DNA/RNA ratios were set at 1×10^7 and 1.5×10^7 , respectively. That is, 0.5 μgm of DNA were used per cpm of the 'complete sequence' α RNA, while 0.75 μgm of DNA were used per cpm of the 3'-end containing fragment.

The final results of each hybridization are presented in Table 7. These results confirm the previous observation that the 'complete sequence' α RNA hybridizes to a greater extent with J558 DNA, and to a

TABLE 7. Percent Hybrid Formed by H2020 α RNA 'complete sequence' and 3'-end containing fragment with H2020, 104E and J558 DNA's.

| DNA | H2020 α RNA | Log $C_{10}t$ | | |
|----------|----------------------------|---------------|------|------|
| | | 2 | 4 | 4.4 |
| H2020 #2 | complete sequence | 10.9 | 33.9 | 37.8 |
| | 3'-end containing fragment | 9.4 | 28.8 | 36.5 |
| 104E | complete sequence | 7.1 | 22.4 | 23.0 |
| | 3'-end containing fragment | 7.7 | 21.5 | 21.9 |
| J558 | complete sequence | | 43.2 | 46.6 |
| | 3'-end containing fragment | | 43.0 | 47.9 |

DNA concentration = 22.5 mg/ml.

Ratio of DNA to RNA = 1×10^7 for the 'complete sequence' H2020 α RNA
 1.5×10^7 for the 3'-end containing fragment.

lower extent with 1041 DNA, than with its homologous RNA. Furthermore, in no instance were significant differences observed between the final level of hybridization of this complete sequence and the final level of the 3' end containing fragment.

A more extensive investigation was then carried out by determining the kinetics of hybridization of the 3' end containing fragment with 1041 DNA, in comparison with those of the complete sequence of a RNA. Again, the DNA excess was adjusted to meet that in each case, with the final DNA concentration being 200 $\mu\text{g/ml}$. The results are presented in Figure 18, where the two sets of curves are seen to be indistinguishable within the range of experimental error.

Effect of the DNA Excess on the Final Hybridization Level

Unless hybridizations are performed under conditions where the amount of DNA vastly exceeds, on a sequence basis, the amount of RNA, the final level of hybridization will be affected by the actual extent of the DNA excess (Melli et al, 1971). Although all possible efforts were made to keep the excess constant in the above experiments, the possibility cannot be excluded that some of the variations observed were due to unknown and unintentional differences in the DNA excess. Therefore, an experiment was performed where the ratio of DNA to RNA was altered purposely and the effect of these alterations on the final hybridization level was studied.

A standard ratio was set at 0.5 μgm of DNA per cpm of 'complete sequence' H2020 α RNA. Using the assumed specific activity of 2×10^7 cpm/ μgm for the RNA, this gives a DNA/RNA ratio of 1×10^7 . Since the

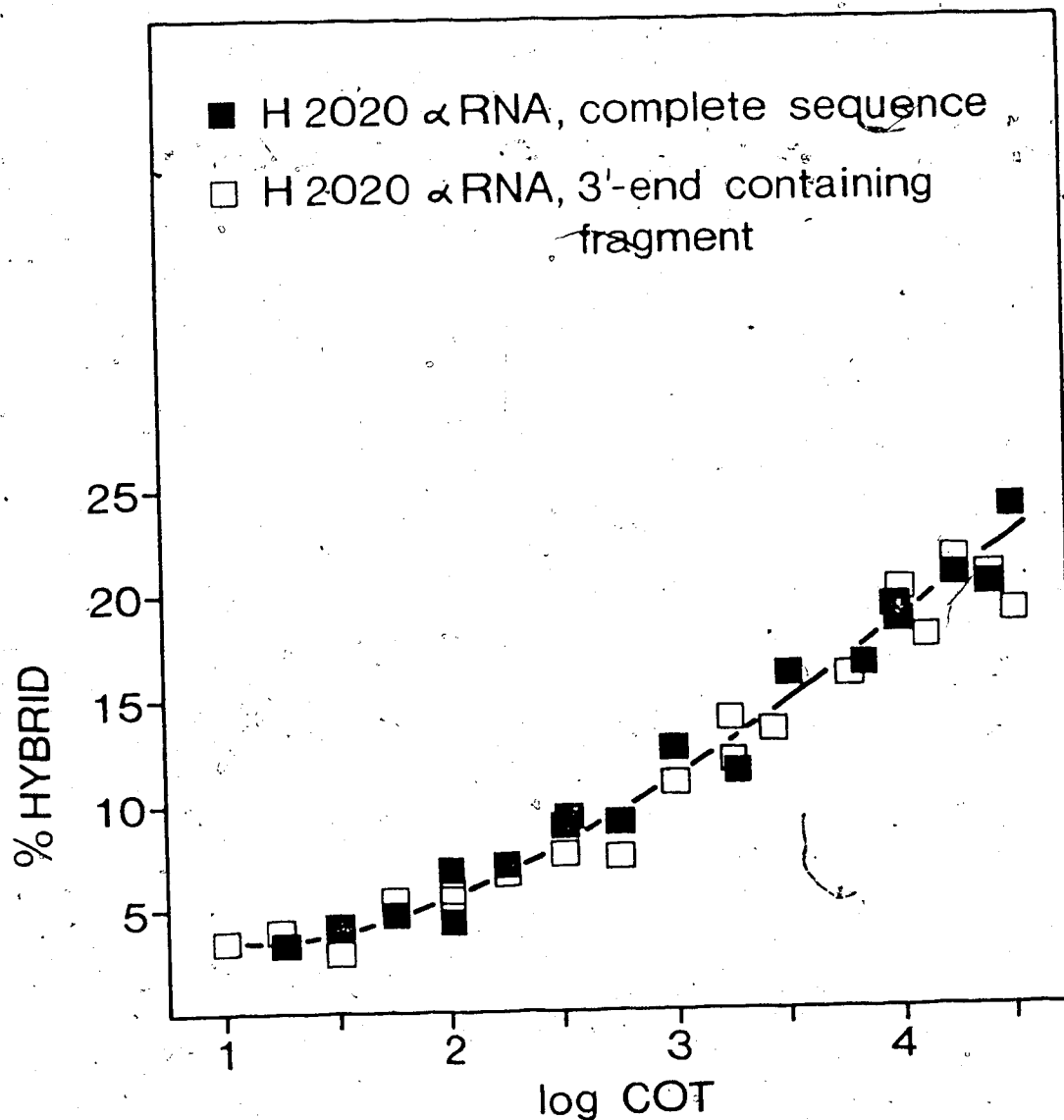


Figure 18. Hybridization kinetics of H2020 α RNA 'complete sequence' and 3'-end containing fragment with 104E RNA (#2). DNA concentration, 22.5 mgm/ml. Ratio of DNA to RNA: ■, 1×10^7 ; □, 1.5×10^7 . Intrinsic RNase resistant factor: ■, 2.76%; □, 1.58%.

sequence ratio of mouse DNA to H2020 α RNA is equal to 3×10^6 (as calculated above), the resulting DNA excess is approximately 3-fold.

Hybridizations were then performed between H2020 and J558 DNA's and H2020 α RNA at ratios of 1.5 μgm DNA/cpm RNA, 0.5 μgm DNA/cpm RNA, and 0.167 μgm DNA/cpm RNA. These ratios are therefore equivalent to DNA excesses of approximately 9, 3 and 1. Results are presented in Table 8. No significant differences, corresponding to the DNA excesses used, were found in the final hybridization levels.

TABLE 8. Effect of the DNA Excess on the Final Hybridization Level

| Type of DNA | Amount of DNA (mgm) | Amount of H2020 & RNA (#2) (cpm) | DNA/RNA | DNA Excess | % Hybrid at log Cot 4 | % Hybrid at log Cot 4.5 |
|-------------|---------------------|----------------------------------|--------------------|------------|-----------------------|-------------------------|
| J558 | 3.0 | 2000 | 3×10^7 | 9 | 39.6 | 46.6 |
| | 1.0 | 2000 | 1×10^7 | 3 | — | 49.4 |
| | 1.0 | 6000 | 0.33×10^7 | 1 | 42.2 | 43.1 |
| H2020 #2 | 3.0 | 2000 | 3×10^7 | 9 | 33.9 | 33.0 |
| | 1.0 | 2000 | 1×10^7 | 3 | 35.5 | 38.1 |
| | 1.0 | 6000 | 0.33×10^7 | 1 | 33.9 | 37.0 |

DNA concentration = 22.5 mg/ml.

DISCUSSION

Three general points of significance are apparent from the experiments described above: firstly, heavy chain mRNA's could be isolated from mouse myelomas with a high degree of purity; secondly, hybridizations of these mRNA's to mouse liver DNA suggested that heavy chain genes are not reiterated more than a few times in the genome of an undifferentiated cell; thirdly, hybridizations of these mRNA's to homologous and heterologous myeloma DNA's showed certain significant variations in the final levels and in the kinetics of hybridization. Each of these points will be presented in greater detail in the following discussion.

Purification and Characterization of Heavy Chain mRNA's

The method described for the purification of the H2020 α and 104E μ mRNA's followed basically methods which had been previously used for immunoglobulin light chain mRNA's. However, several modifications have been introduced in the present work which have permitted the isolation of the α RNA, in particular, to a greater degree of purity than previously reported for any heavy chain mRNA. Firstly, the heat treatment before oligo(dT)-cellulose chromatography allowed a more complete purification of that small percentage of RNA which contains poly(A) sequences. In all previous reports showing sucrose gradient scans of the poly(A)-containing RNA obtained by oligo(dT)-cellulose chromatography, significant proportions of material in the 18S region are clearly visible (Brownlee *et al.*, 1972; Brownlee *et al.*, 1973; Tonegawa and Baldi, 1973; Mach *et al.*, 1973; Premkumar *et al.*, 1974).

This is probably due to aggregation between RNA molecules, resulting in some rRNA being indiscriminately bound to the oligo(dT) along with the mRNA's. With light chain mRNA's, this has not been so great a problem, as their molecular shapes and sizes permit their further purification from 18S rRNA by physical methods (for example, preparative sucrose density gradient centrifugation and polyacrylamide gel electrophoresis). However, the greater molecular weights of heavy chain mRNA's result in physical behavior very similar to that of 18S rRNA: μ mRNA sediments at essentially the same S value as 18S rRNA in sucrose density gradients (see Figure 7), and α mRNA shows an electrophoretic mobility only very slightly less than 18S rRNA in formamide gels (see Plate 8). Therefore, it is essential to remove as much of the non-poly(A)-containing material as possible during the oligo(dT) chromatographic step. The heat treatment described here causes the disaggregation of RNA molecules by the breakage of intermolecular hydrogen bonds, thereby improving the selectivity of binding to oligo(dT).

The second modification involved the method of polyacrylamide gel electrophoresis. Since this technique was used both for analytical purposes and as the final step in the purification procedure, it was essential to use gels with a high degree of resolution, in order to correctly detect that portion of the gel containing the desired mRNA. Gels prepared by the method described above (that is, polymerization in water followed by equilibration to 99% formamide) show a much lower UV-absorbing background than gels prepared by the previously-used method of polymerization directly in 99% formamide (Gould and Hamlyn, 1973). This is likely due to the leaching out of interfering materials during

the equilibration step. Consequently, the resolution of the gels and the purity of the eluted RNA's described here appear to be greater than that achieved in previous reports.

The heavy chain mRNA's prepared in this study were characterized by their abilities to stimulate protein synthesis in a cell-free translation system. In the case of H2020 α RNA, the majority of products produced definitely corresponded to authentic IgA heavy chains, both by their electrophoretic mobilities in SDS gels (see Plate 2) and by the type of peptides formed with trypsin digestion (see Plates 6 and 7). The high purity suggested by this analysis of cell-free products was further supported by the physical characteristics of the H2020 RNA preparation, particularly by its relatively homogeneous migration in formamide gels. The 104E μ RNA preparation also stimulated the synthesis of proteins in the cell-free translation system, but with 25% less efficiency than the H2020 α RNA. The analysis of its cell-free products confirmed the presence of polypeptides closely related to authentic μ chains; however, it was unable to provide a good estimate of the apparent contribution of mRNA's coding for other polypeptides. Furthermore, the formamide gel electrophoresis showed a considerable background in the region of the 104E μ RNA, as well as some residual contamination by 18S rRNA despite the stringent oligo(dT) chromatography. Even after judicious elution of the 104E μ RNA from preparative gels, this rRNA component was shown by competition hybridization experiments to comprise a minimum of 5% of the final preparation.

Therefore, it must be concluded that the purity of the 104E μ RNA preparation is significantly less than that of the H2020 α RNA

preparation. *A priori*, it would be expected that the purification techniques described above would be equally effective in both cases. However, the relative quantities of material in the heavy regions of the RNA sucrose gradients suggest that 104E myeloma cells contain a lower percentage of the corresponding heavy chain mRNA than do the H2020 cells. This observation is consistent with the relative amounts of immunoglobulin per cell as determined by the immunofluorescent staining pattern. Consequently, in the 104E cells more contaminating mRNA molecules are present per molecule of desired mRNA than in the H2020 cells; this is likely a major factor responsible for the differences in the purities of the final α and μ RNA preparations.

Hybridization Kinetics of H2020 α and 104E μ RNA's with Mouse Liver DNA

Previous reports of the hybridization kinetics of complete immunoglobulin mRNA's (summarized in Table 1) invariably showed distinctly biphasic C_0t curves, with a major fraction hybridizing at high $C_0t_{1/2}$ values (representing unique or almost unique gene frequencies) and a minor fraction hybridizing at lower $C_0t_{1/2}$ values. The actual gene frequency of this more rapidly hybridizing fraction, as well as its relative proportion, varies extensively among reports. Considering the heavy chain mRNA's in particular, Bernardini *et al.* (1974) found that a maximum of 23% of their γ mRNA seemed to be derived from genes reiterated about 300 times, and they hypothesized that these sequences comprise the external untranslated section of the γ gene; Premkumar *et al.* (1974) found that 29% of their α mRNA hybridized with a $C_0t_{1/2}$ of 1.5 (corresponding to a gene reiteration frequency of 5000), and on the

basis of purely *ad hoc* arguments, they interpreted this rapidly hybridizing portion as representing the heavy chain variable gene. However the present results, particularly those obtained with the H2020 α RNA, are in opposition to both of these interpretations. Although the C_0t curve did extend over a wider range than expected for a purely homogeneous RNA (see the comparison with 18S rRNA in Figure 13), the H2020 α RNA hybridized to mouse liver DNA with apparently monophasic kinetics. The improvements in the purification procedure discussed above suggest that it is the purity of the mRNA probe which is responsible for this discrepancy between the previous and the present reports in regard to the nature of the C_0t curves. This interpretation is supported by the correlation between the purities of the H2020 and the 104E RNA preparations and their hybridization characteristics: from its physical properties and the analysis of its cell-free products, the 104E μ RNA was determined to be significantly less pure than the H2020 α RNA; correspondingly, it shows a larger proportion of sequences hybridizing at C_0t values less than 10^2 . It follows, then, that those rapidly hybridizing sequences responsible for the biphasic kinetics in previous reports, and for the tails on the C_0t curves in this report, are more likely due to repetitive portions of contaminating mRNA's than of the mRNA's coding for the immunoglobulin chain in question. A similar conclusion has recently been drawn for the light chain mRNA's (S. Tonegawa, personal communication).

The H2020 α and 104E μ mRNA's hybridized to mouse liver DNA with apparent C_0t_2 of 790 and 630 mol-sec/l, respectively. The corresponding nominal reiteration frequencies of 7 and 8 are an upper limit

and must be corrected, as described by Bishop *et al.* (1972), for finite DNA/RNA ratios and for heat degradation of RNA; such considerations result in corrected reiteration frequencies of 3 and 4, respectively. On the basis of the monophasic nature of the C_0t curves obtained, there is no evidence whatsoever to prevent the assignment of these reiteration frequencies to both the variable and the constant regions of the α and μ mRNA's. Therefore, the problem now becomes the following: Are these three or four copies of V_H variable regions, which form stable hybrids with H2020 α and 104E μ mRNA's, sufficient to account for antibody diversity on the basis of the "germ line gene" hypothesis, or must somatic generators of antibody diversity be invoked? This problem can only be resolved by detailed studies on the sequence homology of all V_H regions of mouse myelomas. In any case, no evidence whatsoever was found to suggest the existence of thousands of cross-hybridizable V_H region germ line genes, as was previously reported for another IgA-producing myeloma (Premkumar *et al.*, 1974).

Hybridization Studies with Myeloma DNA's

These studies were undertaken with the hope of relating phenotypic events occurring during lymphocyte differentiation and development with events occurring at the gene level. The phenotypic events implicated are those involving the integration of V and C region genetic information and the subsequent commitment of a nondifferentiated cell to the production of a particular immunoglobulin. As discussed in the Introduction, two models (the translocation model of Dreyer and Bennett and the DNA-network model of Smithies) have been proposed by which integration could occur within the DNA; both of these models are very difficult

to test at the molecular level. However, it is also possible to envision a model in which a V gene is joined to a particular C gene by excision of the interspersing DNA material. In this respect, the heavy chain genetic region is particularly interesting, since genetic studies with allotypic markers have shown, as discussed in the Introduction, that the genes coding for each of the constant regions of heavy chain molecules (C_H genes) form one linkage group together with the gene(s) coding for variable regions (V_H genes). Based on this linkage relationship, a very simplistic form of an excision model for gene integration is presented in Figure 19. If the excised DNA is subsequently lost, such a model has one critical implication at the molecular level: the DNA composition of differentiated lymphocytes (in particular, the numbers and types of C_H genes) will differ with the class of immunoglobulin produced. In the present study, an attempt was made to detect the possible existence of such differences by DNA/RNA hybridizations.

Considering the relative purities of the two heavy chain mRNA's, as discussed above, the results obtained with the H2020 α RNA are likely to be more definitive; therefore, they will be predominantly considered in the following discussion. Basically, these results are as follows: taking the hybridization with its homologous myeloma DNA as a standard, H2020 α RNA hybridized with S28 (γ_1), MPC11 (γ_{2b}) and Y5781 (μ) DNA's to an equal extent, with J558 (α) DNA to a greater extent, and with 104E (μ) DNA to a lesser extent. It can be concluded with a reasonable degree of confidence that these differences are not merely experimental artifacts: firstly, the results were well-substantiated with various preparations of RNA and of each DNA; secondly, the possibility that varying background levels of RNase activity in the DNA preparations were responsible for the varying levels of hybridization was discounted by

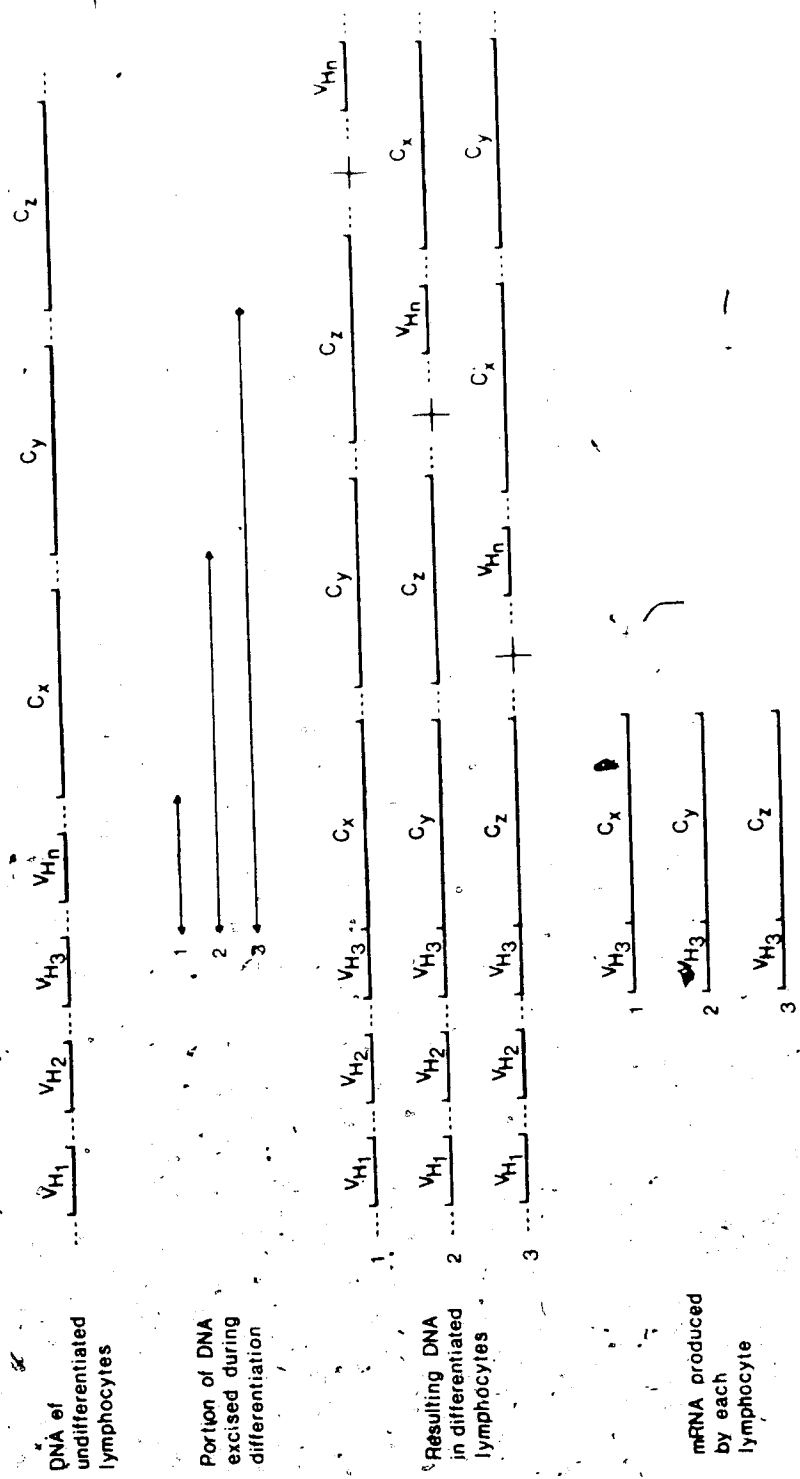


Figure 19. Simplistic model of V-C gene integration by excision of interspersing DNA sequences. Dotted lines indicate that the nature and extent of the DNA sequences are unspecified. C_H genes are labelled as X, Y, and Z to avoid any inference of gene order. This model is independent of the number of V genes.

the equal levels obtained with the 104E RNA preparation (regardless of the purity of this preparation, it would have been affected to the same extent as H2020 α RNA by a greater than average RNase activity in the 104E DNA or by a less than average activity in the J558 DNA); thirdly, the results were not affected by intentional variations in the DNA/RNA ratio, indicating that the experiments had actually been carried out at an even greater DNA excess than that calculated. (This was likely due to the difficulty of determining accurately the specific activity of the iodinated RNA.)

Furthermore, the possibility that these differences in hybridization are related solely to V_H genes must be rejected for the following two reasons:

1. The final levels of hybridization with both the 104E and J558 DNA's varied by approximately 13% from the average level of 38% obtained with the H2020 DNA (values estimated from the C_0t curves in Figure 17). This corresponds to 34% of the total sequences hybridized. However, as evident from the structure of the α mRNA depicted above, the V_H sequences only correspond to approximately 20% of the total ^{125}I -labelled sequences of the α RNA molecule.

2. A 3'-end containing fragment of the α mRNA was prepared in such a way that it should have contained no sequences corresponding to the variable region or the presumptive 5'-end external region. If the differences in hybridization observed among the J558, H2020 and 104E DNA's were actually related to V_H genes, the substitution of this 3'-end containing fragment for the 'complete sequence' α RNA should have obliterated these differences. The results presented in Table 7 and Figure 18 show that this was not the case.

Therefore, it can be tentatively concluded that the observed differences in hybridization are primarily attributable to differences in

the C_H (α) gene composition of the J558, H2020, and 1041 DNA's. That is, during the development of the particular lymphocyte which eventually resulted in each of these myeloma lines, some sort of gene rearrangement appears to have occurred, involving the specific loss of DNA sequences corresponding to a particular C_H gene.

Two apparently puzzling aspects still remain: the lack of class specificity (for example, only one of the two μ DNA's showed a reduced level of hybridization with the α RNA), and the existence of a heterologous hybridization combination (J558 DNA with H2020 α RNA) which gave a higher level of hybridization than the homologous combination. Evidently many complicating factors exist; for example, eukaryotic genes are usually present in two copies on homologous chromosomes; the presumptive excision events cannot be assumed to occur precisely at gene boundaries; subclasses of α - and μ -chains are thought to exist but the crosshybridization abilities of such subclasses are as yet unknown. Further work is required before the simplistic model of Figure 19 can be meaningfully expanded to include these factors. Initially such work should involve: the additional purification of μ mRNA; the isolation of more heavy chain mRNA's from different immunoglobulin classes (particularly γ mRNA) and from different myelomas; the extension of all hybridizations to reciprocal combinations.

The previously proposed models of V and C gene integration (that is, the translocation model of Dreyer and Bennett and the DNA-network model of Smithies) contain no implications whatsoever of differential DNA composition in different immunoglobulin classes; consequently, they do not predict the sort of hybridization data obtained in the present

work. On the other hand, these data suggest that the commitment of a particular lymphocyte to the production of a specific immunoglobulin class occurs concurrently with the loss of certain λ_H genetic sequences. A mechanism of λ_H gene integration based on excision of heteroduplex DNA material seems, therefore, to be implicated. The extension of the present study to include the reciprocal hybridizations of all heavy chain immunoglobulin classes and possible subclasses should not only provide conclusive evidence in this regard, but should also be significant in the determination of λ_H gene order.

BIBLIOGRAPHY

- AVIV, H. and Leder, P. (1972). Purification of biologically active globin mRNA by chromatography on oligothymidylic-acid cellulose. Proc. Nat. Acad. Sci. (USA) 69: 1408.
- BERNARDINI, A. and Tonegawa, S. (1974). Hybridization studies with an antibody heavy chain mRNA. FEBS Lett. 41: 73.
- BERNS, A., Janssen, P. and Bloemendal, H. (1974). The molecular weight of the 14S calf lens messenger RNA. Biochem. Biophys. Res. Comm. 59: 1157.
- BISHOP, J.O. (1972). Molecular hybridization of ribonucleic acid with a large excess of deoxyribonucleic acid. Biochem. J. 126: 171.
- BISHOP, J.O., Pemberton, R., and Baglioni, C. (1972). Reiteration frequency of haemoglobin genes in the duck. Nature New Biol. 235: 231.
-
- BLOBEL, G. and Potter, V.R. (1966). Relation of ribonuclease and ribonuclease inhibitor to the isolation of polysomes from rat liver. Proc. Nat. Acad. Sci. (USA) 55: 1283.
- BRITTEN, R.J., Graham, D.E. and Neufeld, B.R. (1974). Analysis of repeating DNA sequences by reassociation. Methods in Enzymology 29: 363.
- BROWNLEE, G.G., Cartwright, E.M., Cowan, N.J., Jarvis, J.M. and Milstein, C. (1973). Purification and sequence of mRNA for immunoglobulin light chains. Nature New Biol. 244: 236.
- BROWNLEE, G.G., Harrison, T.M., Mathews, M.B. and Milstein, C. (1972). Translation of mRNA for immunoglobulin light chains in a cell-free system from KrebsII ascites cells. FEBS Lett. 23: 244.

- BURNET, F.M. (1969). Cellular Immunology, Melbourne University Press, Cambridge, U.K.
- COMMERFORD, S.L. (1971). Iodination of nucleic acids *in vitro*. Biochemistry 10: 1993.
- DELOVITCH, T.L. and Baglioni, C. (1973). Immunoglobulin genes: a test of somatic vs germ line hypothesis by RNA/DNA hybridization. Cold Spring Harbor Symp. Quant. Biol. 38: 739.
- DREYER, W.J. and Bennett, J.C. (1965). The molecular basis of antibody formation: a paradox. Proc. Nat. Acad. Sci. (USA) 54: 864.
- EDELMAN, G.M. and Gall, W.E. (1966). The antibody problem. Ann. Rev. Biochem. 38: 415.
- EISEN, H.N., Simms, E.S. and Potter, M. (1968). Mouse myeloma proteins with antihapten antibody activity: the protein produced by plasma cell tumor MOPC-315. Biochemistry 7: 4126.
-
- FUDENBERG, H.H., Pink, J.R.L., Stites, D.P. and Wang, A.-C. (1972). Basic Immunogenetics. Oxford University Press, New York.
- GALLY, J.A. and Edelman, G.M. (1970). Somatic translocation of antibody genes. Nature 227: 341.
- GILHAM, P.T. (1964). The synthesis of polynucleotide celluloses and their use in the fractionation of polynucleotides. J. Am. Chem. Soc. 86: 4982.
- GOULD, H.J. and Hamlyn, P.H. (1973). The molecular weight of rabbit globin messenger RNA's. FEBS Lett. 30: 301.
- HERZENBERG, L.A., McDevitt, H.O., and Herzenberg, L.A. (1968). Genetics of antibodies. Ann. Rev. Genet. 2: 209.
- HILSCHMANN, N. and Craig, L.C. (1965). Amino acid sequence studies with Bence-Jones proteins. Proc. Nat. Acad. Sci. (USA) 53: 1403.

- HOLBOROW, E.J. and Johnson, G.D. (1967). Immunofluorescence. In: Handbook of Experimental Immunology, ed. D.M. Weir. Blackwell Scientific Publications, Oxford. p. 571.
- HOOD, L. and Talmage, D.W. (1970). Mechanism of antibody diversity: germ line basis for variability. *Science* 168: 325.
- JERNE, N.K. (1970). The somatic generation of immune recognition. *Eur. J. Immunol.* 1: 1.
- LAEMMLI, U.K. (1970). Cleavage of structural proteins during the assembly of the head of bacteriophage T4. *Nature* 227: 680.
- LEDER, P., Honjo, T., Packman, S., Swan, D., Nau, M. and Norman, B. (1974). The organization and diversity of immunoglobulin genes. *Proc. Nat. Acad. Sci. (USA)* 71: 5109.
- LEE, S.Y., Mendecki, J. and Brawerman, G. (1971). A polynucleotide segment rich in adenylic acid in the rapidly-labeled polyribosomal RNA component of mouse sarcoma 180 ascites cells. *Proc. Nat. Acad. Sci. (USA)* 68: 1331.
- LIBERMAN, R. and Potter, M. (1966). Close linkage in genes controlling IgA and IgG heavy chain structure in Balb/C mice. *J. Mol. Biol.* 18: 516.
- MACH, B., Faust, C. and Vassalli, P. (1973). Purification of 14S messenger RNA of immunoglobulin light chain that codes for a possible light chain precursor. *Proc. Nat. Acad. Sci. (USA)* 70: 451.
- MELLI, M., Whitfield, C., Rao, K.V., Richardson, M. and Bishop, J.O. (1971). DNA-RNA hybridization in vast DNA excess. *Nature New Biol.* 231: 8.

- MILSTEIN, C., Adetugbo, K., Brownlee, G.G., Cowan, N.J., Proudfoot, N.J., Rabbitts, T.H. and Secher, D.S. (1975). Immunoglobulin genes in a mouse myeloma and in mutant clones. *Molecular Approaches to Immunology*, Miami Winter Symposium 9, ed. E.E. Smith and D.W. Ribbons.
- PREMKUMAR, E., Shoyab, M., and Williamson, A.R. (1974). Germ line basis for antibody diversity: immunoglobulin V_H - and C_H gene frequencies measured by DNA-RNA hybridization. *Proc. Nat. Acad. Sci. (USA)* 71: 99.
- SCHARFF, M.D., Birshtein, B., Dharmgongartama, B., Frank, L., Kelly, T., Kuehl, W.M., Margulies, D., Morrison, S.L., Preud'homme, J.-L. and Weitzman, S. (1975). The use of mutant myeloma cells to explore the production of immunoglobulin. *Molecular Approaches to Immunology*, Miami Winter Symposium 9, ed. E.E. Smith and D.W. Ribbons.
- SCHREIBER, M.H. and Staehlin, T. (1973). Initiation of mammalian protein synthesis: the importance of ribosome and initiation factor quality for the efficiency of *in vitro* systems. *J. Mol. Biol.* 33: 329.
- SCHUBERT, D. (1970). Immunoglobulin biosynthesis. IV. Carbohydrate attachment to immunoglobulin subunits. *J. Mol. Biol.* 51: 287.
- SHERR, C.J. and Uhr, J.W. (1970). Immunoglobulin synthesis and secretion. V. Incorporation of leucine and glucosamine into immunoglobulin on free and bound polyribosomes. *Proc. Nat. Acad. Sci. (USA)* 66: 1183.
- SINGER, S.J. and Doolittle, R.F. (1966). Antibody active sites and immunoglobulin molecules. *Science* 153: 13.
- SMITHIES, O. (1968). Immunoglobulin genes: arranged in tandem or in parallel? *Cold Springs Harbor Symp. Quant. Biol.* 38: 725.

- STORB, U. (1974). Evidence for multiple immunoglobulin genes. *Biochem. Biophys. Res. Comm.* 57: 31.
- STUDIER, F.W. (1965). Sedimentation studies of the size and shape of DNA. *J. Mol. Biol.* 11: 373.
- SWAN, D., Aviv, H. and Leder, P. (1972). Purification and properties of biologically active mRNA for a myeloma light chain. *Proc. Nat. Acad. Sci. (USA)* 69: 1967.
- TONEGAWA, S. and Baldi, I. (1973). Electrophoretically homogeneous myeloma light chain mRNA and its translation *in vitro*. *Biochem. Biophys. Res. Comm.* 51: 81.
- TONEGAWA, S., Bernardini, A., Weimann, B. and Steinberg, C. (1974). Reiteration frequency of antibody genes: studies with κ -chain mRNA. *FEBS Lett.* 40: 92.
- TONEGAWA, S., Steinberg, C., Dube, S. and Bernardini, A. (1974). Evidence for somatic generation of antibody diversity. *Proc. Nat. Acad. Sci. (USA)* 71: 4027.
- TOSI, S.L., Mage, R.G. and Dubiski, S. (1970). Distribution of allotypic specificities A1, A2, A14 and A15 among immunoglobulin G molecules. *J. Immunol.* 104: 641.
- WANG, A.-C., Wilson, S.K., Hopper, J.E., Fudenberg, H.H. and Nisonoff, A. (1970). Evidence for control of synthesis of the variable regions of the heavy chains of immunoglobulins G and M by the same gene. *Proc. Nat. Acad. Sci. (USA)* 66: 337.
- WU, T.T. and Kabat, E.A. (1970). An analysis of the sequences of the variable regions of Bence-Jones proteins and myeloma light chains and their implications for antibody complementarity. *J. Exp. Med.* 132: 211.